The Role of Fa2p in Ciliary and Cell Cycle Regulation

by

Moe R. Mahjoub
B.Sc., Simon Fraser University, 2002

THESIS SUBMITTED IN PARTIAL FULFILLMENT OF
THE REQUIREMENTS FOR THE DEGREE OF

DOCTOR OF PHILOSOPHY

In the Department
of
Molecular Biology and Biochemistry

SIMON FRASER UNIVERSITY

Fall 2006

APPROVAL

Name: **Moe R. Mahjoub**

Degree: **Doctor of Philosophy**

Title of Thesis: **The Role of Fa2p in Ciliary and Cell Cycle Regulation**

Examining Committee:

Chair: **Dr. Esther M. Verheyen**
Associate Professor, Department of Molecular Biology and Biochemistry, Simon Fraser University

---

Dr. Lynne M. Quarmby
Senior Supervisor
Associate Professor, Department of Molecular Biology and Biochemistry, Simon Fraser University

---

Dr. Michel R. Leroux
Supervisor
Associate Professor, Department of Molecular Biology and Biochemistry, Simon Fraser University

---

Dr. Christopher T. Beh
Supervisor
Assistant Professor, Department of Molecular Biology and Biochemistry, Simon Fraser University

---

Dr. Bruce P. Brandhorst
Internal Examiner
Professor, Department of Molecular Biology and Biochemistry, Simon Fraser University

---

Dr. Winfield S. Sale
External Examiner
Professor, Department of Cell Biology, Emory University

Date Defended/Approved: Nov. 6, 2006

ABSTRACT

Cilia are microtubule based organelles with roles in motility and sensory perception. An emerging pattern suggests that various human diseases are caused by defects in the assembly, maintenance or function of cilia. Some ciliopathies, such as the polycystic kidney diseases and Bardet-Biedl syndrome, involve aberrant cell proliferation in conjunction with ciliary defects. Recent data suggests that the cilium serves as a highly conserved organizing center for early steps in signal transduction pathways that control cell growth and division. As such, signaling molecules important for growth, mitosis or differentiation have been localized to cilia. The relationship between cilia and cell cycle progression is poorly defined, but may involve regulation by the NIMA-family of kinases (Neks). Our discovery that the Nek Fa2p is important for ciliary function and cell cycle progression in *Chlamydomonas* provides a direct link between these two processes. Fa2p was originally identified from a screen for deflagellation-defective mutants in *Chlamydomonas* and shown to be defective in calcium-induced severing of the axonemal microtubules. We subsequently showed that *fa2* mutants are delayed in transit through at least two points in the cell cycle: (1) G_2/M transition; (2) assembly of flagella after exit from mitosis.

In this study, we show that Fa2p localizes to a unique site at the proximal end of cilia in *Chlamydomonas* and kidney epithelial cells, suggesting a high level of conservation of this signaling complex. In both cell types, Fa2p localization is dynamic; when cells enter the cell cycle, Fa2p becomes reduced in the cilium and accumulates at the base of the basal bodies/centrioles. It remains associated with the spindle poles throughout the cell cycle and is assembled on cilia when they begin to regenerate after exit from mitosis. Importantly, Fa2p kinase activity is required for deflagellation, but does not appear to be essential for localization and efficient cell cycle progression. Furthermore, we show that two mammalian Nek homologs of Fa2p (mNek1 and mNek8), which are defective in murine models of polycystic kidney diseases, localize to primary cilia and centrosomes. Finally, biochemical analysis reveals the interaction of two proteins (~20 and ~60 kDa) with Fa2p *in situ*.

Keywords: Deflagellation, Cilia, Kinase, Cell-cycle, Centriole, *Chlamydomonas*

DEDICATION

To my parents Shahla and Mansour, for all the sacrifices they have made to make this possible. For having the vision and foresight, and for their never ending support, I dedicate this to them. To my brothers, Ali and Amir, and my sister Saghar, who have always been there for me. And to Crystal, for the sacrifices she is about to make.

ACKNOWLEDGEMENTS

I wish to express my utmost gratitude to my mentor, Dr. Lynne Quarmby, for being a wonderful teacher, scientist and friend. I am forever thankful for her constant support and encouragement, and for allowing me to study in her lab. I would like to extend my sincerest thanks to all the members of the Quarmby lab, past and present: Rip Finst and Benjamin Goh for helping with my training in the early days; Ben Montpetit, Apollos Kim and James Wagner for their help in developing my research ideas; Brian Bradley, Jeremy Parker, Mark White, Melissa Trapp and Jaime Kirschner for the stimulating discussions and for sharing ideas; Qasim Rasi for his friendship and for being there with me right from the start of the lab; and the numerous undergraduate students who have contributed to various aspects of my research project.

I am also grateful to members of my PhD committee, Drs. Chris Beh and Michel Leroux, for their time and effort, helpful suggestions and encouragement. I would like to thank members of the Leroux lab (Muneer Esmail, Junchul Kim, Oliver Blacque and Victor Lundin) for their experimental advice and help. Finally, a special thank you to all the labs in the MBB department for sharing of materials and resources.

TABLE OF CONTENTS

LIST OF FIGURES AND TABLES

Glossary

fa	Flagellar Autotomy
IFT	Intraflagellar Transport
IMCD	Inner Medullary Collecting Duct
jck	Juvenile Cystic Kidney
kat	Kidney, Anemia, Testis
NIMA	Never In Mitosis Aspergillus
Nek	NIMA-related Expressed Kinase
PCM	Pericentriolar Material
pf	Paralyzed Flagella
PKD	Polycystic Kidney Disease
QFC	Quadraflagellate Cell
SOFA	Site Of Flagellar Autotomy

CHAPTER 1:

General Introduction

1.1 The Cilium: Structure and Function

Cilia and flagella are evolutionarily conserved, microtubule-based organelles that provide cells with diverse motility and sensory functions (reviewed in Pazour and Witman, 2003). They are found in a wide array of organisms, ranging from alga to humans, and are structurally highly conserved (Mitchell, 2004). Motile cilia can provide cellular movement, for example to sperm cells or protists. Alternatively, they are involved in extracellular fluid propulsion overlying the epithelial surfaces in higher organisms (reviewed in Davis *et al.*, 2006). Immotile cilia have diverse roles in sensory perception, including the detection of light in the vertebrate eye, odorants in the nose and flow in the kidney nephron (Pazour and Witman, 2003; Davis *et al.*, 2006).

At the core of the cilium is the axoneme, composed of nine outer doublet microtubules (Figure 1-1A; reviewed in Silflow and Lefebvre, 2001). In motile cilia, the outer nine doublets surround an additional pair of singlet microtubules. These cilia also contain dynein motor complexes and radial spokes that provide the mechanical movement of the cilium (Figure 1-1A; Dutcher, 1995; Silflow and Lefebvre, 2001). This entire structure is encased by a membrane that is continuous with the plasma membrane of the cell, but is a separate domain with a unique complement of proteins (Bloodgood,

1990). The axoneme is templated by and nucleated from a basal body. Basal bodies are differentiated centrioles, hollow cylinders composed of 9 triplet microtubules (tubules A, B and C). The nine outer doublet microtubules of the axoneme extend from the A and B tubules of the basal body (Dutcher, 1995). The axoneme extends through an electron-dense structure called the flagellar transition zone, located at the distal end of the basal body (Figure 1-1B)

Cilia are dynamic organelles that undergo growth and turnover at their distal tips (Johnson and Rosenbaum, 1992). Assembly and maintenance of cilia is dependent on transport of ciliary building blocks by microtubule-based motors, a process first discovered in *Chlamydomonas* and referred to as *I*ntra*f*lagellar *T*ransport (IFT; Kozminski *et al.*, 1993). Cells assemble cilia by a complex mechanism that involves: (1) pre-assembly of ciliary precursors in the cell body; (2) targeting of pre-assembled components to the basal bodies; and (3) the movement of protein particles (known as IFT rafts), carrying ciliary precursors, from the base to the tip of the flagellum by kinesin (Cole, 2003). Cells disassemble their cilia by one of two mechanisms: (1) Resorption, an IFT-dependent process by which the ciliary components are retracted into the cell by cytoplasmic dynein (Cole, 2003), usually occurring prior to cell division (Figure 1-2A); or (2) Deflagellation/deciliation, an IFT-independent shedding of cilia in response to external stimuli (Figure 1-2B; reviewed in Quarmby, 2004). Although the mechanisms of resorption and deciliation appear distinct, recent evidence suggests that the two pathways share regulatory elements (Parker and Quarmby, 2003; Pan *et al.*, 2004).

Deflagellation is the process by which microtubules of the axoneme are severed to release the flagellum. It involves an influx of extracellular Ca^{2+}, which triggers a signal

transduction pathway that culminates in the precise severing of the nine outer doublet microtubules at the base of the flagellum (for a comprehensive review see Quarmby, 2004). Deflagellation is a ubiquitous and highly conserved cellular response: respiratory and olfactory epithelia, sperm, sea urchin embryos, rabbit oviduct and rat cerebral ependymal cells all deciliate in response to stress (Quarmby, 2004).

Due to the broad and varied tissue and cellular distribution of cilia, as well as the highly conserved functions of this organelle, it is not surprising that dysfunction of cilia can lead to a broad range of human diseases. Specifically, mutations in genes influencing ciliary formation (assembly and disassembly) or function (signaling from cilia) lead to a variety of human diseases we refer to as ciliopathies (Pan *et al.* 2005; Eley at al., 2005; Yoder, 2006; Guay-Woodford, 2006).

1.2 Ciliopathies: The Cilia-Cell Cycle Connection

Defects in cilia are associated with a range of human diseases, such as polycystic kidney disease (PKD), hydrocephalus, primary ciliary dyskinesia and retinal degeneration (Pan *et al.* 2005; Eley *et al.*, 2005; Yoder, 2006; Guay-Woodford, 2006). Furthermore, recent evidence suggests that ciliary defects can lead to a broader set of developmental phenotypes, such as Bardet-Biedl syndrome, Alstrom syndrome and Meckel-Gruber syndrome (Badano *et al.*, 2006). As more and more molecular data is collected, there is an emerging pattern of evidence suggesting that the proximal cause of some ciliopathies is dysregulation of cell proliferation due to ciliary defects (Wilson, 2004). One example of this comes from studies of polycystic kidney disease.

Primary cilia in kidneys are found on epithelial cells lining the nephron extending into the apical lumen, and play roles in mechano-sensation of urinary flow (Praetorius and Spring, 2001). It has been suggested that flow sensing by the cilium regulates the fine balance between cell proliferation and differentiation, and helps maintain intra-luminal diameters and architecture (Boletta and Germino, 2003). Consequently, a failure in ciliary signaling could release cells from growth inhibition, leading to compensatory growth of the tubular cells in an attempt to overcome what appears to be a lack of fluid flow (Calvet, 2003). The increased rate of cell proliferation leads to formation of renal cysts, which increase in size and number until they replace much of the normal kidney tissue, leading to end-stage renal failure (Wilson, 2004).

The most common, and well studied, of the human polycystic kidney diseases is autosomal dominant PKD, caused by mutations in the *PKD1* and *PKD2* genes. These encode a pair of interacting membrane proteins, polycystin-1 and polycystin-2, the latter being a calcium-permeant ion channel (Hanaoka *et al.*, 2000). Both proteins have been localized to cilia and are implicated in mediating the mechano-sensation signals from urinary flow (Praetorius and Spring, 2001). The normal flow of urine leads to an influx of calcium through polycystin-2. This increase in cytosolic calcium is presumed to lead to inhibition of regulated intra-membrane proteolysis of polycystin-1 (Low *et al.*, 2006). Cessation of fluid flow (and hence ciliary signaling) causes proteolytic cleavage of the cytoplasmic tail of polycystin-1, which subsequently translocates to the nucleus along with the associated transcription factor STAT6 and the coactivator P100 (Low *et al.*, 2006). Although the identity of the genes induced by these transcription factors is unknown, it is likely that they are involved in cell proliferation. This illustrates a

mechanism of transducing a ciliary signal into changes in gene expression leading to cell proliferation, and more examples are presented below to address the question: How does signalling from the cilium regulate cell division?

One fundamental relationship between cilia and cell cycle progression is that, in many cells, ciliary disassembly precedes entry into the cell cycle, and exit from mitosis is accompanied by ciliary assembly. This relationship may reflect the use of the basal bodies/centrioles as mitotic spindle poles (Ehler *et al.*, 1995; Wheatley *et al.*, 1996). As such, cell cycle proteins localized to and organized within the cilium or basal bodies may provide signals regarding the state of assembly/disassembly of the cilium, triggering re-entry into the cell cycle. There is likely to be a reciprocal relationship in which signals from the cell body stimulate ciliary loss in anticipation of cell division and ciliary assembly upon exit from mitosis. Importantly, recent work has tied the function of several classes of growth and developmental regulators to cilium-generated signaling (Pazour and Witman, 2003; Huangfu *et al.*, 2004). For example, loss of targeting of the receptors and effectors of Hedgehog to cilia abrogates Hedgehog function (Huangfu *et al.*, 2003; Corbet *et al.*, 2005). Specifically, the transmembrane-protein Smoothened, as well as the Gli transcription factors, have been localized to primary cilia. As such, mutations in IFT proteins (e.g. IFT88/Polaris) that affect ciliogenesis disrupt targeting, processing and function of these transcription factors (Huangfu *et al.*, 2003; Corbet *et al.*, 2005).

Additionally, inversin (a cystogenic protein localized to the cilium) has been shown to act as a regulator of Wnt signaling cascades. Specifically, depletion of inversin was shown to prevent the switch between canonical and non-canonical (often called the

Planar Cell Polarity pathway; PCP) Wnt signaling cascades, a crucial step in renal development required to prevent cyst formation (Simons *et al.*, 2005). In this model, fluid flow over primary cilia results in the increased expression of inversin, which somehow results in the degradation of Dishevelled in the cytoplasm. However, membrane-associated Dishevelled protein (at cell-cell junctions) is unaffected, and can mediate the Wnt signal through various pathways responsible for planar cell polarity, including the JNK and Rho pathways (Logan and Nusse, 2004; Veeman *et al.*, 2003). In the perceived absence of fluid flow, cytoplasmic Dishevelled is not degraded and canonical Wnt signaling leads to aberrant proliferation of cells (Simons *et al.*, 2005).

The role of planar cell polarity in pathogenesis of cystic kidney disease was further demonstrated in elegant experiments by Fisher and colleagues (2006), who showed that the alignment of the mitotic spindles of tubular epithelial cells is aberrant in mice with a renal-specific inactivation of Tcf2, a transcription factor that is essential for the expression of genes involved in PKD, including polycystin-2. They propose a model whereby flow-induced ciliary bending relays signals (most likely through the centrioles/basal bodies) to the epithelia cells of the nephron. These signals are crucial for proper orientation and polarity of the cells, and ultimately, the developing nephron (Fisher *et al.*, 2006). Finally, a recent study in *Xenopus* demonstrated the requirement for core PCP proteins in ciliogenesis (Park *et al.*, 2006). Specifically, the authors identified an unexpected role for Inturned and Fuzzy function in the response to Hedgehog signals during early developmental stages (such as convergent extension and neural tube closure). They discovered that these PCP proteins regulate ciliogenesis by organizing the cytoskeleton at the apical cell surface, thus affecting the orientation of ciliary

microtubules (Park *et al.*, 2006). This data further implicates ciliogenesis as a central prerequisite for Hedgehog signaling and planar cell polarity.

Another class of developmental regulators that have been implicated in signaling from the cilium are the PDGF (Platelet-derived growth factor) family of proteins and receptors. Specifically, the PDGFRα receptor tyrosine kinase has been localized to the cilium, and *in vitro* stimulation of the receptor leads to activation of downstream MAP kinase pathways (Schneider *et al.*, 2005). Furthermore, in mice with mutations in IFT88/Polaris, PDGFRα was localized to the site where cilia would normally have been assembled, but was unable to confer signaling when stimulated by ligand (Schneider *et al.*, 2005). Finally, proteins with well established mitotic functions have been shown to play roles in ciliary assembly, including EB1 (Pederson *et al.*, 2003), a paralog of aurora kinase CALK (Pan *et al.*, 2004), and a MAP kinase (Berman *et al.*, 2003). One simple hypothesis is that signals received from the cilia can maintain cells in a differentiated state, and that loss of cilia or ciliary signaling can be a trigger for re-entry into the cell cycle (Guay-Woodford, 2006; Calvet, 2003). Our discovery that a NIMA-related kinase, Fa2p, is important for ciliary function and cell cycle progression in *Chlamydomonas* provides a direct link between these two processes (Mahjoub *et al.*, 2002).

1.3 Fa2p: A Kinase with Dual Roles

The *FA2* (*F*lagellar *A*utotomy) gene was originally identified from a screen for deflagellation-defective mutants in *Chlamydomonas*, and shown to be defective in Ca^{2+}-induced severing of axonemal microtubules (Finst *et al.*, 1998). *FA2* encodes a 68 kDa protein with high sequence identity (~40%) to members of the NIMA family of expressed kinases (Neks). A phylogenetic analysis of the Nek proteins indicates that this family has

expanded in organisms that have ciliated cells (Figure 1-3). Furthermore, Neks have been shown to play essential roles in cell cycle regulation, assuming overlapping but non-identical roles in the regulation of cell cycle progression (summarized in Table 1-1; also reviewed in O'Connell *et al.*, 2003; Quarmby and Mahjoub, 2005). Motivated by the homology of Fa2p with a family of cell cycle regulatory proteins, we undertook a detailed study of cell cycle progression in *fa2* mutant cells.

The first indication of a cell cycle abnormality occurred when, as an undergraduate student in the Quarmby lab, I noticed that *fa2* cells were larger in size compared to wild-type. This difference was confirmed and quantified in both asynchronous and synchronous populations of cells (Mahjoub *et al.*, 2002). Subsequent analysis of DNA content and cell division rates indicated that *fa2* cells are delayed in transit through at least two points in the cell cycle: (1) the G_2/M transition; and (2) in the assembly of flagella after exit from mitosis. The role of Fa2p at each of these points is non-essential because *fa2* mutant cells transit through the cell cycle, albeit more slowly than wild type cells (Mahjoub *et al.*, 2002). The intriguing combination of ciliary and cell cycle phenotypes of *fa2* mutants lead me to this dissertation research in an effort to dissect the relationship between cilia and cell cycle regulation.

1.4 Research Aims

My first goal was to investigate the spatial and temporal localization of Fa2p. Two other proteins involved in the deflagellation pathway, Fa1p and Katanin, have been localized to the basal body region in *Chlamydomonas* (Finst *et al.*, 2000; Lohret *et al.*, 1999). Similarly, I hypothesized that Fa2p is localized to basal bodies, possibly at the distal end close to the site of flagellar severing. To facilitate detection of the protein I: (1)

generated peptide antibodies against Fa2p; (2) built an epitope-tagged *FA2* construct which was transformed into *fa2* mutants to rescue the deflagellation and cell cycle phenotypes. Using these tools, I first determined the sub-cellular localization of the protein by biochemical fractionation of cells. I refined this localization by immunofluorescence microscopy, starting with interphase cells then following Fa2p localization as cells undergo division. Another important question addressed in this thesis is whether the kinase activity of Fa2p is essential for its role in deflagellation, cell cycle progression, or both.

My next goal was to identify proteins that interact with Fa2p. Using biochemical fractionation methods that have been successfully employed in *Chlamydomonas*, I attempted to purify proteins that bind to, and interact with, Fa2p. In an alternate approach, I conducted a genetic suppressor screen of *fa2* mutants to isolate mutations that rescue the deflagellation defect in those cells. Identification of these genes will shed light on proteins that may regulate, or are regulated by, Fa2p.

Finally, I am interested in identifying a potential mammalian ortholog of Fa2p. Comparison of the amino acid sequence of Fa2p with the 11 Neks expressed in humans and mice does not lead to a well-defined ortholog. This is because most of the homology between the Neks occurs in the N-terminal kinase domain; the C-terminal regions of these proteins are highly divergent (O'Connell *et al.*, 2003; Quarmby and Mahjoub, 2005). Therefore, I investigated the subcellular localization of selected mammalian Neks by immunofluorescence microscopy as a means to identify functional equivalents of Fa2p in mammals. Two interesting candidates are Nek1 and Nek8, mutations in which cause polycystic kidney disease in mice (Upadhya *et al.*, 2000; Liu *et al.*, 2002). Based on the

ciliary hypothesis of PKD, we predicted that Nek1, Nek8 and possibly other Neks localize to cilia or basal bodies.

1.5 Figures

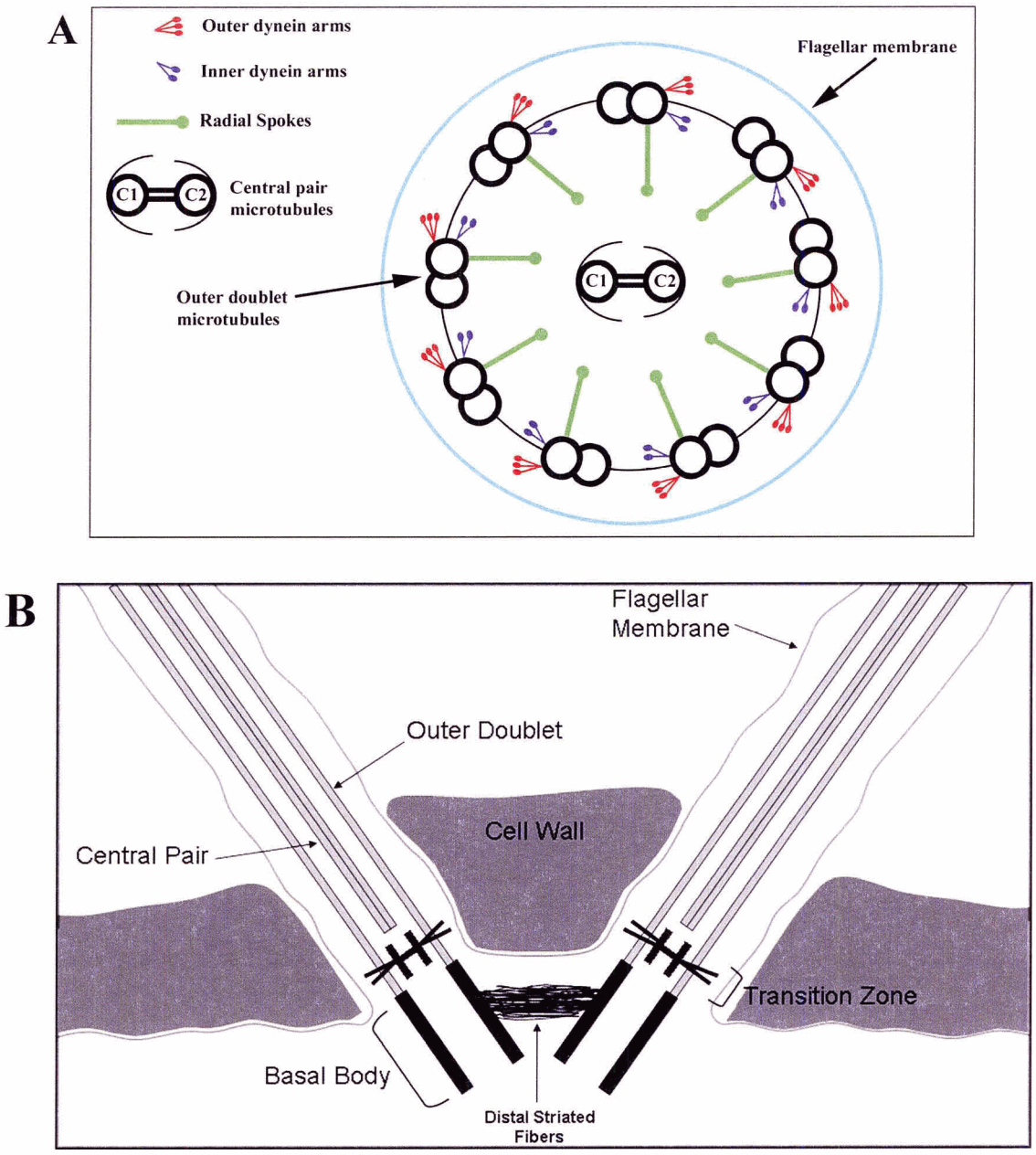

Figure 1-1 Schematic diagrams of flagellar and basal-body structures.
(A) Cross-section through a motile cilium. The 9 outer-doublet microtubules anchor the inner and outer dynein arms, multi-subunit ATPases that generate relative sliding movements between the outer doublet microtubules. The radial spokes and central pair microtubules with their associated projections coordinate the dynein-induced sliding. (B) Schematic of a longitudinal section through the flagella and basal-bodies of *Chlamydomonas*. The nine outer doublet microtubules of the axoneme are nucleated by and continuous with the basal-bodies. The axoneme extends through an electron-dense structure called the flagellar transition zone, located at the distal end of the basal body.

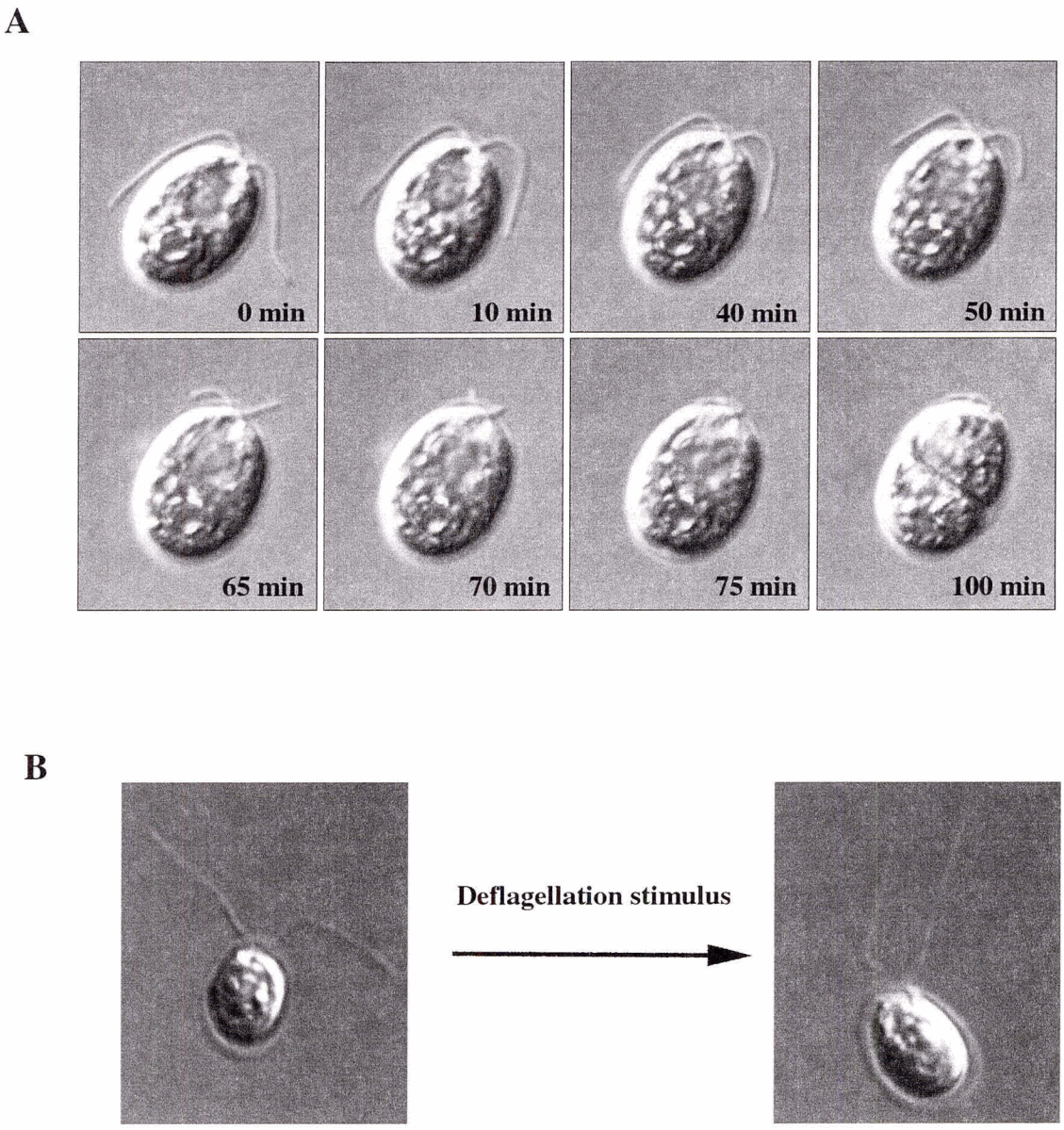

Figure 1-2 Two ways to lose your cilia.
(A) Resorption of cilia prior to cell division. Ciliary components are disassembled at the ciliary tip and retracted into the cell. This is a relatively slow process that takes between 70-90 minutes. (B) Cells can also shed their cilia by a process called deflagellation/deciliation. This involves the precise severing of axonemal microtubules at the base of the cilia in response to various external stimuli (reviewed in Quarmby, 2004). This is a rapid process (<1 sec) which allows cells to quickly shed their cilia.

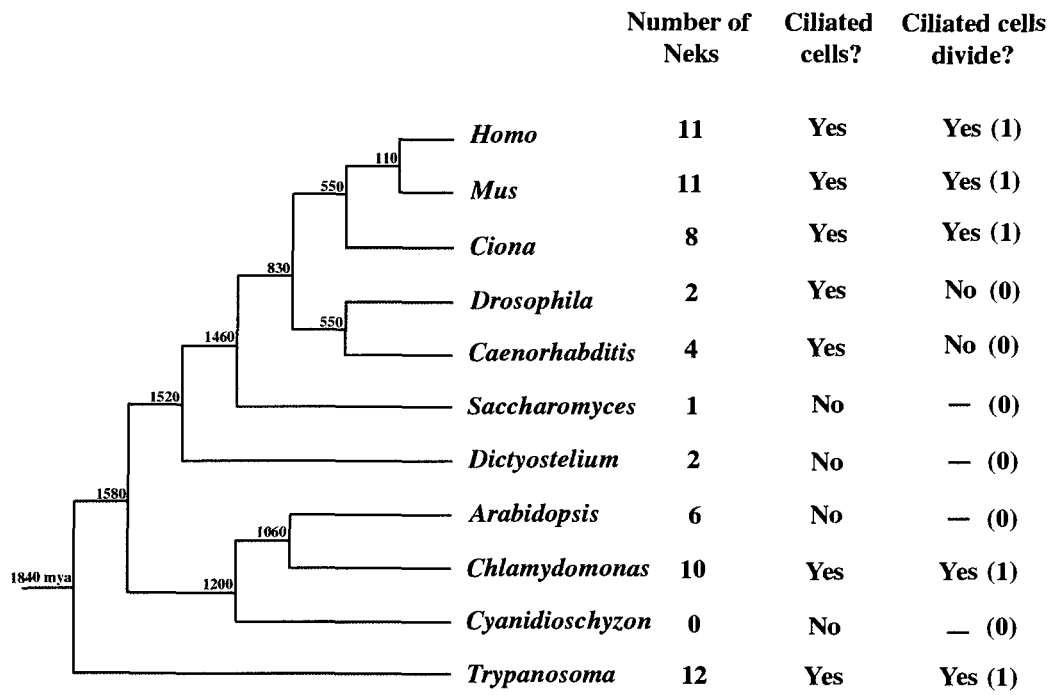

Figure 1-3 Phylogenetic tree of model organisms indicating the number of Neks and the presence or absence of cilia.

NIMA kinase homologs were identified using genome-wide BLAST searches with the *Aspergillus* NIMA protein sequence. Candidate genes were used in reciprocal BLAST searches against the NCBI protein database (http://www.ncbi.nlm. nih.gov/BLAST/) to identify true Nek homologs. The data were codified as follows: '1' was assigned to organisms that possess ciliated cells that re-enter the cell cycle, and '0' was assigned to organisms that do not have ciliated cells that undergo cell division (numbers presented in brackets). The tree is adapted from Quarmby and Mahjoub (2005).

1.6 Tables

Table 1-1 Proposed functions of the mammalian Neks.

Protein	Proposed functions & localizations	References
Nek1	**hNek1**	
	- Interacts with polycystic kidney disease (PKD) proteins	Surpili *et al.*, 2003
	mNek1	
	- Causal mutation in *kat* mouse model of progressive PKD	Upadhya *et al.*, 2000
	- Role in DNA damage response pathway	Polci *et al.*, 2004
	- Role in chromosome condensation	Feige *et al.*, 2006
Nek2	**hNek2**	
	- Localizes to centrosomes and kinetochores.	Fry *et al.*, 1998b
	- Phosphorylates C-Nap1and Nlp at centrosomes	Fry *et al.*, 1998a;
	- Regulates centrosome splitting at G_2/M	Rapley *et al.*, 2005
	- Phosphorylates Hec1 at kinetochores; possible role in spindle checkpoint	Chen *et al.*, 2002
Nek3	**hNek3**	
	- Associates with Vav2; modulates prolactin receptor signalling	Miller *et al.*, 2005
	mNek3	
	- Predominantly localized to cytoplasm; no cell cycle-dependent changes in Nek3 activity detected	Tanaka and Nigg, 1999
Nek4	- No known functions	
Nek5	- No known functions	
Nek6 & Nek7	**hNek6 and hNek7**	
	- Nek6 and 7 bind to C-terminal tail of Nek9. Nek9 phosphorylates and activates Nek6 during mitosis	Belham *et al.*, 2003
	- Inhibition of Nek6 function arrests cells in metaphase and triggers apoptosis.	Yin *et al.*, 2003

Protein	Proposed functions & localizations	References
Nek8	***h*Nek8**	
	- Overexpressed in primary human breast tumors	Bowers and Boylan, 2004
	mNek8	
	- Causal mutation in *jck* mouse model of recessive juvenile cystic kidney disease	Liu *et al.*, 2002
Nek9	***h*Nek9**	
	- Associates with and phosphorylates Bicd2 *in vivo*	Holland *et al.*, 2002
	- Regulates chromosome alignment and segregation in mitosis	Roig *et al.*, 2002
	- Mediates centrosomal and chromosomal microtubule organization	Roig *et al.*, 2005
	- Activates Nek6 during mitosis	Belham *et al.*, 2003;
	- Regulates G_1 and S progression via interaction with FACT complex.	Tan and Lee, 2004
Nek10	- No known functions	
Nek11	**hNek11**	
	- DNA replication/damage stresses-responsive kinases; may play a role in the S-phase checkpoint	Noguchi *et al.*, 2002
	- Colocalized with Nek2A in nucleoli; is activated by Nek2A in G_1/S-arrested cells	Noguchi *et al.*, 2004

Abbreviations: h, human; m, mouse; FACT, "Facilitates Transcription of Chromatin Templates". Adapted and modified from Quarmby and Mahjoub (2005); references are found therein.

1.7 Reference List

Badano J.L., Mitsuma N., Beales P.L., Katsanis N. (2006). The ciliopathies: an emerging class of human genetic disorders. Annu. Rev. Genomics Hum. Genet. 7: 125-148.

Benzing T., Walz G. (2006). Cilium-generated signaling: a cellular GPS? Curr. Opin. Nephr. Hypert. 15: 245-249.

Berman S.A.,Wilson N.F., Haas N.A.,Lefebvre P.A.. (2003). A novel MAP kinase regulates flagellar length in Chlamydomonas. Curr. Biol. 13: 1145-1149.

Bloodgood R.A. (1990). Ciliary and flagellar membranes. New York, Plenum Press. Pp 1-431.

Boletta A., Germino G.G. (2003). Role of polycystins in renal tubulogenesis. Trends Cell Biol. 13: 484.

Calvet, JP (2003). Ciliary signalling goes down the tubes. *Nat. Genet.* 33: 113-114.

Cole, D.G. (2003). The intraflagellar transport machinery of *Chlamydomonas reinhardtii*. *Traffic* 4, 435-442.

Corbit K.C., Aanstad P., Singla V., Norman A.R., Stainier D.Y., Reiter J.F. (2005) Vertebrate Smoothened functions at the primary cilium. *Nature* 437: 1018-1021.

Davis E.E. (2006). The emerging complexity of the vertebrate cilium: new functional roles for an ancient organelle. *Dev Cell* 11: 9-19.

Dutcher S.K. (1995). Flagellar assembly in two hundred and fifty easy-to-follow steps. *Trends Genet* 10:398-404.

Ehler, L.L., Holmes, J.A., Dutcher, S.K. (1995). Loss of spatial control of the mitotic spindle apparatus in a *Chlamydomonas reinhardtii* mutant strain lacking basal bodies. *Genetics* 141, 945-960.

Eley L., Yates L.M., Goodship J.A. (2005). Cilia and disease. *Curr. Opin. Gen. Dev.* 15: 308-314.

Finst R.J., Kim P.J., Quarmby L.M. (1998) Genetics of the deflagellation pathway in *Chlamydomonas reinhardtii. Genetics* 149, 927-936.

Finst, R.J., Kim P.J, Griffis E., Quarmby L.M. (2000). Fa1p is a 171 kDa protein essential for axonemal microtubule severing in *Chlamydomonas. J. Cell Science* 113: 1963-1971.

Fisher E., Legue E., Doyen A., Nato F., Nicolas J.F., Torres V., Yaniv M., Pontoglio M. (2006). Defective planar cell polarity in polycystic kidney disease. *Nat. Genet.* 38: 21-23.

Guay-Woodford L.M. (2006). Renal cystic kidneys: diverse phenotypes converge on the cilium/centrosome complex. *Pediatr. Nephrol.* Epub.

Hanaoka K., Qian F., Boletta A., Bhunia A.K., Piontek K., Tsiokas L., Sukhatme V.P., Guggino W.B., Germino G.G. (2000). Co-assembly of polycystin-1 and polycystin-2 produces unique cation-permeable currents. *Nature* 408: 990-994.

Huangfu D., Liu A., Rakeman A.S., Murcia N.S., Niswander L., Anderson K.V. (2003). Hedgehog signalling in the mouse requires intraflagellar transport proteins. *Nature* 426: 83-87.

Huangfu D., Liu A., Rakeman A.S., Murcia N.S., Niswander L., Anderson K.V. (2003). Hedgehog signaling in the mouse requires intraflagellar transport proteins. *Nature* 426: 83-87

Johnson K.A., Rosenbaum J.L. (1992). Polarity of flagellar assembly in *Chlamydomonas. J. Cell Biol.* 119: 1605-1611.

Kozminski K.G., Johnson K.A., Forscher P., Rosenbaum J.L. (1993). A motility in the eukaryotic flagellum unrelated to flagellar beating. *Proc Natl Acad Sci U S A* 90, 5519-5523.

Liu S., W. Lu T. Obara S. Kuida J. Lehoczky K. Dewar I.A. Drummond I. A., Beier D.R. (2002). A defect in a novel Nek-family kinase causes cystic kidney disease in the mouse and in zebrafish. *Development* 129: 5839-5846.

Logan C.Y., Nusse R. (2004). The Wnt signaling pathway in development and disease. Annu. Rev. Cell Dev. Biol. 20: 781-810.

Lohret T.A., Zhao L., Quarmby L.M. (1999). Cloning of *Chlamydomonas* p60 katanin and localization to the site of outer doublet severing during deflagellation. *Cell Motil Cytoskeleton* 43, 221-231.

Low S.H., Vasanth S., Larson C.H., Mukherjee S., Sharma N., Kinter M.T., Kane M.E., Obara T., Weimbs T. (2006). Polycystin-1, STAT6, and P100 function in a pathway that transduces ciliary mechanosensation and is activated in polycystic kidney disease. *Dev. Cell* 10: 57-69.

Mahjoub M.R., Montpetit B., Zhao L., Finst R.J., Goh B., Kim A.C., Quarmby, L.M. (2002). The FA2 gene of Chlamydomonas encodes a NIMA family kinase with roles in cell cycle progression and microtubule severing during deflagellation. J *Cell Sci* 115, 1759-1768.

Mitchell, D.R. (2004). Speculations on the evolution of 9+2 organelles and the role of central pair microtubules. *Biol Cell* 96, 691-696.

O'Connell M.J., Krien M.J.E., Hunter T. (2003). Never say never. The NIMA-related protein kinases in mitotic control. *Trends Cell Biol* 13: 221–228

Pan, J., Wang, Q., Snell, W.J. (2005). Cilium-generated signaling and cilia-related disorders. *Laboratory Investigation* 1-12

Pan, J., Wang, Q., Snell, W.J. (2004). An aurora kinase is essential for flagellar disassembly in Chlamydomonas. *Dev Cell* 6, 445-451.

Park T.J., Haigo S.L., Wallingford J.B. (2006). Ciliogenesis defects in embryos lacking inturned or fuzzy function are associated with failure of planar cell polarity and Hedgehog signaling. *Nat. Genet.* 38: 303-311.

Parker, J.D., Quarmby, L.M. (2003). *Chlamydomonas fla* mutants reveal a link between deflagellation and intraflagellar transport. *BMC Cell Biol* 4, 11.

Pazour, G.J., Witman, G.B. (2003). The vertebrate primary cilium is a sensory organelle. *Curr Opin Cell Biol* 15, 105-110.

Pedersen, L.B., Geimer S., Sloboda R.D., Rosenbaum J.L. (2003). The microtubule plus end-tracking protein EB1 is localized to the flagellar tip and basal bodies in *Chlamydomonas reinhardtii. Curr. Biol.* 13: 1969-1974.

Praetorius, HA and KR Spring. 2001. Bending the MDCK cell primary cilium increases intracellular calcium. *J. Membr. Biol.* 184: 71-79

Quarmby, L.M. (2004). Cellular deflagellation. *Int Rev Cytol* 233, 47-91.

Quarmby L.M., Mahjoub M.R. (2005) Caught Nek-ing: Cilia and centrioles. *J Cell Sci* 118: 5161-5169.

Schneider L., Clement C.A., Telmann S.C., Pazour G.J., Hoffmann E.K., Satir P., Christensen S.T. (2005). PDGFRα signaling is regulated through the primary cilium in fibroblasts. *Curr. Biol.* 15: 1861-1866.

Silflow C.D., Lefebvre P.A. (2001). Assembly and motility of eukaryotic cilia and flagella. Lessons from *Chlamydomonas reinhardtii. Plant Physiol.* 127: 1500-1507.

Simons M., Gloy J., Ganner A., Bullerkote A., Bashkurov M., Kronig C., Schermer B., Benzing T., Cabello O.A., Jenny A., Mlodzik M., Polok B., Dreiver W., Obara T., Walz G. (2005). Inversin, the gene product mutated in nephronophthisis type II, functions as a molecular switch between Wnt signaling pathways. *Nat. Genet.* 37: 537-543.

Upadhya P., Birkenmeier E.H., Birkenmeier C.S., Barker J.E. (2000). Mutations in a NIMA-related kinase gene, *Nek1*, cause pleiotropic effects including a progressive polycystic kidney disease in mice. *Proc. Nat. Acad. Sci. (U.S.A.)* 97: 217-221.

Veeman M.T., Axelrod J.D., Moon R.T. (2003). A second canon. Functions and mechanism of β-catenin-independent Wnt signaling. *Dev. Cell* 5: 367-377.

Wheatley, D.N., Wang, A.M., Strugnell, G.E. (1996). Expression of primary cilia in mammalian cells. *Cell Biol Int* 20, 73-81.

Wilson P.D. (2004). Mechanisms of disease: Polycystic kidney disease. *N. Engl. J. Med.* 350: 151.

Yoder B.K. (2006). More than just postal service: Novel roles for IFT proteins in signal transduction. *Dev. Cell* 10: 541-542.

CHAPTER 2:

A NIMA-related Kinase, Fa2p, Localizes to a Novel Site in the Proximal Cilia of *Chlamydomonas* and Mouse Kidney Cells

The following chapter has been published in Molecular Biology of the Cell (2004), Vol 15, 5172-5186. The authors of the paper were as follows:

Moe R. Mahjoub, M. Qasim Rasi, and Lynne M. Quarmby

Department of Molecular Biology and Biochemistry, Simon Fraser University, Burnaby, British Columbia, Canada V5A 1S6

As the first author, I conducted all of the experiments and interpreted the results presented in this study. I also contributed to the preparation of the manuscript. M.Q. Rasi conducted the RT-PCR experiments to clone the *FA2* cDNA. L.M. Quarmby was heavily involved in the conception and design of experiments, analysis of data, as well as the writing of the manuscript.

2.1 Abstract

Polycystic kidney disease and related syndromes involve dysregulation of cell proliferation in conjunction with ciliary defects. The relationship between cilia and cell cycle is enigmatic, but it may involve regulation by the NIMA-family of kinases (Neks). We previously showed that the Nek Fa2p is important for ciliary function and cell cycle in *Chlamydomonas*. We now show that Fa2p localizes to an important regulatory site at the proximal end of cilia in both *Chlamydomonas* and a mouse kidney cell line. Fa2p is also associated with the proximal end of centrioles. Its localization is dynamic during the

cell cycle, following a similar pattern in both cell types. The cell cycle function of Fa2p is kinase independent, whereas its ciliary function is kinase dependent. Mice with mutations in Nek1 or Nek8 have cystic kidneys; therefore, our discovery that a member of this phylogenetic group of Nek proteins is localized to the same sites in *Chlamydomonas* and kidney epithelial cells suggests that Neks play conserved roles in the coordination of cilia and cell cycle progression.

2.2 Introduction

The Nek family of kinases is defined by sequence similarity to NIMA, the *Aspergillus* kinase that is essential for entry into mitosis (reviewed by Morris and Enos, 1992; O'Connell *et al.*, 2003). Fungi and higher plants encode only one or a few members of this family (Kambouris *et al.*, 1993; Pu *et al.*, 1995; Krien *et al.*, 1998; Wang *et al.*, 2003), but in organisms with centrioles and cilia, such as humans and *Chlamydomonas*, the family is expanded to 10 or more members (O'Connell *et al.*, 2003; Bradley *et al.*, 2004; Bradley and Quarmby, unpublished data), some of which affect ciliary length (Wloga et al., 2006). We recently reported that the *Chlamydomonas* Nek Fa2p participates in ciliary function and cell cycle progression (Mahjoub *et al.*, 2002).

An emerging pattern suggests that a variety of human syndromes are related to defects in the assembly, maintenance, or function of cilia (Ong and Wheatley, 2003; Pazour and Witman, 2003; Li *et al.*, 2004; Sun *et al.*, 2004). Ciliopathies, including polycystic kidney disease, Bardet-Beidl syndrome, and nephronophthisis include kidney cyst formation as an important component of a pleiotropic syndrome (Mykytyn and Sheffield, 2004; Wilson, 2004). This important consequence of these diseases arises, in part, from dysregulation of cell proliferation in conjunction with ciliary dysfunction. Of

particular relevance to the current study are reports that mutations in vertebrate Nek1 and Nek8 cause cystic kidneys in mice and zebrafish (Upadhya *et al.*, 2000; Liu *et al.*, 2002).

The relationship between cilia and cell cycle progression is poorly understood. In many cells, entry into the cell cycle is preceded by ciliary disassembly, and exit from mitosis is accompanied by ciliary assembly, a relationship that may reflect the use of the basal bodies/centrioles as mitotic spindle poles (Tucker and Pardee, 1979; Ehler *et al.*, 1995; Wheatley *et al.*, 1996). Consistent with this idea, signaling pathways important for growth or differentiation have been reported to localize to cilia (Huangfu *et al.*, 2003; Pazour and Witman, 2003) and some *Chlamydomonas* mutants defective in ciliary assembly have cell cycle progression phenotypes (Mahjoub *et al.*, 2002; Parker and Quarmby, unpublished data). In addition, members of protein families known for their mitotic functions have been found to play roles in ciliary assembly, including EB1 (Pedersen *et al.*, 2003); a distant paralog of aurora kinase, CALK (Pan *et al.*, 2004); and a mitogen-activated protein kinase (Berman *et al.*, 2003). The simplest hypothesis is that cells can be maintained in a differentiated state by signals received from their cilia and that loss of cilia or ciliary signaling can be a trigger for re-entry into the cell cycle. This is likely to be a reciprocal relationship in which signals from the cell body stimulate ciliary loss in anticipation of cell division and ciliary re-growth upon exit from mitosis. The Nek proteins may play roles in this reciprocal signaling.

Fa2p was originally identified from a screen for deflagellation-defective mutants in *Chlamydomonas reinhardtii* and shown to be defective in calcium-induced severing of the axonemal microtubules (Finst *et al.*, 1998). We noticed that *fa2* cells are larger than wild-type and went on to show that this is due to a delay at the G_2/M transition (Mahjoub

et al., 2002). The preponderance of Nek family members in organisms with cilia, and the intriguing combination of ciliary and cell cycle phenotypes of *fa2* mutants, lead us to pursue this protein in our efforts to dissect the enigmatic relationship between cilia and the cell cycle.

Here, we report that Fa2p localizes to a specific site at the proximal end of the cilia, in both *Chlamydomonas* and cultured kidney epithelial cells. When cells enter the cell cycle, Fa2p accumulates at the base of the basal bodies/centrioles. It remains associated with the spindle poles throughout the cell cycle and moves to the cilia when they begin to regenerate after deciliation or exit from the cell cycle. Importantly, Fa2p kinase activity is required for deflagellation, but not for localization and efficient cell cycle progression.

2.3 Materials and Methods

2.3.1 Cell Strains and Culture

Chlamydomonas strains B214 and G1 (obtained from G. Pazour, University of Massachusetts, Amherst, MA) and strains cc620 and cc621 (obtained from the *Chlamydomonas* Genetics Center, Durham, NC) were used as the wild-type strains. Mutant strains *fa2-1*, *fa2-2*, *fa2-3*, and *fa2-4* were isolated in our laboratory as described previously (Finst *et al.*, 1998). Cells were maintained in liquid TAP medium or on plates containing 1.5% agar (Harris, 1989) at 22°C with constant illumination. All *ble* transformants were grown on 1.5% TAP plates supplemented with Zeocin (30 μg/ml; Invitrogen, Carlsbad, CA). All chemicals were purchased from Sigma-Aldrich (St. Louis, MO) unless otherwise indicated.

2.3.2 Epitope Tagging and *Chlamydomonas* Transformations

The 4.6-kb wild-type genomic construct pFA2 (*Sac*I-*Sal*I) (Mahjoub *et al.*, 2002) was engineered to contain three copies of the hemagglutinin (HA) epitope in the carboxy terminus of the predicted product. The FA2 (*Sac*I-*Sal*I) plasmid was linearized at a unique *Nru*I site at base position 3108 in the second to last exon. Next, the p3XHA (a plasmid encoding 3 repeats of the 9-amino acid hemagglutinin epitope; Finst *et al.*, 2000) was digested with *Sma*I and *Nae*I to excise the 3XHA cassette. The *Sma*I-*Nae*I fragment was blunt-end ligated into the *Nru*I-linearized FA2 construct to produce plasmid pFA2HA (3108), which encodes a Fa2p-HA chimera with the HA tag following directly after amino acid 536. To introduce the selectable marker *ble* into this construct, plasmid pSP124S (kindly provided by Saul Purton, University College London, United Kingdom; England; Lumbreras *et al.*, 1998) was digested with *Hind*III to release the gene cassette. This cassette was subsequently ligated into the p3XHAFA2(3108) after digestion at a unique *Hind*III site upstream of the 5'UTR, to produce the final plasmid pble-FA2HA (3108).

Nuclear transformation was performed as described previously (Finst *et al.*, 1998). Transformants were selected on 1.5% TAP medium plates supplemented with Zeocin and assayed for deflagellation as described previously (Finst *et al.*, 1998).

2.3.3 Antibodies and Immunoblot Analysis

Based on the predicted Fa2p amino acid sequence, peptides 364–380 (QIPYLPHQRPGSGRSPG) and 562–575 (YQAPQYGRRRNPE) were synthesized, conjugated to keyhole limpet hemocyanin and used as antigens to raise rabbit polyclonal antibodies (Sigma Genosys, The Woodlands, TX). Polyclonal antiserum from one

positively reactive rabbit (10495, immunized by peptide 562-575) was affinity purified using a peptide column per manufacturer's instructions (UltraLink biosupport medium; Pierce Chemical, Rockford, IL) to produce anti-Fa2p-10495, used in these experiments as anti-Fa2p.

For immunoblot analysis, whole cell lysate from wild type, a series of mutant cells carrying various *fa2* alleles, *fa2*-1; *FA2* (*fa2*-1 cells transformed with the wild-type *FA2* genomic clone), and *fa2*-1; *FA2*-HA strains (*fa2*-1 cells transformed with the FA2-HA construct) were used. Protein concentration was determined using the Advanced Protein Assay (Cytoskeleton, Denver, CO). Whole cell extract (30 μg) was separated by SDS-PAGE (10%) and electroblotted to supported nitrocellulose (Bio-Rad, Hercules, CA). To confirm efficient transfer of protein samples, membranes were stained with Ponceau S (Allied Chemicals, Morristown, NJ) and then washed with 0.05% Tween 20 in Tris-buffered saline/Tween (TBST). The membrane was blocked in 5% skim milk in TBST for 1 h at room temperature, and then incubated overnight at 4°C with affinity-purified anti-Fa2p-10495 (1:250). The membrane was washed with TBST and incubated with horseradish peroxidase-linked donkey anti-rabbit IgG (1:10,000; Amersham Biosciences, Baie d'Urfe', Québec, Canada) at room temperature with rocking for 1 h. For detection of Fa2p-HA, the membrane was incubated overnight with rat monoclonal anti-HA (1:1000; clone 3F10; Roche Diagnostics, Berkeley, CA), washed with TBST, and then incubated with horseradish peroxidase-linked goat anti-rat IgG (1:2500; Amersham Biosciences). For loading control, blots were stripped using the ReBlot Plus kit (Chemicon International; Temecula, CA), and then probed with mouse monoclonal anti-α-tubulin (1:10,000; clone B-5-1-2; Sigma-Aldrich). After washes with TBST, blots

were incubated with horseradish peroxidase-linked horse anti-mouse IgG (1:10,000; Vector Laboratories, Burlingame, CA). Immunoreactive proteins were visualized using the ECL chemiluminescent detection system (Amersham Biosciences).

2.3.4 Subcellular Fractionation

Deflagellation was induced by dibucaine, and cell bodies, flagella, axonemes, and membrane plus matrix fractions were isolated as described previously (Witman, 1986). We substituted 1% IGEPAL CA 630 (Sigma-Aldrich) for 0.5% NP-40. Cell equivalents of each fraction were used for immunoblot analysis.

2.3.5 Indirect Immunofluorescence Imaging of *Chlamydomonas* Cells

For indirect immunofluorescence, *fa2* mutants and *fa2*-1; *FA2*-HA strains were harvested from suspension by centrifugation and treated with gametic lytic enzyme to remove their cell walls (Saito and Matsuda, 1991). The cells were pelleted by centrifugation and resuspended in MT buffer (30 mM Tris-acetate, pH 7.3, 5 mM MgSO4, 5 mM EDTA, 25 mM KCl, 1 mM dithiothreitol), and then affixed to coverslips coated with 0.1% polyethylenimine. Cells were fixed in 100% ice-cold methanol at -20°C for 20 min, rehydrated by three 5-min washes in phosphate-buffered saline (PBS), and blocked with 3% bovine serum albumin in PBS for 1 h. The coverslips with fixed cells were incubated overnight at 4°C with rat monoclonal anti-HA (diluted 50-fold), together with the mouse monoclonal anti-α-tubulin (diluted 500-fold) and a mouse monoclonal anti-centrin (clone 20H5, diluted 400-fold; generously provided by J. Salisbury, Mayo Clinic, Rochester, MN). The next day, coverslips were rinsed three times in PBS and then incubated for 1 h with the appropriate secondary antibody, depending on the experiment:

Texas Red- or -Alexa Fluor 488-conjugated goat anti-rat IgG (for Fa2p-HA), Alexa Fluor 350- or 488-conjugated goat anti-mouse IgG (for centrin), and Alexa Fluor 488, 568, or CY-5–conjugated goat anti-mouse IgG (for α-tubulin). All secondary antibodies were purchased from Molecular Probes (Eugene, OR) and diluted 200-fold in PBS before use. The cells were rinsed in PBS and mounted in an antifade medium containing 0.1 mg/ml Mowiol (Calbiochem, San Diego, CA), 50% glycerol, and 100 mM Tris, pH 8.5.

To visualize cells immediately after deflagellation, live cultures of a *fa2*-1; *FA2*-HA strain were affixed to coverslips coated with 0.1% polyethylenimine for 1 min. Deflagellation was induced by addition of a drop of 25 mM dibucaine, and samples were immediately fixed with ice-cold methanol. To study localization of Fa2p-HA during flagellar regeneration, cells were deflagellated by pH shock as described previously (Finst *et al.*, 1998). Cells were pelleted, resuspended in TAP medium and allowed to regenerate their flagella. Samples were taken at 5, 30, 60, and 90 min post-deflagellation. Cells were fixed, processed, and stained as described above.

A series of digital optical sections of the fixed samples were obtained using an Olympus IX70 epifluorescence inverted microscope in a DeltaVision imaging station (Applied Precision, Issaquah, WA). The system is fitted with a computer-controlled stage with Nanomotion micropositioning technology with a stepping motor (0.2-μm step size), 100X (1.35 numerical aperture) Olympus objective and fluorescein, rhodamine, 4,6-diamidino-2-phenylindole (DAPI), and CY-5 filter set. Stacks of digital images were acquired with a cooled charge-coupled device camera (Roper Scientific, Tucson, AZ). Out of-focus fluorescence and restoration of optical Z-sections was achieved by deconvolution by using the constrained iterative algorithm and point spread functions

supplied with the DeltaVision system. Three-dimensional reconstructions were produced by stacking a set of deconvolved sections and projecting them around the *x*- or *y*-axis.

Differential interference contrast optics were used for cell size measurements, as described previously (Mahjoub *et al.*, 2002). Cells were fixed with 2% glutaraldehyde in culture medium and measured using software provided with the Delta Vision system (Applied Precision).

2.3.6 Cell Synchrony and Mating

Synchronization of cells was carried out as described by Umen and Goodenough (2001) with modification. Cultures were grown in M-medium (Harris, 1989) at 25°C with shaking. Flasks were bubbled with 5% CO2 and grown asynchronously to a density of 5 X 10^6 cells/ml in the light, and then placed in the dark at 1 X 10^6 cells/ml for 24 h. Cultures were then moved back to the light, and aliquots were sampled over the next 24 h. Cells were fixed, processed, and stained as described above.

For zygotic resorption experiments, vegetative wild-type and *fa2*-1; *FA2*-HA strains were pelleted and resuspended in medium lacking nitrogen (M-N is M medium, Harris, 1989, excluding NH_4NO_3) for 16 h to induce gametogenesis. The resulting gametes were mixed together and allowed to form quadraflagellate cells (QFCs). Samples were taken at 30-min intervals over the next 4 h. Cells were fixed, processed, and stained as described above.

For mitotic index experiments, we examined 300 fixed cells (from each sample) microscopically for cleavage furrows to determine the fraction of cells that had entered M

phase. In *Chlamydomonas*, incipient cleavage furrows form at preprophase and are visible throughout mitosis and cytokinesis (Kirk, 1998).

2.3.7 Construction of Kinase-dead Fa2p

The QuikChange site-directed mutagenesis kit (Stratagene, La Jolla, CA) was used to introduce an A-to-G change at base position 137 (from the start codon). The resulting translated product substitutes the invariant lysine (aa 46 in Fa2p) of the ATP-binding loop to arginine. The plasmid pFA2 (*Sac*I-*Sal*I) was used as template, and site-directed mutagenesis was performed following manufacturer's instructions, to produce pFA2-K46R. To introduce this change in the FA2 construct containing the HA-tag and *ble* marker, a *Bam*HI-*Pml*I cassette (containing the A-to-G change) was excised and substituted into pble-FA2HA (3108) digested with *Bam*HI-*Pml*I, to produce the final vector pble-FA2HA-K46R. Integrity of the final construct was confirmed by DNA sequencing (DNA sequencing laboratory, University of British Columbia). The construct was transformed into *fa2* mutants, and transformants were analyzed as described above.

2.3.8 Fa2p Expression in Mammalian Cells

To express green fluorescent protein (GFP)-tagged Fa2p in mouse kidney collecting duct epithelial cells (murine inner medullary collecting duct cells; mIMCD-3), *FA2* cDNA was isolated using methods described by Finst *et al.* (2000). Primers were used to introduce an *Eco*RI (5') and *Sal*I (3') sites in the *FA2* cDNA, which was subsequently cloned into the pEGFP-C2 vector (BD Biosciences Clontech, Palo Alto, CA) digested with *Eco*RI-*Sal*I, to give vector pEGFP-FA2. The resulting product is an EGFP-Fa2p chimeric protein. IMCD-3 cells were maintained in 1:1 mixture of DMEM

(Invitrogen) and Ham's F-12 medium (Invitrogen), supplemented with 10% fetal bovine serum (FBS), at 37°C in the presence of 5% CO_2. Cells were cultured to 70–80% confluence and transfected with either pEGFP or pEGFP-FA2 by using the Polyfect transfection reagent per manufacturer's instruction (QIAGEN, Valencia, CA). Cells were collected 24 h after transfection, resuspended in 1X SDS sample buffer, and analyzed by immunoblot with anti-GFP (1:2000; Roche Diagnostics) as described above. Alternatively, cells were grown on coverslips, transfected as described above, and then fixed in -20°C methanol for 10 min, rehydrated in PBS, and blocked with 5% BSA in PBS. Samples were incubated 1 h with mouse monoclonal anti-acetylated tubulin (Sigma, clone 6–11B-1, diluted 10,000-fold) and mouse monoclonal anti-gamma tubulin (clone GTU-88, diluted 1000-fold; Sigma-Aldrich). After washing with PBS, cells were incubated for 1 h with Alexa Fluor 568-conjugated rabbit anti-mouse IgG (diluted 200-fold), and then rinsed in PBS. Nuclei were stained by incubating with DAPI for 10 min. Coverslips were mounted in Prolong antifade reagent (Molecular Probes), and immunofluorescence microscopy was performed as described above.

2.4 Results

2.4.1 Epitope Tagging, Transformation Rescue, and Antibody Characterization

To determine the spatial and temporal localization of Fa2p, we undertook two approaches. First, we inserted an HA epitope tag near the carboxy terminus of the predicted Fa2p product (Figure 2-1A). The construct also carried the antibiotic resistance gene *ble*, allowing selection of transformants on Zeocin plates. *fa2-1* mutants were transformed with this construct and assayed for deflagellation phenotype by pH shock and for Fa2p-HA expression by immunoblot. Of the transformants, ~30% (n = 65)

expressed the expected 73- kDa fusion protein (Figure 2-1B). All of the colonies expressing the fusion protein showed rescue of the deflagellation defect (Figure 2-1B).

We also raised antibodies against Fa2p peptides. Based on the Fa2p amino acid sequence, peptides 364–380 (in the middle region) and 562–575 (near the extreme C terminus) were used as antigens. Polyclonal antibodies against Fa2p were affinity purified from one positively reactive rabbit injected with peptide 562–575. The affinity purified anti- Fa2p recognizes a single protein of expected size on immunoblots of wild-type cells (Figure 2-1C). As expected, this band is not detected in any of four *fa2* mutant strains (Mahjoub *et al.*, 2002), but is present in *fa2-1* cells that were transformed with the *FA2* gene. Additionally, the antibody recognizes the HA-tagged Fa2 protein (Figure 2-1C).

2.4.2 Subcellular Localization of Fa2p

Given that *fa2* mutants have defects in deflagellation and in cell cycle progression (Mahjoub *et al.*, 2002), it was of interest to determine whether Fa2p was associated with the flagella or the cell body. Wild-type cells were deflagellated by treatment with 5 mM dibucaine (Witman, 1986) and cell-equivalent equivalent amounts of whole cell, cell bodies, and flagella were analyzed by immunoblot. Fa2p is detected in the flagellar fraction but not cell bodies of wild-type cells (Figure 2-2A, left). The same result was obtained in cell fractions of the *fa2-1*; FA2-HA strains (Figure 2-2A, right). Flagella were further fractionated by detergent extraction to yield a membrane plus matrix fraction and an axonemal fraction. Western analysis showed that Fa2p is an axonemal protein (Figure 2-2B).

2.4.3 Fa2p Localizes to a Unique Site at the Proximal End of Flagella

We next performed indirect immunofluorescence to refine the localization of Fa2p in the axoneme. Repeated attempts at immunofluorescence with the anti-Fa2p antibodies were unsuccessful, so we used the *fa2*-1; *FA2*-HA strains for the following localization experiments. We are confident that the Fa2p-HA localization with anti-HA antibody accurately reflects the localization of endogenous Fa2p because 1) Fa2p-HA is expressed at levels below or comparable with endogenous Fa2p (Figure 2-1C), 2) Fa2p-HA rescued the deflagellation defect of *fa2* cells (Figure 2-1B), and 3) the subcellular fractionation of Fa2p-HA was indistinguishable from Fa2p (Figure 2-2).

Indirect immunofluorescence staining of *fa2*-1; *FA2*-HA cells with anti-HA reveals two distinct sites of localization of Fa2p-HA. All of the ~1000 cells examined showed staining near the base of each flagellum (Figure 2-3A, top). In addition, some of the cells reveal a signal in the basal body region (Figure 2-3). Centrin is known to localize with the distal striated fibers that connect the two basal bodies, as well as to form the nucleus-basal body connectors (Salisbury *et al.*, 1988; Sanders and Salisbury, 1989). Based on comparison with the centrin signal, the distinct Fa2p-HA flagellar signals occur above the distal striated fiber, near the transition zone region at the proximal end of the flagella (Figure 2-3). We refer to this protein as axonemal-Fa2p (ax-Fa2p). The basal body-associated signal is clearly below the distal striated fibers, in the region where the proximal ends of the two basal bodies are in juxtaposition (Figure 2-3). We refer to this subset of the total Fa2p-HA as basal body associated-Fa2p (bb-Fa2p). In a population of asynchronously growing cells, bb-Fa2p comprises a small fraction of total Fa2p, as indicated by the immunoblots (Figure 2-2).

Deflagellation is a consequence of calcium-induced severing of axonemal microtubules at the distal end of the transition zone, near the base of the flagella (reviewed in Quarmby, 2004). Our biochemical fractionation (Figure 2-2) indicated that the ax-Fa2p was located on the axonemal side of this site. To confirm this, live *fa2*-1; *FA2*-HA cells were allowed to adhere briefly to coverslips, deflagellated with dibucaine (~2 sec), and fixed immediately. Due to the briefness of the deflagellation treatment, not all cells shed both flagella. In cells that did not shed their flagella, Fa2p-HA was observed at the base of the flagella as described above (Figure 2-4, left column). In cases where a cell had shed one flagellum, the Fa2p-HA signal remained with the corresponding severed flagellum and was localized to the proximal tip (Figure 2-4, middle column). Note that no Fa2p-HA signal from the severed flagellum was retained by the cell body, indicating that ax-Fa2p is distal to the transition zone. Similarly, when both flagella were shed, Fa2p-HA was detected at the proximal ends of each (Figure 2-4, right column). In the ~800 cells that were examined, every shed flagellum had a signal at the proximal end, and no ax-Fa2p-HA signal was retained by the cell body. The localization of axonemal Fa2p exclusively to the proximal end of the axoneme, and distal to the transition zone microtubule severing region, defines a novel region of the axoneme. Although other axonemal proteins have been found in this region, for example, a minor fraction of epsilon-tubulin (Dutcher *et al.*, 2002), Fa2p is the only protein identified so far whose axonemal localization is specific to a site entirely distal to the transition region.

2.4.4 Distribution of Fa2p between the Proximal Axoneme and the Basal Body Correlates with Flagellar Resorption and Regeneration

Chlamydomonas cells are flagellated during interphase; they resorb their flagella before entering mitosis, and grow new flagella at the onset of G_1 (Johnson and Porter, 1968; Cavalier- Smith, 1974). We hypothesized that the subset of cells with bb-Fa2p-HA were cells either entering or exiting mitosis. It is well established that axonemal components are transported into and out of the axoneme by IFT particles and motors and that basal bodies are the docking site for IFT particles and cargo (reviewed by Rosenbaum and Witman, 2002). Consequently, cells with a strong bb-Fa2p signal might be in the process of resorbing or regenerating their flagella. To test this idea, we synchronized the growth of *fa2*-1; *FA2*-HA cells as described previously (Mahjoub *et al.*, 2002) and harvested cells when they were resorbing their flagella before mitosis. As predicted, we observed an increase in the bb-Fa2p signal in cells that were resorbing their flagella (Figure 2-5A).

We also examined zygotic resorption of flagella. Biflagellate gametes of opposite mating types (+ and -) will fuse and form a temporary QFC or zygote, which will eventually undergo meiosis, producing four haploid cells. Flagellar resorption begins 2–4 h after QFC formation and occurs simultaneously in many cells (Cavalier-Smith, 1974). We mated *fa2*-1; *FA2*-HA and wild-type gametes and allowed 30min for QFC formation. The wild-type strain does not express an HA epitope and thus acts as an internal control. Within a few minutes of QFC formation, ax-Fa2p signals are observed on only two flagella, presumably the ones derived from the Fa2p-HA expressing gamete (Figure 2-5B, 8.4 μm). As the flagella shorten, there is an increase in bb-Fa2p levels, similar to what was observed during pre-mitotic flagellar resorption (Figure 2-5A). Interestingly,

the basal bodies from the wild-type cell also begin to show a Fa2p-HA signal as the flagella shorten (Figure 2-5B, 1.5 and 0.5 μm).

To study changes in Fa2p-HA localization during flagellar regeneration, we deflagellated *fa2*-1; *FA2*-HA cells by pH shock and harvested cells at various stages of flagellar assembly. At 5 min post deflagellation, a robust bb-Fa2p-HA signal is observed, along with faint staining of ax-Fa2p-HA (Figure 2-5C). As the flagella grow, the intensity of the ax-Fa2p-HA signal increases, whereas the bb-Fa2p-HA signal diminishes (Figure 2-5C). Finally, by 90 min when the flagella have attained full length, no bb-Fa2p signal is observed (Figure 2-5C). These observations suggest that newly synthesized Fa2p is targeted to basal bodies and is deposited at the severing site as soon as the flagella grow past the transition zone.

2.4.5 Fa2p-HA Localization during Mitosis

We have previously reported that *fa2* cells delay at the G_2/M transition of the cell cycle (Mahjoub *et al.*, 2002). It was, therefore, of interest to determine Fa2p localization during mitosis. *fa2*-1; *FA2*-HA cells were synchronized for growth, harvested during mitosis, and stained for Fa2p-HA. The cells also were stained for centrin and α-tubulin to identify the position of the basal bodies and microtubular structures, respectively. During prophase (an incipient cleavage furrow is visible at this stage; Kirk, 1998), the flagella have completely resorbed, the basal bodies have duplicated and are slightly separated at the anterior end of the cell (Figure 2-6, prophase). Note the colocalization of Fa2p-HA with each of the basal body spots. As cells progress through metaphase/anaphase, the basal bodies separate further and begin to serve as spindle pole microtubule organizing centers (Silflow and Lefebvre, 2001). In these cells, the Fa2p-HA signal is more diffuse

and is associated with the proximal regions of the mitotic spindle (Figure 2-6, top, in metaphase/anaphase). As cells progress through nuclear division and cytokinesis, Fa2p-HA remains tightly associated with the basal bodies in each newly formed daughter cell (Figure 2-6, cytokinesis). During the onset of G1 phase, daughter cells begin to assemble flagella. The ax-Fa2p-HA signals are apparent at this early stage of post-mitotic flagellar assembly (Figure 2-6, G1 onset). Images from this stage are comparable with the signals observed in cells that are regenerating their flagella 5 min after deflagellation (Figure 2-5C).

2.4.6 Fa2p Kinase Activity Is Required for Deflagellation, but not for Cell Cycle Progression

Although Fa2p is essential for calcium-induced deflagellation (Finst *et al.*, 1998), and we have now shown that this kinase localizes to the site of axonemal severing (Figure 2-4), previous data suggested that kinase activity was not required for axonemal severing. Lohret *et al.* (1998) found that in vitro activation of axonemal severing by calcium did not require the addition of ATP and was not blocked by non-hydrolyzable ATP analogues or ADP. Based on these data, we hypothesized that the kinase activity of Fa2p plays a role in the assembly of a severing complex, rather than a signaling role during stress-induced deflagellation. To test this idea, we constructed a presumptive catalytically inactive (kinase-dead) version of the protein, by using site-directed mutagenesis to convert the invariant lysine in the ATP-binding loop to an arginine (Figure 2-7A, Fa2p-HA-K46R). The cognate mutation has been shown to inactivate kinase activity in several other Nek kinases (Noguchi *et al.*, 2002; Faragher and Fry, 2003; Yin *et al.*, 2003; Twomey *et al.*, 2004). The construct was transformed into *fa2-1*

mutant cells, and transformants were assayed for expression of the protein. Approximately 18% of transformants (n = 33) expressed a protein of the expected size (Figure 2-7A). Whereas *fa2* mutants expressing the Fa2p-HA were rescued for the deflagellation defect, none of the cells expressing the Fa2p-HA-K46R were rescued (Figure 2-7A). This result indicates that kinase activity is necessary for deflagellation.

To determine whether failure to rescue the deflagellation defect was due to mislocalization of the kinase-dead protein, we stained the cells with anti-HA antibodies. The Fa2p-HA-K46R localizes to the same region of the axoneme as Fa2p-HA (Figure 2-7B). This indicates that kinase activity of Fa2p is not required for its localization to the site of severing. The role of Fa2p kinase activity in the deflagellation pathway remains to be determined.

We next asked whether the cell cycle function of Fa2p requires its kinase activity. Our presumptive kinase-dead Fa2p-HA-K46R localized correctly to both the proximal axoneme and basal bodies (Figure 2-7B; our unpublished data) but did not fulfill the deflagellation function of wild-type Fa2p. This provided us with an opportunity to test whether the G_2/M delay of *fa2* mutants was a consequence of defects in axonemal severing, or due to some other function of the protein. We hypothesized that the cell cycle delay would be directly related to the deflagellation defect because flagella are resorbed at G_2/M and the mechanisms of resorption and deflagellation share common features (Parker and Quarmby, 2003). We initially used cell size as a proxy for cell cycle progression (Mahjoub *et al.*, 2002). As shown in Figure 2-7C, Fa2p-HA-K46R rescues the cell size phenotype of *fa2* mutant cells. To directly assess whether the mutant protein had indeed rescued the cell cycle progression delay, we measured mitotic index. Figure

2-7D shows that *fa2*-1; *FA2*HA-K46R cells enter mitosis at the same time as wild-type cells, ~4h sooner than *fa2*-1 cells. Although we did not predict this result, it is consistent with recent observations in *Xenopus* mitosis, where a vertebrate NIMA-related kinase, Nek2B, plays an important role in centrosome assembly (Fry *et al.*, 1998). A confirmed kinase-dead mutant Nek2B localizes correctly to the centrosome and satisfies the centrosome duplication function of Nek2B (Twomey *et al.*, 2004).

2.4.7 Fa2p Localization in Mouse Kidney Cells

Deflagellation (or deciliation) is a ubiquitous cellular response to stress (reviewed in Quarmby, 2004). We previously noted that expansion of the Nek family of proteins correlates with the presence of cilia (Bradley *et al.*, 2004). Although we cannot identify a mammalian ortholog of Fa2p on the basis of sequence data, it falls in the same phylogenetic group as Nek 1/3/4/8 (Bradley *et al.*, 2004). We anticipate that this group retains responsibility for the conduct of certain fundamental cellular functions, such as deflagellation and cell cycle progression. Consequently, we hypothesized that Fa2p would localize in mammalian cells as it does in *Chlamydomonas*, reflecting the localization of an as yet unidentified functional ortholog. To express Fa2p in mammalian cells, the *FA2* cDNA was cloned into a mammalian expression vector containing the gene encoding the enhanced green fluorescence protein (EGFP). The resulting product would be expressed as an EGFP-Fa2p chimera.

The EGFP-FA2 construct was transfected into mouse kidney collecting duct epithelial cells (IMCD-3). Immunoblots of whole cell lysate with anti-GFP antibodies showed a single band of the expected molecular weight in transfected cells (Figure 2-8A, left). This band is not detected in control cells transfected with EGFP-only. Immunoblots

of the same cell lysates with the anti-Fa2p antibody recognized the same band (Figure 2-8A, right).

Fluorescence microscopy revealed an EGFP-Fa2p signal at the base of the primary cilium (Figure 2-8, B and C). Localization of Fa2p to the proximal end of the cilium is of particular interest because the simplest hypothesis is that it is axonemal Fa2p that is required for deflagellation in *Chlamydomonas*. Although it is not clear that deciliation is a part of the normal physiology of epithelial cells, many different cell types have been observed to deciliate in response to stress (reviewed in Quarmby, 2004). Independent of the physiological relevance of deciliation, ax-Fa2p (or its ortholog) may play a role in coordinating ciliary assembly/disassembly and cell cycle progression, for example, by sequestration of Fa2p (or associated proteins) in the cilia when cells are in interphase.

There is also a distinct EGFP-Fa2p signal associated with the proximal end of the centrioles in the kidney cells (Figure 2-8, B and C). Note that in mammalian cells the centrioles are orthogonally positioned, so that the proximal regions of each centriole are distant from one another. This is in contrast to the closely apposed proximal regions of the *Chlamydomonas* basal bodies (Figure 2-3; reviewed in Kirk, 1998). The centriolar staining pattern observed in Figure 2-8 supports our suggestion that bb-Fa2p is associated with the proximal end of basal bodies. In transfected IMCD-3 cells undergoing division, EGFP-Fa2p remained associated with centrioles throughout mitosis (Figure 2-9). As in *Chlamydomonas*, Fa2p signals were observed associated with the base of each new daughter centriole (Figure 2-9, top). As cells progressed into metaphase, there was robust EGFP-Fa2p staining at the spindle poles (Figure 2-9, middle). Finally, as cells

approached cytokinesis, EGFP-Fa2p was tightly associated with the centrioles in the new daughter cells (Figure 2-9, bottom). Intriguingly, a significant EGFP-Fa2p signal was associated with acetylated microtubules at the midbody (Figure 2-9, arrow).

2.5 Discussion

The proximal axoneme has received little attention as a specialized functional zone, but there are indications that this is about to change. Recent studies of the role of primary cilia as flow sensors (McGrath *et al.*, 2003; Nauli *et al.*, 2003; Praetorius *et al.*, 2003) suggest that this region of the flagella is likely to play a role in mechanical sensation. It also may be an important site for the regulation of intraflagellar transport (IFT). IFT is the process by which cilia and flagella are built and maintained; it involves anterograde and retrograde transport of flagellar components along the axoneme (reviewed by Rosenbaum and Witman, 2002). When retrograde IFT is blocked, IFT particles and proteins accumulate at the proximal flagellum (Pazour *et al.*, 1999; Porter *et al.*, 1999; Iomini *et al.*, 2004). Similarly, IFT proteins accumulate at this site in differentiated *Chlamydomonas* gametes, presumably in anticipation of a rapid burst of anterograde IFT upon mating (Lucker, Goodenough, and Cole, personal communication; Mesland *et al.*, 1980; Musgrave and van den Ende, 1987). The idea that this site plays an important role in IFT is further supported by observations that many flagellar assembly, or *fla*, mutants have deflagellation phenotypes and the *fa1* and *fa2* deflagellation-defective mutants have flagellar resorption phenotypes (Parker and Quarmby, 2003; Parker and Quarmby, unpublished data). In the present report, we show that a NIMA-family kinase, Fa2p, localizes to the proximal end of the axoneme in both *Chlamydomonas* and mouse kidney cells (Figures 2-2, 3, 4 and 8). In this context, it is

interesting to note that KIF3A (the anterograde kinesin of IFT) has recently been identified as a putative substrate of human Nek1 (Surpili *et al.*, 2003). We propose that this specialized region of the proximal cilium be known as the site of flagellar assembly/autotomy (SOFA). Fa2p lies on the SOFA.

Axonemal Fa2p localizes to the distal side of the site where the outer doublet microtubules are severed during stress-induced deflagellation (Figure 2-4; Lewin and Lee, 1985). This location is perhaps not surprising, given that *fa2*cells are defective in one of the final steps of deflagellation: calcium-activated microtubule severing (Finst *et al.*, 1998). However, the role of a kinase in this pathway is perplexing because earlier in vitro results indicated that ATP is not required for calcium-activated axonemal severing. We previously developed an in vitro assay for axonemal microtubule severing wherein axonemal-basal body complexes are isolated from whole cells in the presence of calcium chelators (Lohret *et al.*, 1998). Calcium, but not ATP, is necessary to activate axonemal severing in this system, and axonemal-basal body complexes from *fa2* cells do not sever in response to calcium addition (Lohret *et al.*, 1998). These data suggest that the Fa2p kinase was not likely to play a direct role in signaling calcium-induced deflagellation, but they may be important for directing assembly of a microtubule severing complex during axonemal assembly (Mahjoub *et al.*, 2002). Therefore, localization of Fa2p near the site of severing suggested that either its role in severing was kinase-independent, or its kinase activity was required for the priming or assembly of additional factors at this site. Correct localization of a kinase-dead Fa2p to the proximal axoneme, without rescue of the deflagellation-defect of *fa2* cells (Figure 2-7) clearly demonstrates that its role in deflagellation is not kinase independent. We conclude that Fa2p itself targets to this site

in a kinase-independent manner, but that its kinase activity is important for the assembly of a severing complex.

To our surprise, the kinase-dead Fa2p rescued the cell cycle progression delay of *fa2* mutant cells (Figure 2-7). Because *fa2;fla10-1* double mutants are slow to resorb their flagella on shift to the restrictive temperature (Parker and Quarmby, 2003), we thought that the G_2/M delay of *fa2* mutants might be a consequence of slow flagellar resorption before M phase. However, another mutant with defective calcium-activated axonemal severing, *fa1*, does not have a G_2/M delay (our unpublished data), yet it is also slow to resorb flagella as a *fa1;fla10-1* double mutant at the restrictive temperature (Parker and Quarmby, 2003). Together, these data support the idea that the cell cycle progression phenotype of *fa2* cells is independent of its kinase-dependent axonemal severing function. Consistent with this is a recent report that Nek2B has a kinase-independent role in centrosome assembly (Twomey *et al.*, 2004).

In *Chlamydomonas* and in kidney cells, Fa2p localized to the proximal end of basal bodies and centrioles respectively (Figures 2-3, 4, 5, 6, 8, and 9). It was observed at the base of daughter as well as mother basal bodies and centrioles, but it is not required for basal body assembly, nor for the assembly of flagella (Finst *et al.*, 1998). In both cell types, Fa2p remained associated with the spindle poles throughout mitosis (Figures 2-6 and 9). In *Chlamydomonas*, Fa2p occurred at the proximal cilium at the onset of G_1 (we did not capture any IMCD-3 cells at this precise stage of cell division). In the IMCD-3 cells, we noticed an additional site of localization of Fa2p during cell division: the midbody or cytoplasmic bridge between two cells at the final stages of cytokinesis. Acetylated microtubules span the midbody (Figure 2-9; our unpublished data) and an

intense Fa2p signal is observed approximately midway along the length of these microtubules (Figure 2-9). The staining that we observed in this region looks very much like the staining of midbody complex proteins, the mitotic kinesin-like protein CHO1 (Matuliene and Kuriyama, 2002), and the calcium-binding protein Annexin 11 (Tomas *et al.*, 2004). The axonemal microtubules whose calcium-induced severing is Fa2p dependent also are acetylated, and we speculate that an ortholog of Fa2p may play a role in the severing of acetylated microtubules during the final stages of cytokinesis in the kidney cells. Fa2p is not predicted to play a similar role in the cytokinesis of *Chlamydomonas* because an analogous structure does not form (Johnson and Porter, 1968; Ehler and Dutcher, 1998).

Mice with mutations in either Nek1 or Nek8 have pleiotropic phenotypes, including cystic kidneys (Upadhya *et al.*, 2000; Liu *et al.*, 2002). Our discovery that a member of this phylogenetic group of Nek proteins, Fa2p, is localized to the same subcellular sites in both *Chlamydomonas* and kidney epithelial cells provides strong support for the concept that this family of kinases plays conserved roles in the coordination of cilia and cell cycle progression. This conservation is important because it will allow the application of the powerful genetic, molecular, and biochemical approaches available in *Chlamydomonas* to critical questions, such as the identification of the key substrates and interacting proteins in this human disease-related pathway.

2.6 Acknowledgments

We are grateful to many members of the research community for stimulating discussions. We are particularly indebted to the following colleagues: Jeff Salisbury and Saul Purton generously provided the centrin antibody and pSP124S vector, respectively.

B.J. Lucker, Ursula Goodenough, and Doug Cole kindly shared their unpublished observations and ruminations on IFT proteins at the proximal flagella of gametes. Wallace Marshall suggested the QFC experiment, and Ben Goh helped generate the kinase-dead FA2 construct. Michel Leroux and Junchul Kim enabled the kidney cell experiments. M.R.M. was supported, in part, by Doctoral Fellowships from the Michael Smith Foundation for Health Research, and the Natural Sciences and Engineering Research Counsel. This work was supported by an operating grant to L.M.Q. from the Canadian Institutes of Health Research (MOP 37861).

2.7 Figures

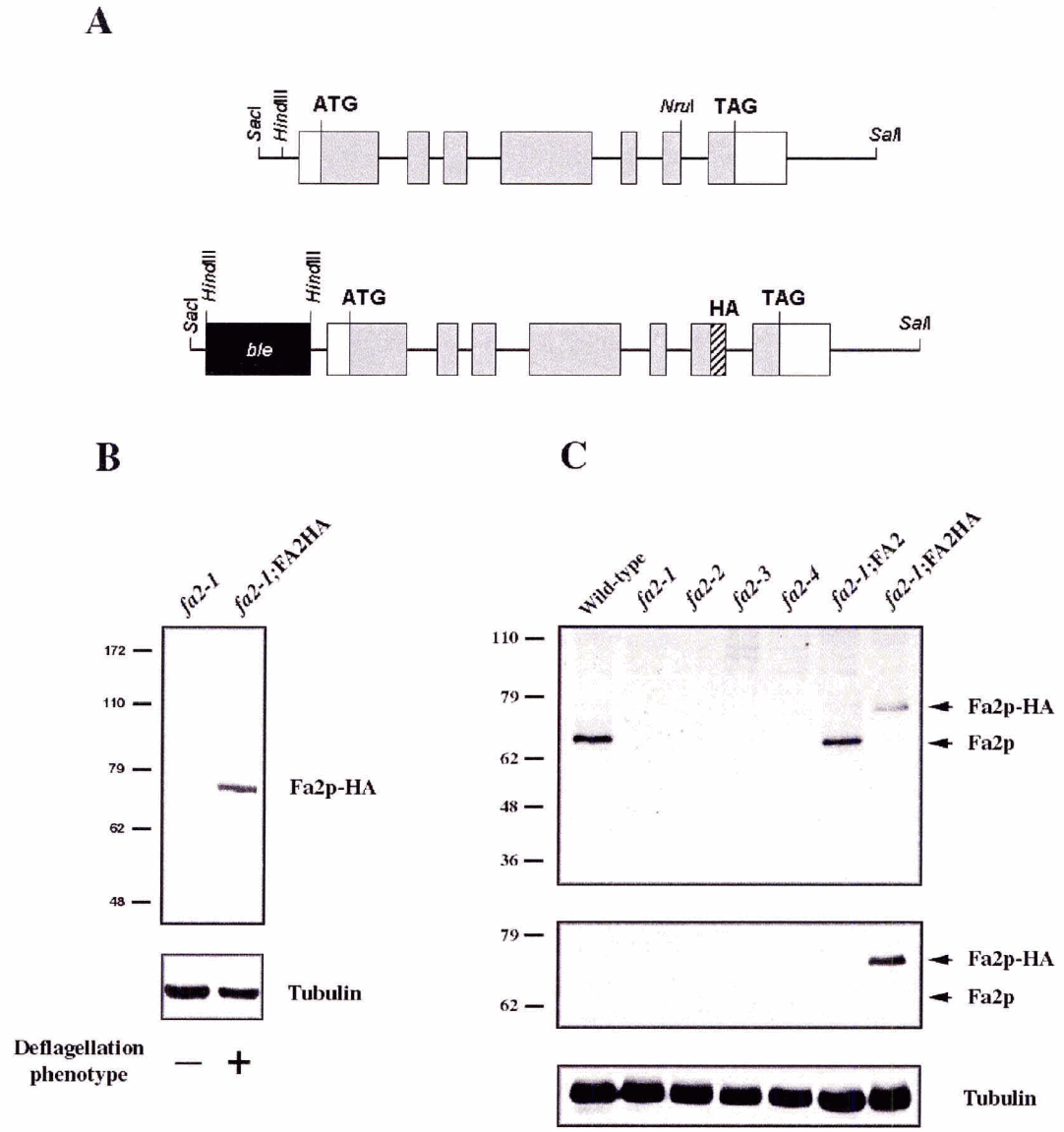

Figure 2-1 Immunoblot analysis of HA-tagged and endogenous Fa2p.
(A) Schematic representation of the genomic *FA2* construct, containing an HA-epitope tag at the C-terminus of Fa2p and the *ble* marker gene. Exons are shown in grey and the UTRs in white. (B) Immunoblot of whole cell lysate from *fa2-1* mutants and *fa2-1* cells rescued for deflagellation with the HA-tagged construct. Protein (30 µg) was loaded in each lane, and the blot was probed with anti-HA antibody. The membrane was stripped and reprobed with anti-α-tubulin antibody for loading control. Molecular mass standards (in kilodaltons) are indicated on the left. (C) Characterization of affinity purified anti-Fa2p antibody against whole cell lysate from wild-type, *fa2-1*, *fa2-2*, *fa2-3*, *fa2-4*, *fa2-1* rescued with the *FA2* gene (*fa2*-1; *FA2*), and *fa2-1* rescued with the HA-tagged FA2 construct (*fa2*-1; FA2-HA). Protein (30 µg) was loaded in each lane, and the blot was probed with anti-Fa2p, then stripped, and reprobed with anti-HA. The membrane was stripped again and reprobed with anti-α-tubulin antibody for loading control.

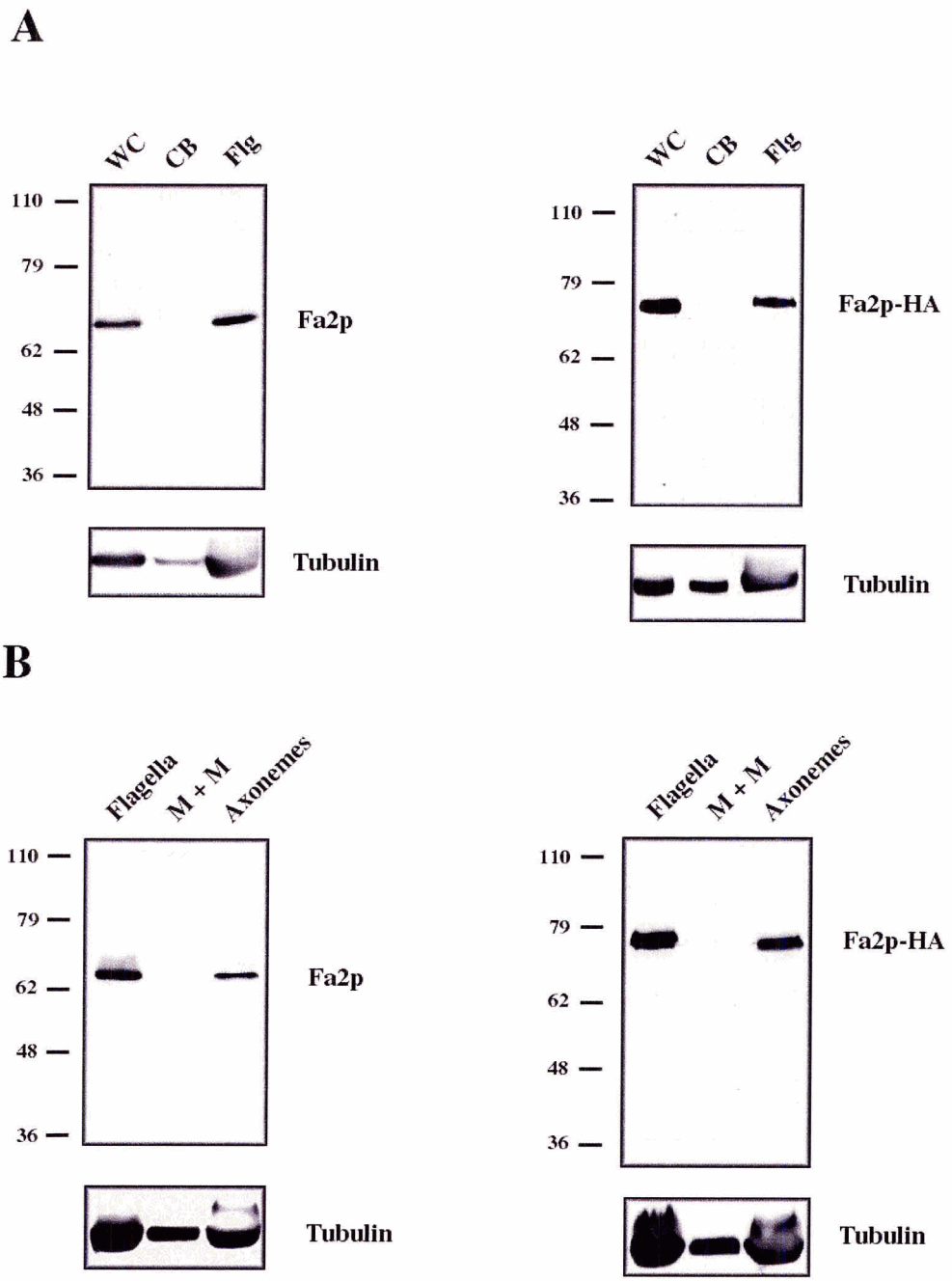

Figure 2-2 Fa2p is an axonemal protein.
(A) Immunoblot of cellular fractions from wild type (left) or *fa2*-1; *FA2*-HA (right) strains shows that Fa2p is found in the flagella. Cells were deflagellated with dibucaine, and equivalent numbers of whole cells (WC), cell bodies (CB), and flagella (Flg) were loaded in each lane. Blots were probed with either anti-Fa2p (left) or anti-HA (right) antibodies. (B) To refine the localization of Fa2p, flagellar membranes were extracted with detergent, and flagellar-equivalent amounts of flagella, membrane plus matrix (M+M), and axonemes were loaded in each lane. Blots were probed with either anti-Fa2p (left) or anti-HA (right) antibodies. All blots were stripped and reprobed with anti-α-tubulin antibody.

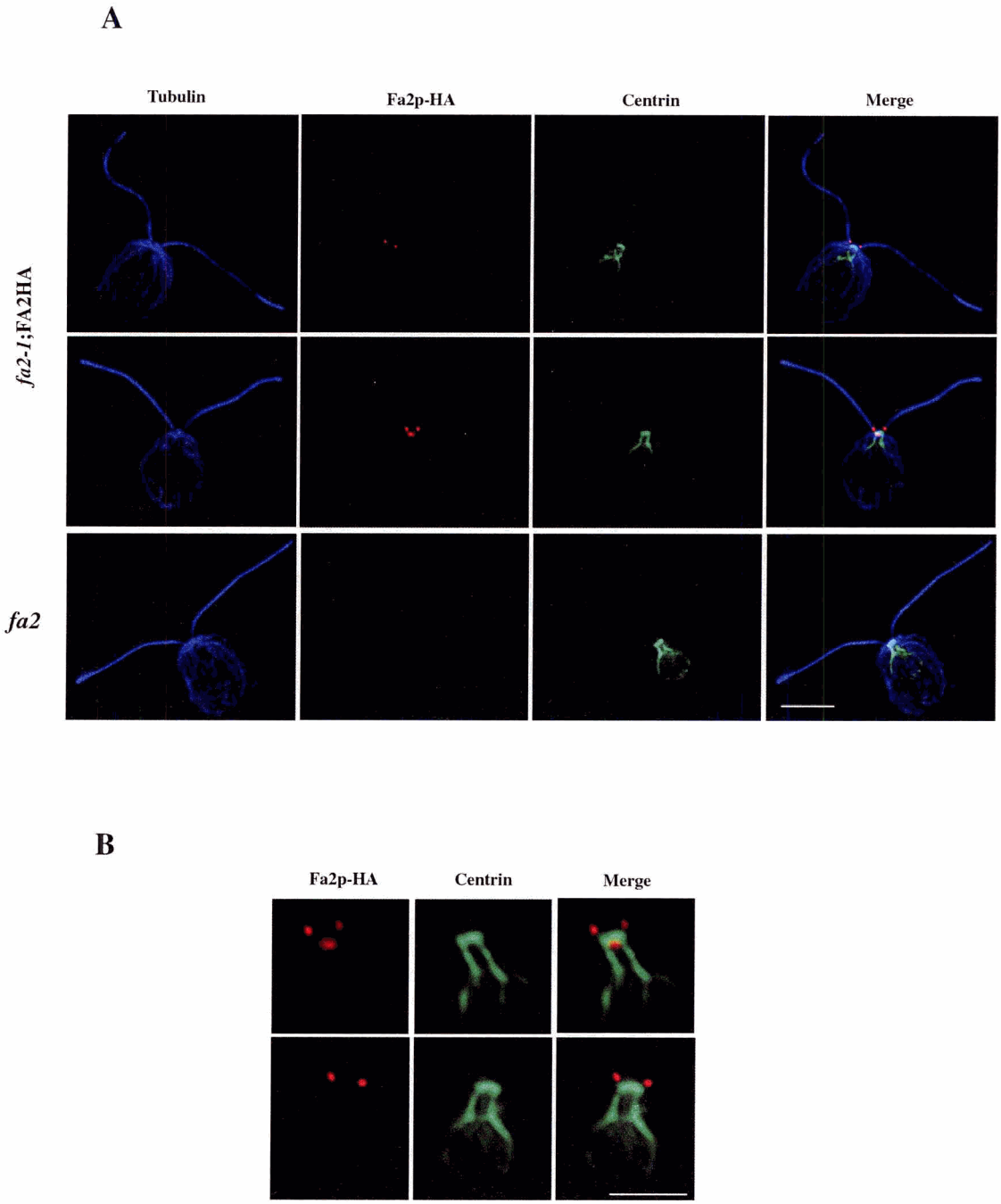

Figure 2-3 Fa2p localization in *Chlamydomonas* cells.
(A) Triple-staining of *fa2-1*; FA2-HA cells (top two rows) and *fa2-1* mutant cells (bottom row) with anti-α-tubulin (blue), anti-HA (red), and anti-centrin (green) antibodies. Bar, 5 μm. (B) Magnification of the basal body-transition zone region showing two examples of Fa2p-HA and centrin costaining. Bar, 2 μm.

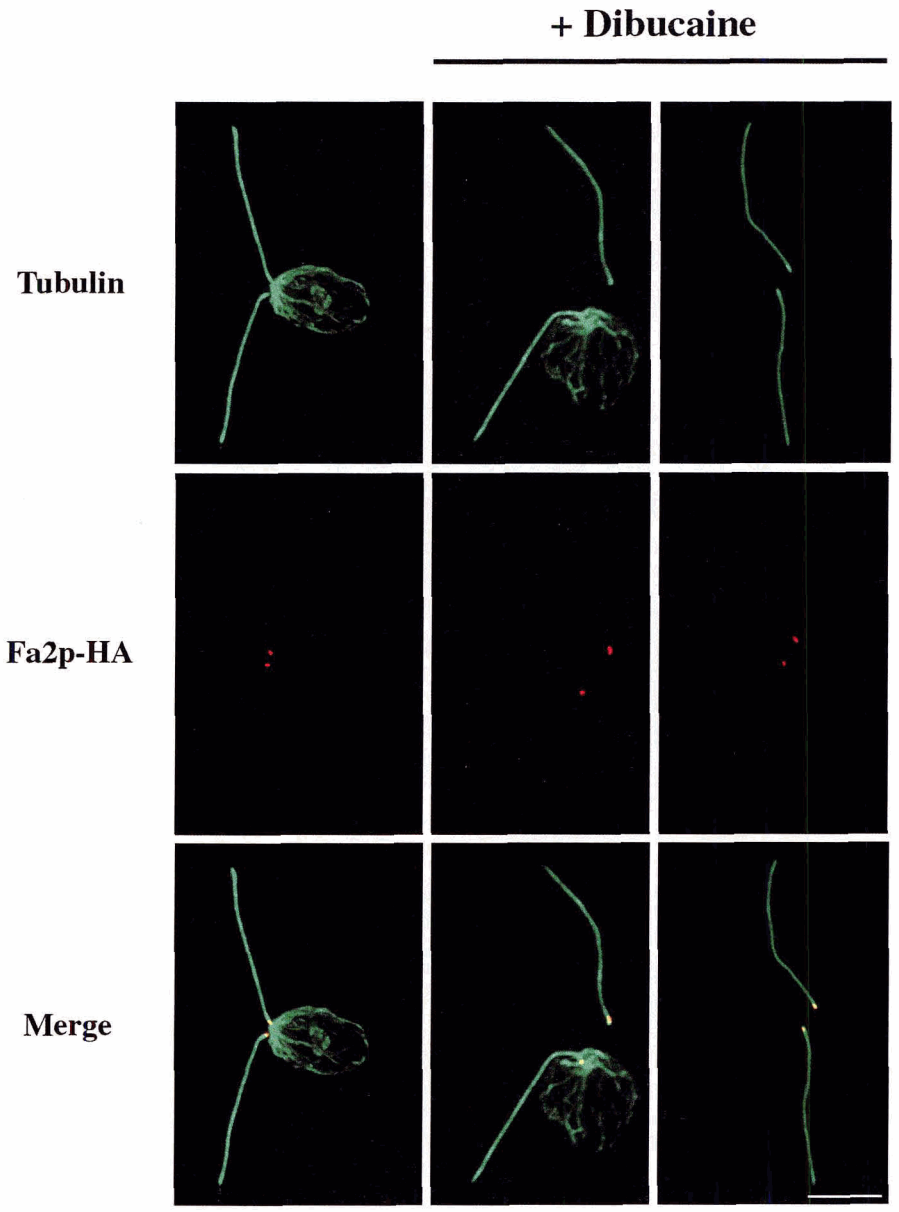

Figure 2-4 Axonemal Fa2p localizes distal to the site of axonemal microtubule severing
fa2-1; *FA2*-HA cells were spotted onto polyethylenimine-coated coverslips and briefly allowed to adhere. Cells were deflagellated by addition of dibucaine and immediately fixed with methanol. Samples were subsequently stained with anti-HA (red) and anti-α-tubulin (green) antibodies. Bar, 5 μm.

Figure 2-5 Dynamic changes in basal body-associated and axonemal Fa2p levels during flagellar resorption (following two pages).

(A) Cultures of *fa2*-1;*FA2*-HA cells were synchronized and harvested during a period of flagellar resorption, before entry into mitosis. Cells were stained with anti-HA (green) and anti-α-tubulin (red) antibodies. Both flagella from the represented cells were measured, and the average length indicated in the bottom panels.

(B) *fa2*-1; *FA2*-HA and wild-type cells were transferred to medium lacking nitrogen and grown overnight to induce gametogenesis. The resulting gametes were mixed together to allow mating and formation of QFCs. To obtain cells at various stages of flagellar resorption, samples were collected at 30-min intervals for the next 4 h. Samples were fixed and stained with anti-HA (green) and anti-α-tubulin (red) antibodies. Both flagella from the original Fa2p-HA-expressing cell were measured, and the average length indicated in the bottom panels.

(C) *fa2*-1; *FA2*-HA cells were deflagellated by pH shock and allowed to regenerate their flagella. Samples were taken at 5, 30 and 90 min post-deflagellation, fixed and stained with antibodies for HA (green) and α-tubulin (red). Bars, 5 μm.

A

Pre-mitotic flagellar resorption

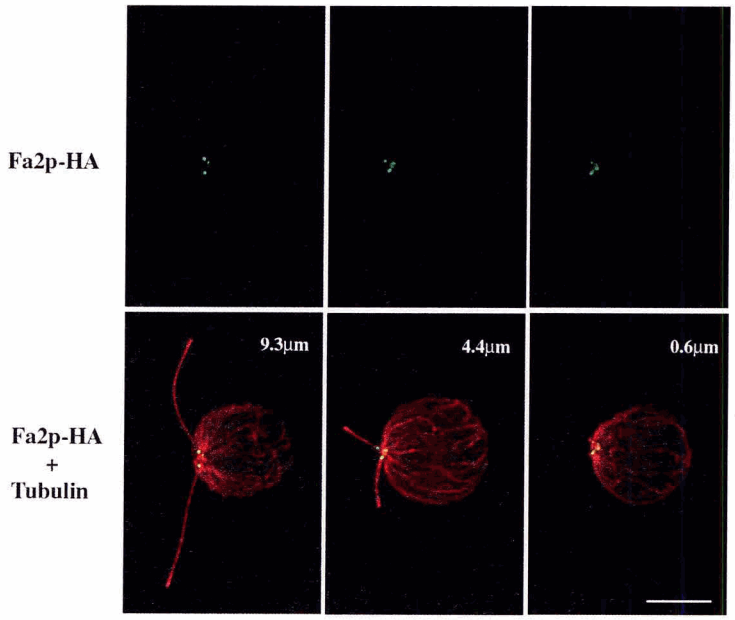

B

Zygotic flagellar resorption

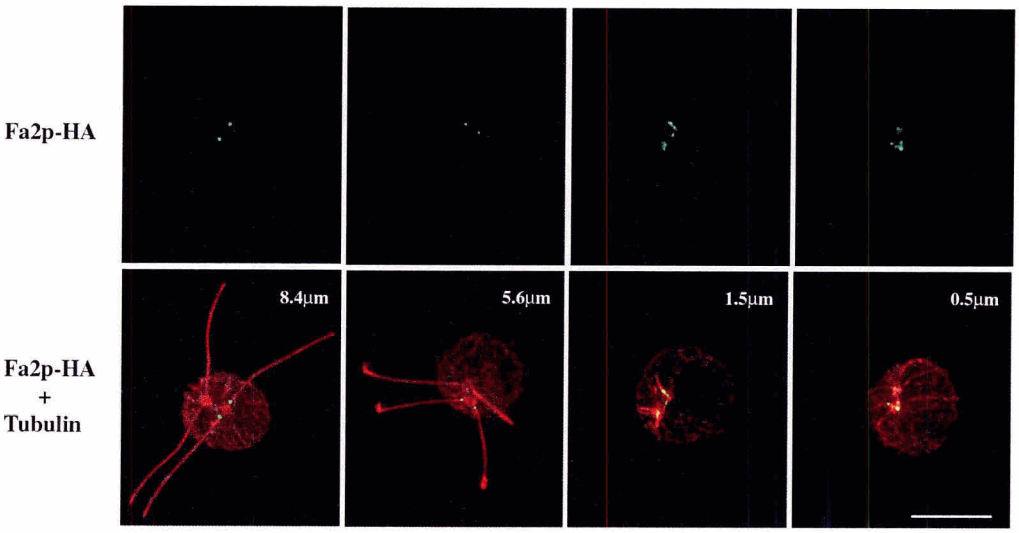

C

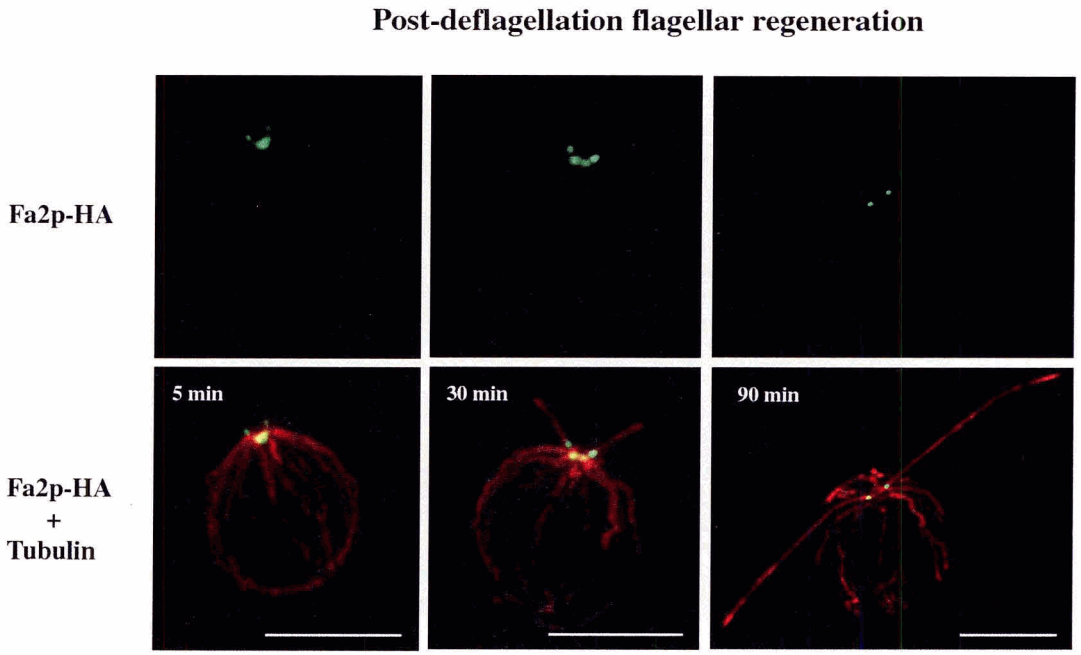
Post-deflagellation flagellar regeneration
Fa2p-HA
Fa2p-HA
+
Tubulin
5 min
30 min
90 min

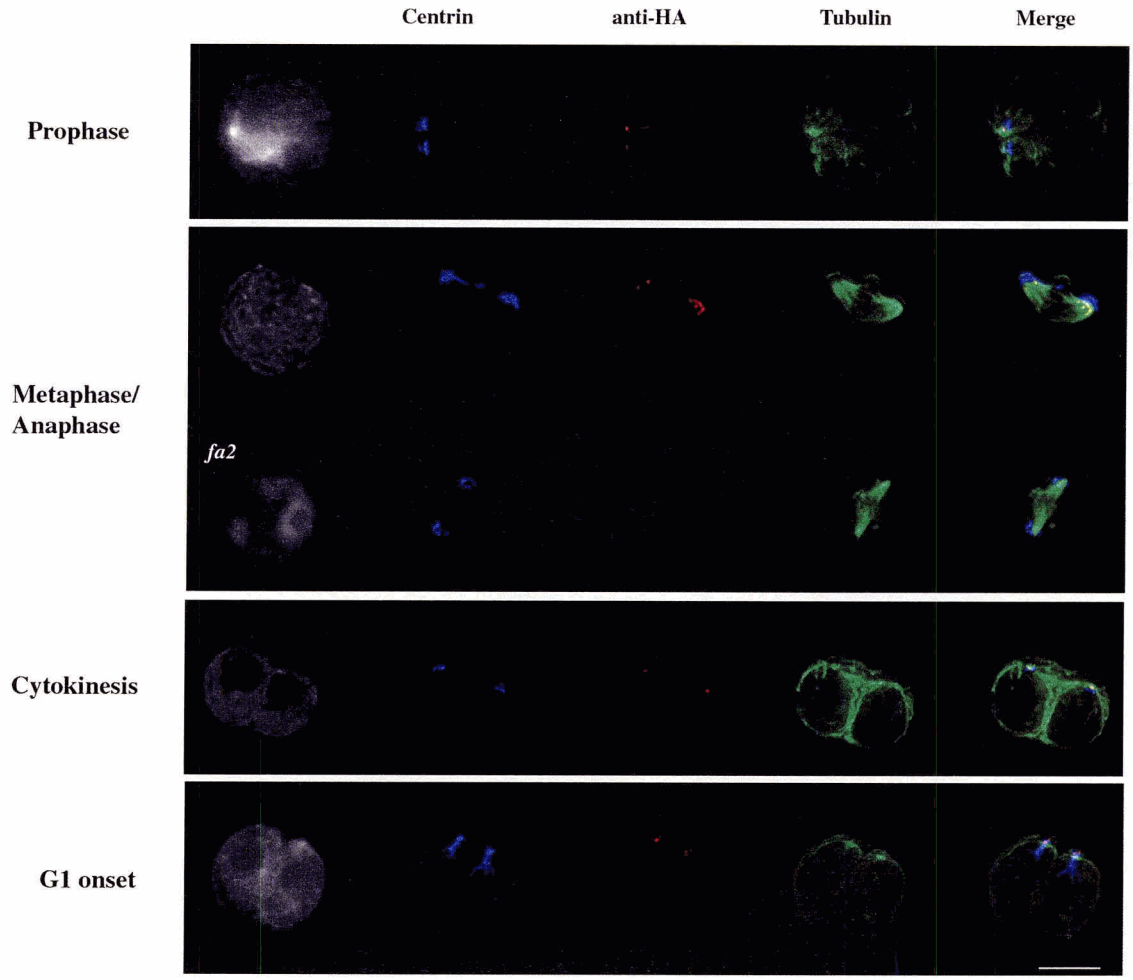

Figure 2-6 Fa2p localization during mitosis.
Synchronized *fa2-1*; FA2-HA cells were harvested as cells were beginning to divide. Samples were fixed and stained with antibodies for centrin (blue), HA (red), and α-tubulin (green). Also, cell autofluorescence is shown in the far-left column and helps identify the position of the nucleus. Representative samples of cells in prophase, metaphase/anaphase, cytokinesis, and the onset of G_1 are shown. To determine the specificity of Fa2p-HA staining in dividing cells, *fa2* mutants were synchronized and stained as described above (our unpublished data, except for a metaphase/anaphase cell, the phase at which we saw the highest non-specific staining).

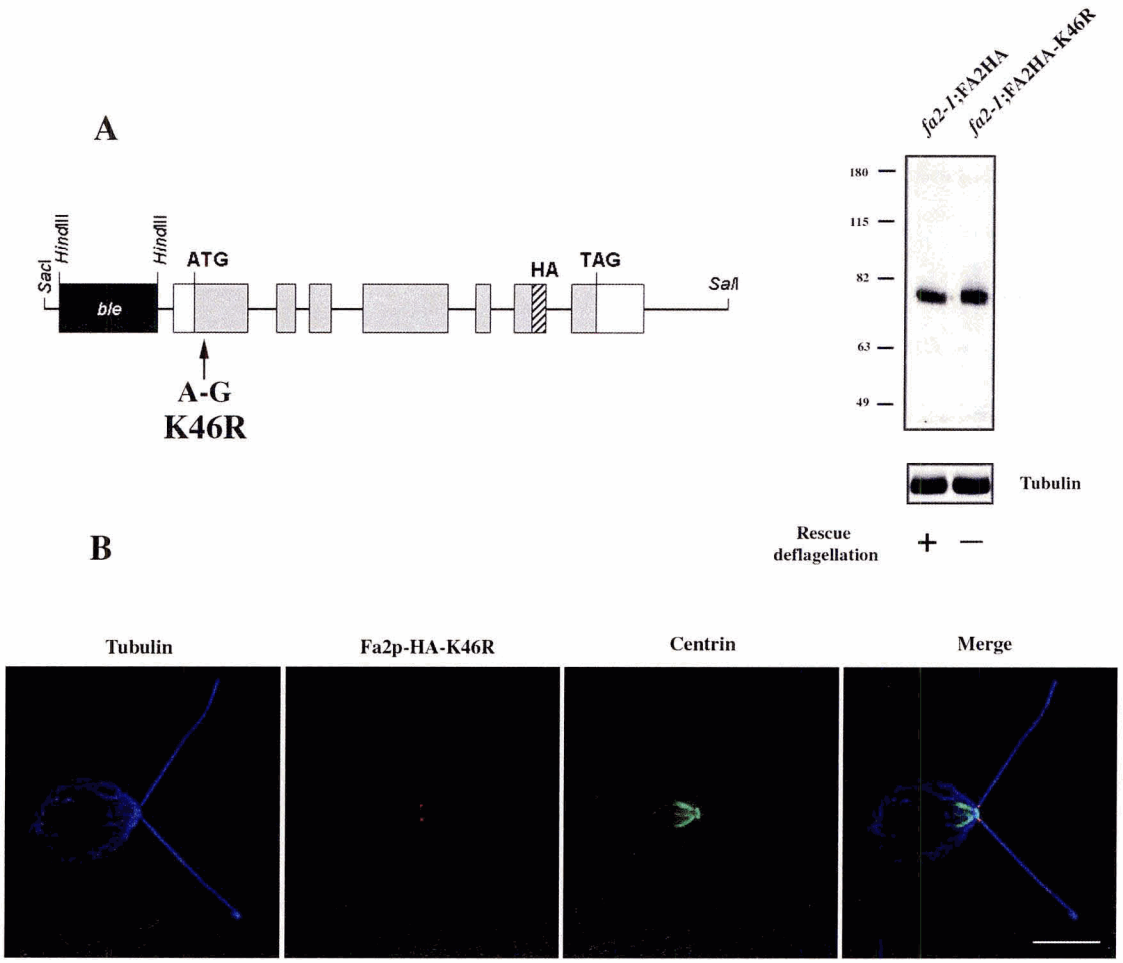

Figure 2-7 Kinase-dead Fa2p assessed for deflagellation activity, localization and cell cycle progression.

(A) Site-directed mutagenesis was performed to introduce an A-to-G change in the HA-tagged FA2 construct. The resulting translated product introduces an amino acid change from the invariant lysine in the ATP-binding loop (aa 46) to an arginine. Immunoblot analysis of *fa2*-1; *FA2*HA-K46R cells shows that the protein is expressed at levels comparable to Fa2p-HA, but unlike Fa2p-HA, the presumptive kinase-dead mutant does not rescue the deflagellation defect of *fa2* cells. (B) *fa2*-1; *FA2*HA-K46R cells were fixed and stained with anti-HA (red), anti-centrin (green), and anti-α-tubulin (blue) antibodies. Bar, 5 μm.

(C, **below**) Cell volume profiles for cells grown asynchronously in M-medium. One hundred cells were measured from each culture. (D, below) Mitotic index of wild-type, *fa2*-1, and *fa2*-1; *FA2*HA-K46R cells. Cultures grown in M medium were incubated in the dark for 24 h and then returned to the light. Aliquots were analyzed microscopically at the indicated time points for evidence of mitotic cleavage furrows. The percentage of cells with visible cleavage furrows was scored as percentage of cells in M phase. Three hundred cells from each time point for each strain were scored.

C

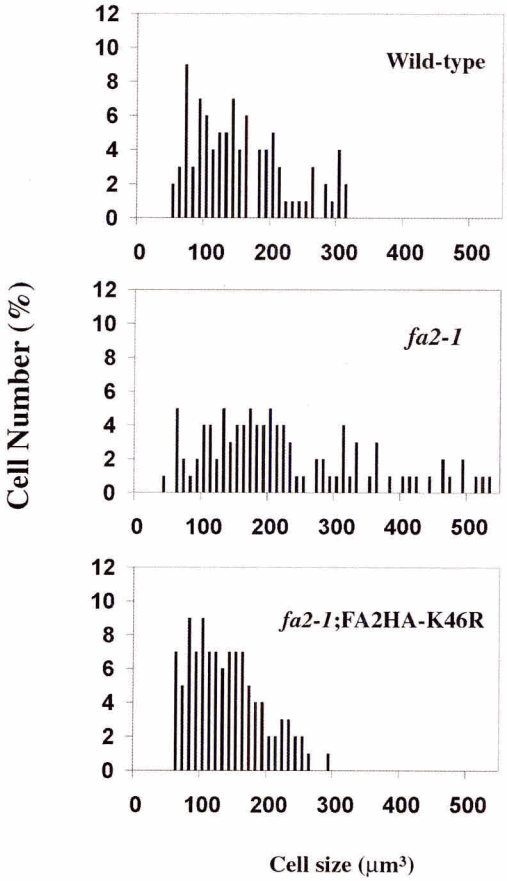
Wild-type
fa2-1
fa2-1;FA2HA-K46R
Cell Number (%)
Cell size (μm³)
0
2
4
6
8
10
12
0
100
200
300
400
500

D

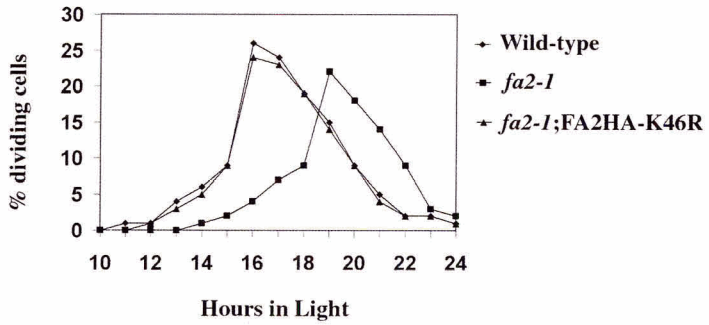
% dividing cells
Hours in Light
Wild-type
fa2-1
fa2-1;FA2HA-K46R
0
5
10
15
20
25
30
10
12
14
16
18
20
22
24

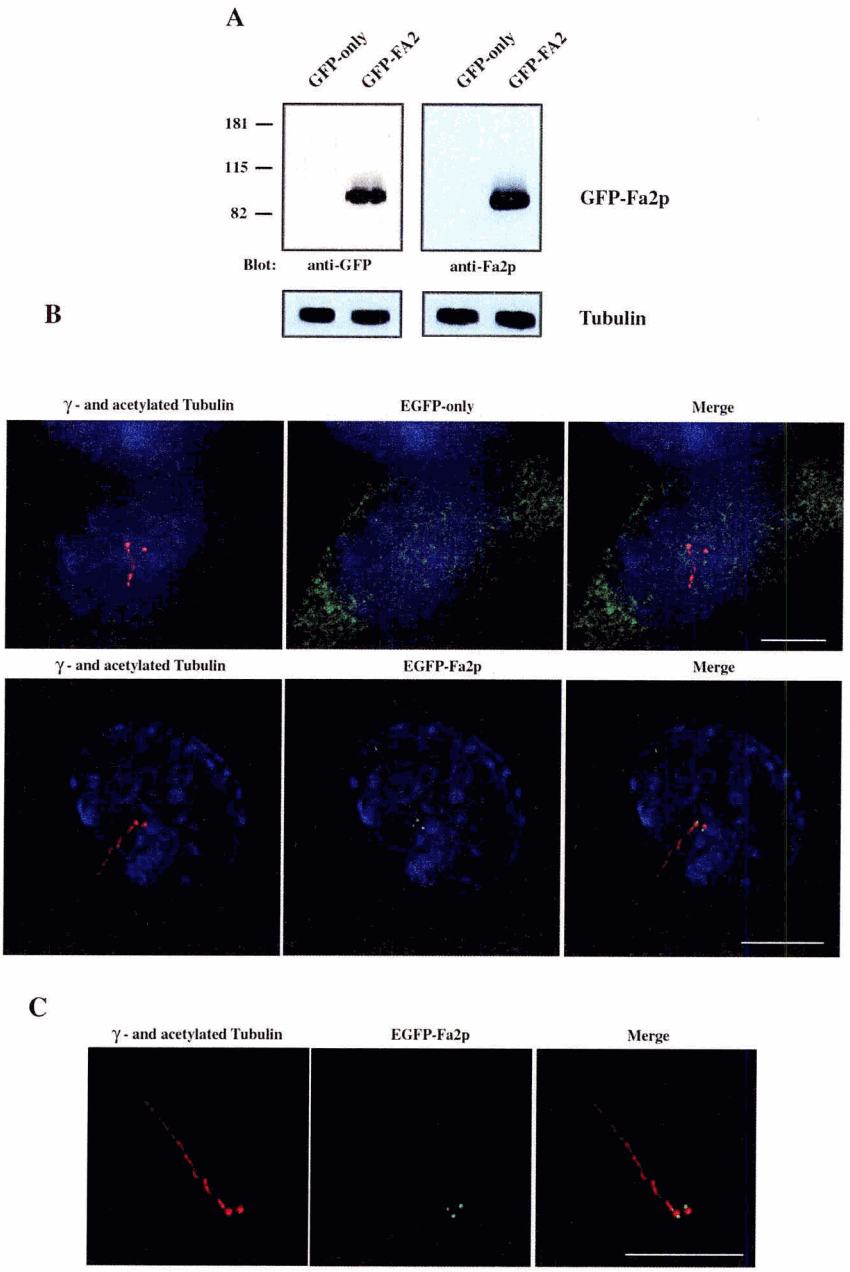

Figure 2-8 Expression of Fa2p in mouse kidney cells.
(A) IMCD-3 cells were transfected with an expression vector containing either EGFP-FA2 or EGFP only as a control. Immunoblots of total protein extract were probed with anti-GFP and anti-Fa2p antibodies. The membranes were stripped and reprobed with anti-α-tubulin antibody for loading control. Molecular mass standards (in kilodlatons) are indicated on the left. (B) Cells transfected with EGFP-only (top) or EGFP-FA2 (bottom) were co-stained with antibodies against α- and acetylated tubulin, to mark the positions of the centrioles and the cilia, respectively. A common secondary antibody was used that allowed visualization of both α- and acetylated tubulin (red), and EGFP-Fa2p was visualized directly using the fluorescein channel (green). DNA was stained with DAPI (blue). (C) Magnified image from EGFP-Fa2p expressing cell in B showing relative position of the centrioles, cilium, and Fa2p. The image was rendered 140° around the *x*-axis and magnified 1.5X. Bars, 5 μm.

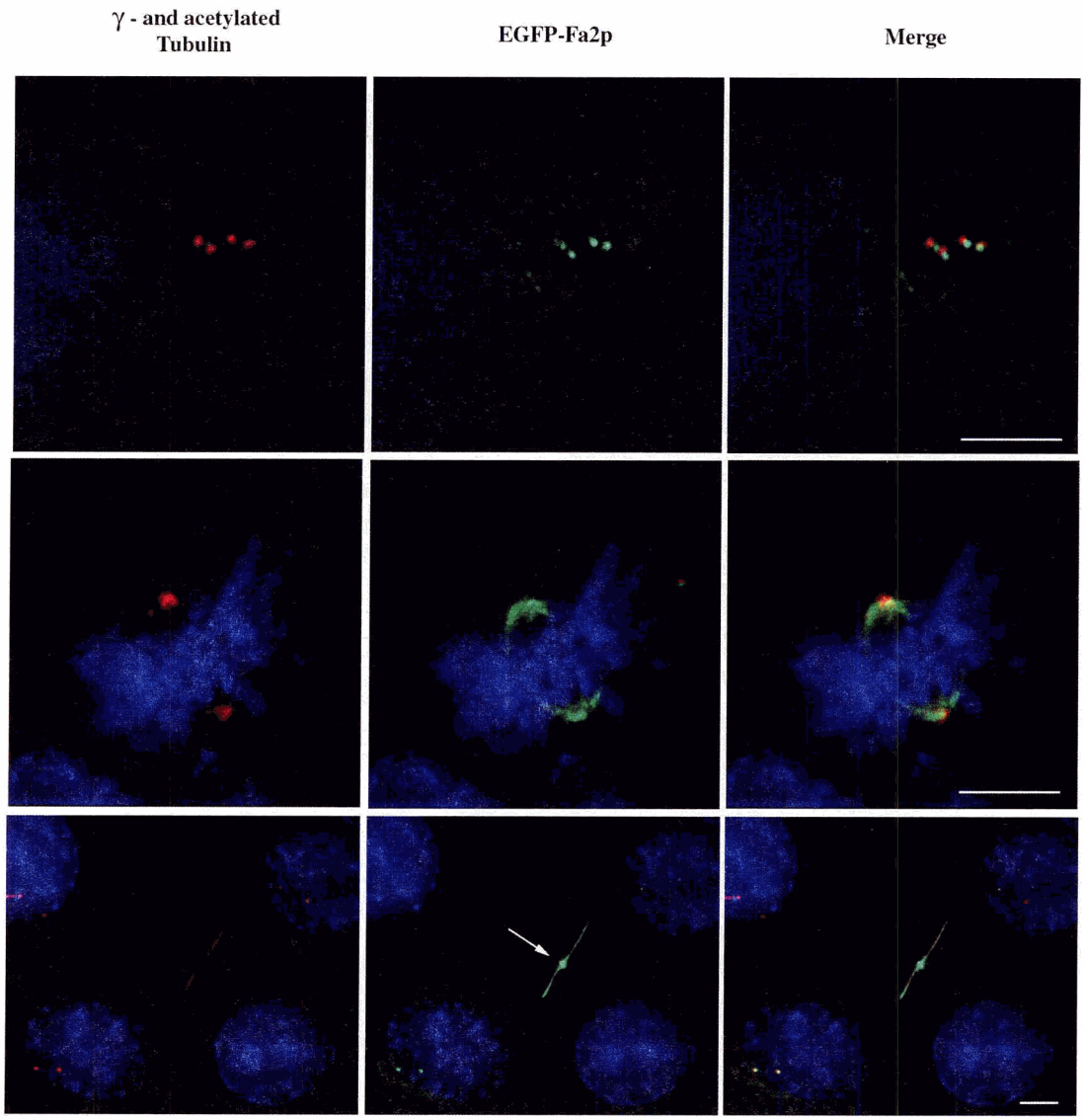

Figure 2-9 Fa2p localization during mitosis in mouse kidney cells.
IMCD-3 cells expressing EGFP-Fa2p were stained for α- and acetylated tubulin (red), and cells were visualized at various stages of division. Images shown are from cells after centriole duplication (top), metaphase (middle), and cytokinesis (bottom). Arrow indicates concentration of EGFP-Fa2p signal in the middle of the cytoplasmic microtubule bridge connecting the dividing cells. Bars, 5 μm.

2.8 Reference List

Berman, S.A., N.F. Wilson, N.A. Haas, and P.A. Lefebvre. 2003. A novel MAP kinase regulates flagellar length in *Chlamydomonas*. Curr. Biol. *13*: 1145-1149.

Bradley, B.A., J.J.D. Wagner, and L.M. Quarmby. (2004) Identification and sequence analysis of six new members of the NIMA-related kinase family in *Chlamydomonas*. J. Euk. Micro. *51*:66-72.

Cavalier-Smith, T. 1974. Basal body and flagellar development during the vegetative cell cycle and the sexual cycle of *Chlamydomonas reinhardtii.* J. Cell Sci. *16*: 529-556.

Dutcher, S.K., N.S. Morrissette, A.M. Preble, C. Rackley, and J. Stanga. 2002. Epsilon-tubulin is an essential component of the centriole. Mol. Biol. Cell. 13: 3859-3869.

Ehler, L.L., J.A. Holmes, and S.K. Dutcher. 1995. Loss of spatial control of the mitotic spindle apparatus in a *Chlamydomonas* reinhardtti mutant strain lacking basal bodies. Genetics. *141*: 945-960.

Ehler, L.L. and S.K. Dutcher. 1998. Pharmacological and genetic evidence for a role of rootlet and phycoplast microtubules in the positioning and assembly of cleavage furrows in *Chlamydomonas reinhardtii.* Cell Motil. Cytoskeleton. *40*: 193-207.

Faragher, A.J. and A.M. Fry. 2003. Nek2A kinase stimulates centrosome disjunction and is required for formation of bipolar mitotic spindles. Mol. Biol. Cell. *14*: 2876-89.

Finst, R.J., P.J. Kim and L.M. Quarmby. 1998. Genetics of the deflagellation pathway of *Chlamydomonas reinhardtii*. Genetics. *149*: 927-936.

Finst, R.J., P.J. Kim, E. Griffis and L.M. Quarmby. 2000. Fa1p is a 171 kDa protein essential for axonemal microtubule severing in *Chlamydomonas*. J. Cell Science *113*: 1963-1971.

Fry, A.M., P. Meraldi, and E.A. Nigg. 1998. A centrosomal function for the human Nek2 protein kinase, a member of the NIMA family of cell cycle regulators. EMBO J. *17*: 470-481.

Harris, E.H. 1989. The *Chlamydomonas* Sourcebook. Academic Press. Inc., Berkeley. CA.

Huangfu, D., A. Liu, A.S. Rakeman, N.S. Murcia, L. Niswander, and K.V. Anderson 2003. Hedgehog signalling in the mouse requires intraflagellar transport proteins. Nature *426*: 83-87.

Iomini, C., K. Tejada, W. Mo, H. Vaananen and G. Piperno. 2004. Primary cilia of human endothelial cells disassemble under laminar shear stress. J. Cell Biol. *164*: 811-817.

Johnson, U.G. and K.R. Porter. 1968. Fine structure of cell division in *Chlamydomonas reinhardi*. Basal bodies and microtubules. J. Cell Biol. *38*: 403-425.

Kambouris N.G., D.J. Burke, and C.E. Creutz. 1993. Cloning and genetic analysis of the gene encoding a new protein kinase in *Saccharomyces cerevisiae.* Yeast. *9*:141-50.

Kirk, D.L. 1998. Volvox. Molecular-genetic origins of multicellularity and cellular differentiation. New York, NY: Cambridge University Press.

Krien, M.J., S.J. Bugg, M. Palatsides, G. Asouline, M. Morimyo, M. and M.J. O'Connell. 1998. A NIMA homologue promotes chromatin condensation in fission yeast. J. Cell Sci. *111*: 967-976.

Lewin, R.A. and K.W. Lee. 1985. Autotomy of algal flagella: electron microscope studies of *Chlamydomonas* (Chlorophyceae) and *Tetraselmis* (Prasinophyceae). Phycologia *24*: 311-316.

Li, J.B., J.M. Gerdes, C.J. Haycraft, Y. Fan, T.M. Teslovich, H. May-Simera, H. Li, O.E. Blacque, L. Li, C.C. Leitch, R.A. Lewis, J.S. Green, P.S. Parfrey, M.R. Leroux, W.S. Davidson, P.L. Beales, L.M. Guay-Woodford, B.K. Yoder, G.D. Stormo, N. Katsanis and S.K. Dutcher. 2004. Comparative Genomics Identifies a Flagellar and Basal Body Proteome that Includes the BBS5 Human Disease Gene. Cell *117*: 541-552.

Liu, S., W. Lu, T. Obara, S. Kuida, J. Lehoczky, K. Dewar, I.A. Drummond, I. A., and D.R. Beier. 2002. A defect in a novel Nek-family kinase causes cystic kidney disease in the mouse and in zebrafish. Development *129*: 5839-5846.

Lohret, T.A., F.J. M^{c}Nally and L.M. Quarmby. 1998. A role for katanin-mediated axonemal microtubule severing in *Chlamydomonas* deflagellation. Mol. Biol. Cell *9*: 1195-1207.

Lumbreras, V., D.R. Stevens, and S. Purton. 1998. Efficient foreign gene expression in *Chlamydomonas reinhardtii* mediated by an endogenous intron. Plant J. *14*: 441-448.

Mahjoub, M., B. Montpetit, L. Zhao, R.J. Finst, B. Goh, A.C. Kim and L.M. Quarmby 2002. The *FA2* gene of *Chlamydomonas* encodes a NIMA family kinase with roles in cell cycle progression and microtubule severing during deflagellation. J. Cell Sci. *115*: 1759-1768.

Matuliene, J., and R. Kuriyama. 2002. Kinesin-like protein CHO1 is required for the formation of midbody matrix and the completion of cytokinesis in mammalian cells. Mol. Biol. Cell. *13*: 1832-1845.

McGrath J., S. Somlo, S. Makova, X. Tian, M. Brueckner. 2003. Two populations of node monocilia initiate left-right asymmetry in the mouse. Cell *114*: 61-73.

Mesland, D.A., J.L. Hoffman, E. Caligor and U.W. Goodenough. 1980. Flagellar tip activation stimulated by membrane adhesions in *Chlamydomonas* gametes. J. Cell Biol. *84*: 599-617.

Morris, N.R., and A.P. Enos. 1992. Mitotic gold in a mold: Aspergillus genetics and the biology of mitosis. Trends Genet. *8*: 32-37.

Musgrave, A. and H. van den Ende. 1987. How *Chlamydomonas* court their partners. Trends Biochem. Sci. *12*: 470-473.

Mykytyn K. and V.C. Sheffield. 2004. Establishing a connection between cilia and Bardet-Biedl Syndrome. Trends Mol. Med. *10*: 106-109.

Nauli, S.M., F.J. Alenghat, Y. Luo, E. Williams, P. Vassilev, X. Li, A.E. Elia, W. Lu, E.M. Brown, S.J. Quinn, et al. 2003. Polycystins 1 and 2 mediate mechanosensation in the primary cilium of kidney cells. Nat. Genet. *33*:129–137

Noguchi K., H. Fukazawa, Y. Murakami, and Y. Uehara. 2002. Nek11, a new member of the NIMA family of kinases, involved in DNA replication and genotoxic stress responses. J Biol Chem. *277*: 39655-39665.

O'Connell, M. J., M.J.E. Krien and T. Hunter. 2003. Never say never. The NIMA-related protein kinases in mitotic control. Trends Cell Biol., *13*: 221-228.

Ong, A.C. and D.N. Wheatley. 2003. Polycystic kidney disease--the ciliary connection. Lancet *361*: 774-776.

Pan, J., Q. Wang, and W.J. Snell. 2004. An aurora kinase is essential for flagellar disassembly in *Chlamydomonas*. Dev. Cell *6*: 445-451.

Parker, J.D.K. and L.M. Quarmby. 2003. *Chlamydomonas fla* mutants reveal a link between deflagellation and intraflagellar transport. BMC Cell Biology. *4*: 11.

Pazour, G.J., B.L. Dickert, and G.B. Witman. 1999. The DHC1b (DHC2) isoform of cytoplasmic dynein is required for flagellar assembly. J. Cell Biol., *144*: 473-481.

Pazour, G.J. and G.B. Witman. 2003. The vertebrate primary cilium is a sensory organelle. Curr. Opin. Cell Biol. *15*: 105-110.

Pedersen, L.B., S. Geimer, R.D. Sloboda, and J.L. Rosenbaum. 2003. The microtubule plus end-tracking protein EB1 is localized to the flagellar tip and basal bodies in *Chlamydomonas reinhardtii.* Curr. Biol. *13*: 1969-1974.

Porter, M.E., R. Bower, J.A. Knott, P. Byrd, and W. Dentler. 1999. Cytoplasmic dynein heavy chain 1b is required for flagellar assembly in *Chlamydomonas.* Mol. Biol. Cell *10*: 693-712.

Praetorius, H.A., J. Frokiaer, S. Nielsen and K.R. Spring. 2003. Bending the primary cilium opens Ca2+-sensitive intermediate-conductance K^+ channels in MDCK cells. J. Membr. Biol. *191*: 193-200

Pu, R. T., G. Xu, L. Wu, J. Vierula, K. O'Donnell, X.S. Ye, and S.A. Osmani. 1995. Isolation of a functional homolog of the cell cycle-specific protein kinase NIMA of *Aspergillus nidulans* and functional analysis of conserved residues. J. Biol. Chem., *270*: 18110-18116.

Quarmby, L.M. (2004). Cellular deflagellation. *Int Rev Cytol* 233, 47-91.

Rosenbaum, J.L. and G.B. Witman. 2002. Intraflagellar transport. Nat. Rev. Mol. Cell Biol. *3*: 813-825.

Saito, T. and Y. Matsuda. 1991. Isolation and characterization of *Chlamydomonas* temperature-sensitive mutants affecting gametic differentiation under nitrogen-starved conditions. Curr. Genet. *19*: 65-71.

Salisbury, J.L., A.T. Baron, and M.A. Sanders. 1988. The centrin-based cytoskeleton of *Chlamydomonas reinhardtii*: Distribution in interphase and mitotic cells. J. Cell Biol. *107*: 635-641.

Sanders, M.A. and J.L. Salisbury. 1989. Centrin-mediated microtubule severing during flagellar excision in *Chlamydomonas reinhardtii.* J Cell Biol. *108*:1751-1760.

Schneider, L., Hoffman, E.K., Satir, P., and Christensen, S.T. (2003). A mechanism

for growth arrest control in the primary cilium based on PDGR-alpha. Mol. Biol. Cell *14*, 323a.

Silflow, C.D. and P.A. Lefebvre. 2001. Assembly and motility of eukaryotic cilia and flagella. Lessons from *Chlamydomonas reinhardtii.* Plant Physiol. *127*: 1500-1507.

Sun, Z., A. Amsterdam, G.J. Pazour, D.G. Cole, M.S. Miller, N. Hopkins. 2004. A genetic screen in zebrafish identifies cilia genes as a principal cause of cystic kidney. Dev. Biol. *In press.*

Surpili, M.J., T.M. Delben and J. Kobarg. 2003. Identification of proteins that interact with the central coiled-coil region of the human protein kinase NEK1. Biochemistry *42*: 15369-15376.

Tomas, A., C. Futter, and S.E. Moss. 2004. Annexin 11 is required for midbody formation and completion of the terminal phase of cytokinesis. J. Cell Biol. *165*: 813-822.

Tucker, R.W., and A.B. Pardee. 1979. Centriole ciliation is related to quiescence and DNA synthesis in 3T3 cells. Cell. *17*:527-535.

Twomey C, S.L. Wattam, MR, Rapley J, Baxter JE, Fry AM. 2004. Nek2B stimulates zygotic centrosome assembly in Xenopus laevis in a kinase-independent manner. Dev. Biol. *265*: 384-398.

Umen, J.G. and U.W. Goodenough. 2001. Control of cell division by a retinoblastoma protein homolog in *Chlamydomonas*. Genes and Dev. *15*: 1652-1661.

Upadhya, P., E.H. Birkenmeier, C.S. Birkenmeier and J.E. Barker. 2000. Mutations in a NIMA-related kinase gene, *Nek1*, cause pleiotropic effects including a progressive polycystic kidney disease in mice. Proc. Nat. Acad. Sci. (U.S.A.) *97*: 217-221.

Wang, D., J.F. Harper, and M. Gribskov. 2003. Systematic trans-genomic comparison of protein kinases between *Arabidopsis* and *Saccharomyces cerevisiae*. Plant Physiol.*132*: 2152-2165.

Wheatley, D.N., A.M. Wang, and G.E. Strugnell. 1996. Expression of primary cilia in mammalian cells. Cell Biol. Int. *20*:73–81

Wilson, P.D. 2004. Polycystic kidney disease. N. Engl. J. Med. *350*: 151-164.

Witman, G.B. 1986. Isolation of *Chlamydomonas* flagella and flagellar axonemes. Methods Enzymol. *134*: 280-290.

Wloga, D., Camba, A., Rogowski, K., Manning, G., Jerka-Dziadosz, M., Gaertig, J. 2006. Members of the NIMA-related kinase family promote disassembly of cilia by multiple mechanisms. Mol. Biol. Cell. *17*: 2799-2810.

Yin, M.J., L. Shao, D. Voehringer, T. Smeal, and B. Jallal. 2003. The serine/threonine kinase Nek6 is required for cell cycle progression through mitosis. J. Biol. Chem. *278*: 52454-52460

CHAPTER 3:

NIMA-Related Kinases Defective in Murine Models of Polycystic Kidney Disease Localize to Primary Cilia and Centrosomes

The following chapter has been published in the Journal of American Society of Nephrology (2005), Vol 16, 3485-3489. The authors of the paper were as follows:

Moe R. Mahjoub*, Melissa L. Trapp*, and Lynne M. Quarmby

Department of Molecular Biology and Biochemistry, Simon Fraser University, Burnaby, British Columbia, Canada V5A 1S6

* These authors contributed equally to this work.

As co-author, I performed all of the experiments and prepared the figures presented in this study. M.L. Trapp assisted with experiments, maintained cell-lines in culture, and prepared the manuscript. L.M. Quarmby was heavily involved in the conception and design of experiments, analysis of data, as well as the writing of the manuscript.

3.1 Abstract

A key feature of the polycystic kidney diseases is aberrant cell proliferation, a consequence of dysfunctional ciliary signaling. The NIMA-related kinases (Nek) Nek1 and Nek8 carry the causal mutations of two of the eight established mouse models of polycystic kidneys. Nek proteins have roles in cell cycle and may contribute to coordinate regulation of cilia and cell-cycle progression. Herein is reported that in a mouse kidney epithelial cell line, mNek1 localizes to centrosomes in interphase and remains associated

with the mitotic spindle pole during mitosis. In contrast, mNek8 localizes to the proximal region of the primary cilium and is not observed in dividing cells. Knockdown of mNek8 by siRNA does not affect ciliary assembly. Taken together with the phenotypes of the mutant mice, these data suggest that mNek1 and mNek8 provide links between cilia, centrosomes, and cell-cycle regulation.

3.2 Introduction

Polycystic kidney disease (PKD) is one of the most common genetic diseases and has a highly variable pathology involving aberrant cell proliferation in the kidney and in other organ systems, such as the liver and the pancreas. Evidence that renal cyst formation is caused by defects in ciliogenesis or ciliary function is substantial (Pazour, 2004). Most dramatically, failure to assemble a primary cilium leads to polycystic pathology in mice (Pazour *et al.*, 2000). In addition, several of the proteins that are implicated in renal cyst formation localize to cilia and/or basal bodies, including polycystin-1 and polycystin-2, which are responsible for autosomal dominant PKD, and fibrocystin- 1, which is responsible for autosomal recessive PKD (Pazour, 2004).

Murine models that contain spontaneously arising mutations have served to identify many of the genes that are involved in the polycystic pathology and to form causal associations between gene and phenotype. Seven proteins have been implicated in eight of the mouse models: Cystin in *cpk*, bicaudal C in *bpk* and *jcpk*, polaris/IFT88 in *orpk*, inversin in *inv*, NPHP3 in *pcy*, Nek1 in *kat*, and Nek8 in *jck* mice (Guay-Woodford, 2003). Nek1 and Nek8 are members of the NIMA-related kinase (Nek) family. Neks are cell cycle kinases that seem to have co-evolved with the bifunctional use of centrioles as spindle poles and basal bodies (Quarmby and Mahjoub, 2005; O'Connel *et al.*, 2003). For

example, the founding member of the Nek family, NIMA, is essential for mitotic entry in *Aspergillus nidulans* (Osmani *et al.*, 1991), and the mammalian Nek2 is involved in centrosome separation and bipolar spindle formation (Faragher and Fry, 2003).

The roles of Neks in ciliary regulation have been studied in the unicellular biciliate *Chlamydomonas reinhardtii* and the ciliated protozoan *Tetrahymena thermophila* (reviewed in Quarmby and Mahjoub, 2005; Quarmby and Parker, 2005). The *Chlamydomonas* Nek Fa2p, which is essential for $Ca2^{+}$-mediated axonemal microtubule severing, is located at a specific region of the proximal cilium, the site of flagellar autotomy (SOFA) (Mahjoub *et al.*, 2004). Several *Tetrahymena* Neks and the *Chlamydomonas* Nek Cnk2p are localized to cilia and regulate ciliary length (Quarmby and Mahjoub, 2005; Bradley and Quarmby, 2005). In addition to their roles in the regulation of cilia, Fa2p and Cnk2p affect the cell cycle. Cells that lack Fa2p have a G_2/M cell-cycle delay and, Cnk2p affects cell size control (Quarmby and Parker, 2005). The dual roles of the Fa2p and Cnk2p kinases, taken together with the murine PKD phenotypes of Nek1 and Nek8 mutations, suggest that Neks are a direct link between cilia and centrosomes and the aberrant cell proliferation of cystic kidneys.

Here we report the localization of endogenous murine Nek1 and Nek8 (mNEK1 and mNEK8) in an inner medullary collecting duct (IMCD-3) cell line. mNek1 was observed in multiple foci associated with the centrosomes during interphase and remained associated with the microtubule organizing center at the mitotic spindle pole. In contrast, the mNek8 signal was restricted to the proximal region of the primary cilia during interphase and was not observed during mitosis. siRNA knockdown of mNek8 resulted in loss of an immunofluorescence signal at the cilia but did not affect ciliary

assembly. These data support the idea that mNek1 and mNek8 are involved in ciliary cell-cycle signaling.

3.3 Materials and Methods

3.3.1 Cell Culture, Synchrony, and Immunofluorescence

IMCD-3 cells were grown in a 1:1 mixture of DMEM and Ham's F12 medium supplemented with 10% FBS (all from Life Technologies, BRL, Auckland, New Zealand). For synchrony, cells that were grown to approximately 50% confluence were incubated with 2 mM thymidine for 18 h and then rinsed briefly with PBS. Cells were incubated with regular growth medium for 14 h, and samples were taken at 2-h intervals. For indirect immunofluorescence, cells were fixed with ice-cold methanol and incubated at -20°C for 10 min, then rehydrated in PBS. The primary antibodies used include rabbit polyclonal anti-mNek1 (diluted 100-fold) and anti-mNek8 (diluted 100-fold [Liu *et al.*, 2002]), mouse monoclonal anti–γ tubulin (clone GTU-88, diluted 1000-fold; Sigma-Aldrich, St. Louis, MO), mouse monoclonal anti-acetylated tubulin (clone 6–11B-1, diluted 10,000-fold; Sigma-Aldrich), and human autoimmune serum M4491 (diluted 3000-fold [Mack *et al.*, 1998]). The secondary antibodies used include Alexa Fluor 488–conjugated goat anti-rabbit IgG (diluted 1000-fold; Molecular Probes, Eugene, OR), Alexa Fluor 594– conjugated goat anti-mouse IgG (diluted 2000-fold; Molecular Probes), Alexa Fluor 594–conjugated goat anti-human IgG (diluted 500-fold; Molecular Probes), and Cy5-conjugated goat anti-mouse IgG (diluted 500-fold; Southern Biotech, Birmingham, AL). All antibody incubations were done at room temperature for 1 h, followed by a wash in PBS. Cell nuclei were stained with 4'-6-diamidino-2-phenylindole for 10 min and coverslips were mounted using Mowiol (Calbiochem, San Diego, CA).

Immunofluorescence microscopy was performed using the Delta Vision system (Applied Precision, Issaquah, WA) as described previously (Mahjoub *et al.*, 2004).

3.3.2 RNA Interference

The siGENOME SMARTpool reagent that contains four different siRNA duplexes that target mNek8 (Dharmacon catalogue no. M-044403- 00) was used to transfect IMCD-3 cells according to the manufacturer's instructions. Untransfected and mock-transfected cells were used as negative controls. Cells were transfected for 24, 48, 72, and 96 h, harvested; and processed as described above.

3.3.3 Western Analysis

IMCD-3 cells were grown to confluence, harvested, and resuspended 1X SDS sample buffer. Immunoblot analysis using rabbit anti-mNek1 (diluted 2000-fold) was performed as described previously (Mahjoub *et al.*, 2004).

3.4 Results and Discussion

3.4.1 mNek1 Localizes to Centrosomes during Interphase and Mitosis

IMCD-3 cells that were stained with polyclonal rabbit anti-mNek1 antibodies showed multiple puncta associated with centrosomes during interphase (Figure 3-1A). In general, we observed more mNek1 foci surrounding the daughter centriole than the mother centriole, which nucleates a cilium. Similar staining was observed in the mouse fibroblast line NIH 3T3 and in the human embryonic kidney cell line HEK 293 (data not shown). During mitosis, mNek1 staining remained associated with the centrosomes in metaphase, anaphase, and cytokinesis (Figure 3-1A).

The multiple foci of mNek1 suggest that it is not a component of the centriole itself. To resolve whether mNek1 localization was specific to pericentriolar material, IMCD-3 cells were costained with Nek1 and a human autoimmune serum (M4491) that is known to stain the pericentriolar proteins CEP 110, ninein, pericentrin/kendrin, and CEP 250 (Mack e al., 1998; Ou and Rattner, 2000). The Nek1 foci appear outside the pericentriolar material (PCM) tube stained by the M4491 serum in IMCD-3 cells (Figure 3-1B) and HeLa cells (data not shown). The spatial localization relative to the M4491-stained PCM tube suggests that mNek1 could be a component of pericentriolar satellites. PCM-1 has been localized to centriolar satellites in a microtubule-dependent manner and is involved in centriolar duplication (Kubo *et al.*, 1999). However, PCM-1 dissociates from centrosomes during mitosis (Kubo *et al.*, 1999), whereas mNek1 remains associated.

3.4.2 mNek8 Localizes to Primary Cilia during Interphase but is not Observed during Mitosis

Indirect immunofluorescence of endogenous mNek8 revealed a specific signal that usually is restricted to the proximal region of primary cilia in IMCD-3 cells during interphase (Figure 3-2). We observed the same localization in NIH 3T3 cells (data not shown). A quantitative analysis revealed that mNek8 was present in the cilia of 96% of ciliated cells. During mitosis, no specific mNek8 staining was observed in cells that were undergoing metaphase, anaphase, or cytokinesis (Figure 3-2).

The ciliary localization of mNek8 is reminiscent of other proteins that are implicated in PKD. Polycystin-1 and polycystin- 2 are found within primary cilia (Pazour *et al.*, 2002; Yoder *et al.*, 2002), as well as fibrocystin- 1 (Ward *et al.*, 2003; Wang *et al.*,

2004), polaris, and cystin (Yoder *et al.*, 2002). The localization of mNek8 is also similar to Fa2p, which localizes to the base of the cilia at the SOFA in *Chlamydomonas* and when exogenously expressed in IMCD-3 cells (Mahjoub *et al.*, 2004). However, the mNek8 signal labels a broader region of the cilium than the tightly focused Fa2p signal.

3.4.3 Knockdown of mNek8 does not Affect Cilia Formation

Renal cyst formation as a result of failure to assemble cilia is often accompanied by pleiotropic pathologies. This is apparent in the *orpk* mouse model, in which a hypomorphic allele of polaris/IFT88, encoding a component of the intraflagellar transport machinery, is defective in ciliary assembly (Pazour at al., 2000). Because mNek8 localized to the cilia, we hypothesized that it could play a role in ciliary assembly. siRNA that targeted Nek8 was transfected into IMCD-3 cells, and mNek8 knockdown was measured at 96 h after transfection. There was a dramatic decrease in the ciliary staining of mNek8 in cells that were treated by siRNA (Figure 3-3A), in which only 34% of ciliated cells contained mNek8 *versus* 96% of untransfected and 94% of mock-transfected cells (Figure 3-3B). However, the percentage of ciliated cells (~90%) in the population did not change when compared with the negative controls. Staining at the plasma membrane was still observed in knockdown cells, suggesting non-specific staining by the polyclonal mNek8 antibody. Western blot analysis of cellular protein indicated knockdown of mNek8 protein below detectable levels (data not shown).

The mNek8 knockdown indicates that ciliogenesis is unaffected by loss of ciliary mNek8 and suggests that mNek8 function is not essential for cilia assembly. The *jck* mutation is a single amino acid substitution in the C-terminus of mNek8 (Liu *et al.*, 2002), and only the kidneys are affected (Atala *et al.*, 1993), unlike other models, in

which multiple organ systems are defective. Taken with our findings that mNek8 knockdown does not affect ciliogenesis strongly suggests that mNek8 is involved in a signaling role specific to the kidney.

Our discovery that mNek1 is centrosomal and mNek8 is ciliary completes the subcellular localization studies of the seven proteins identified in the mouse models of cystic kidney disease. It is interesting that mNek1 is the only gene product of these mouse models that does not localize to the primary cilia. Many of the proteins that are implicated in renal cyst formation are not members of conserved protein families; polycystin-1 and fibrocystin-1 are novel integral membrane proteins (Inter. Poly. Kidney Cons., 1995; Ward *et al.*, 2002), polycystin-2 is a novel cation channel (Mochizuki *et al.*, 1996), cystin is a novel lipid-anchored membrane protein (Hou *et al.*, 2002), and inversin is a novel protein that contains ankyrin repeats and calmodulin-binding motifs (Mochizuki *et al.*, 1998). PKD is a ciliopathy that results in aberrant cell proliferation; therefore, conserved ciliary and cell-cycle proteins are expected to contribute to the mechanism of disease. mNek1 and mNek8 are excellent candidates because they are members of a cell-cycle kinase family that is conserved throughout ciliated eukaryotes, and, as shown here, they localize to basal bodies and cilia. Considering Fa2p and Cnk2p and their roles in regulating ciliary function and cell-cycle progression, Neks may provide a common link between cilia and cell cycle regulation, although the cellular mechanisms remain to be established.

An important aspect of elucidating the signal transduction pathway may lie in identification of modifying loci, as genetic background greatly influences the variable PKD phenotype. Although PKD1, PKD2, and PKHD1 are the genes that are responsible

for PKD, the age of onset and disease severity are highly variable and are affected by additional germline and somatic mutations (Pei, 2003). It is possible that hNek1 and hNek8 are important modifiers of PKD.

3.5 Acknowledgments

This work was funded by an operating grant from the Canadian Institutes of Health Research (MOP 37861) to L.M.Q. M.R.M. and M.L.T are supported by graduate fellowships from the Michael Smith Foundation for Health Research and the Natural Sciences and Engineering Research Council of Canada.

We are deeply indebted to David Beier for the mNek8 antibody, Yumay Chen for the mNek1 antibody, and Jerome Rattner for the M4491 anti-serum. We also thank Michel Leroux and his laboratory members for the use of their facilities.

3.6 Figures

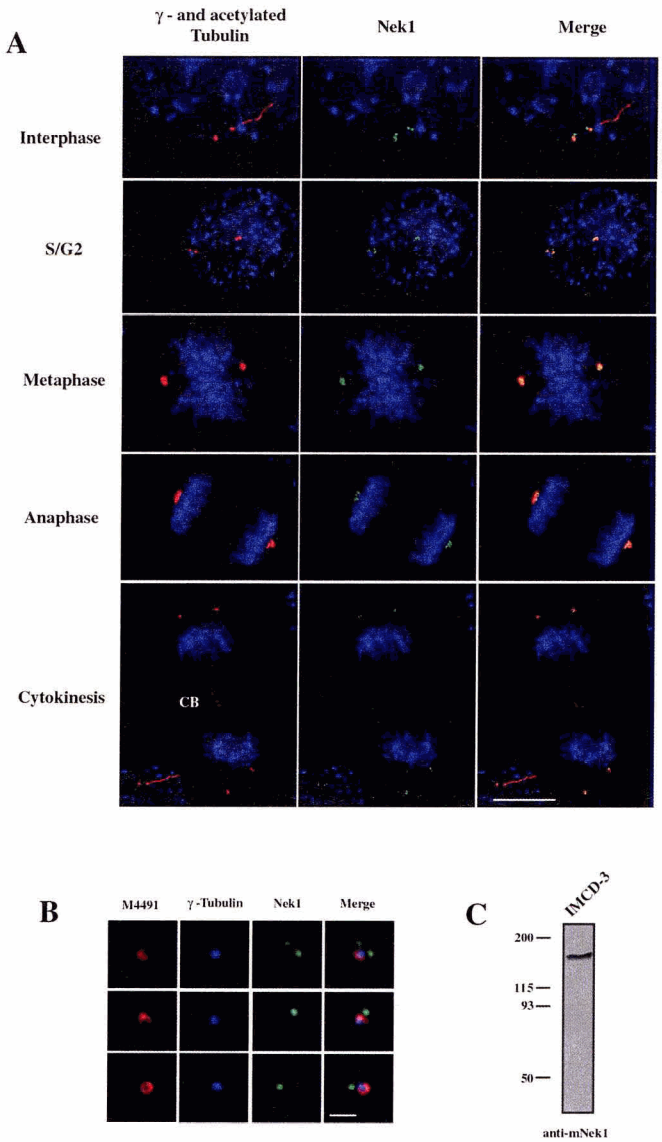

Figure 3-1 Murine NIMA-related kinase 1 (mNek1) is localized to centrosomes throughout the cell cycle.

(A) Synchronized inner medullary collecting duct-3 (IMCD-3) cells were stained with antibodies against γ- and acetylated tubulin (red) to mark the positions of the centrioles and the cilia, respectively. mNek1 (green) was detected using a rabbit polyclonal antibody, and DNA was stained with 4'-6-diamidino-2-phenylindole (blue). CB, cytoplasmic bridge. Bar = 5 μm. (B) To refine the centrosomal localization of mNek1, IMCD-3 cells were stained with the centrosome-reactive human autoimmune serum M4491 (red), which identifies the pericentriolar material (PCM) tube (Mack *et al.*, 1998; Ou and Rattner, 2000). Cells were co-stained with antibodies against γ-tubulin (blue) and mNek1 (green). Bar = 1 μm. (C) Western analysis of IMCD-3 cells showing anti-mNek1 antibody specificity. A single band of expected molecular weight (approximately 143 kDa) is observed after incubation with the rabbit anti-mNek1 antibody.

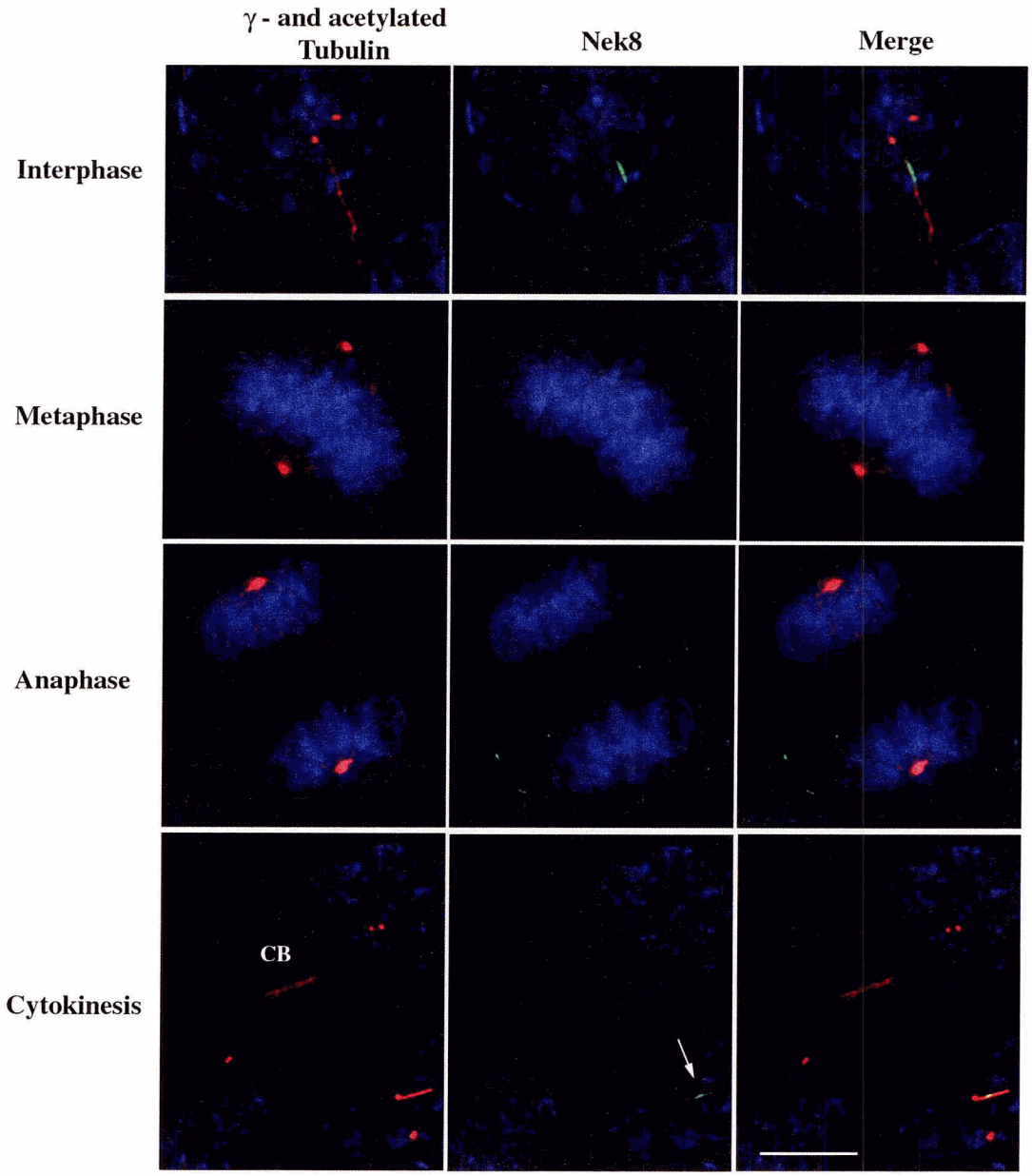

Figure 3-2 mNek8 is localized to the proximal region of primary cilia during interphase. Synchronized IMCD-3 cells were stained for γ- and acetylated tubulin (red), mNek8 (green), and DNA (blue). No mNek8 signal was detected during mitosis and appears only in ciliated cells in interphase (interphase panel and arrow in cytokinesis panel). Bar = 5 μm.

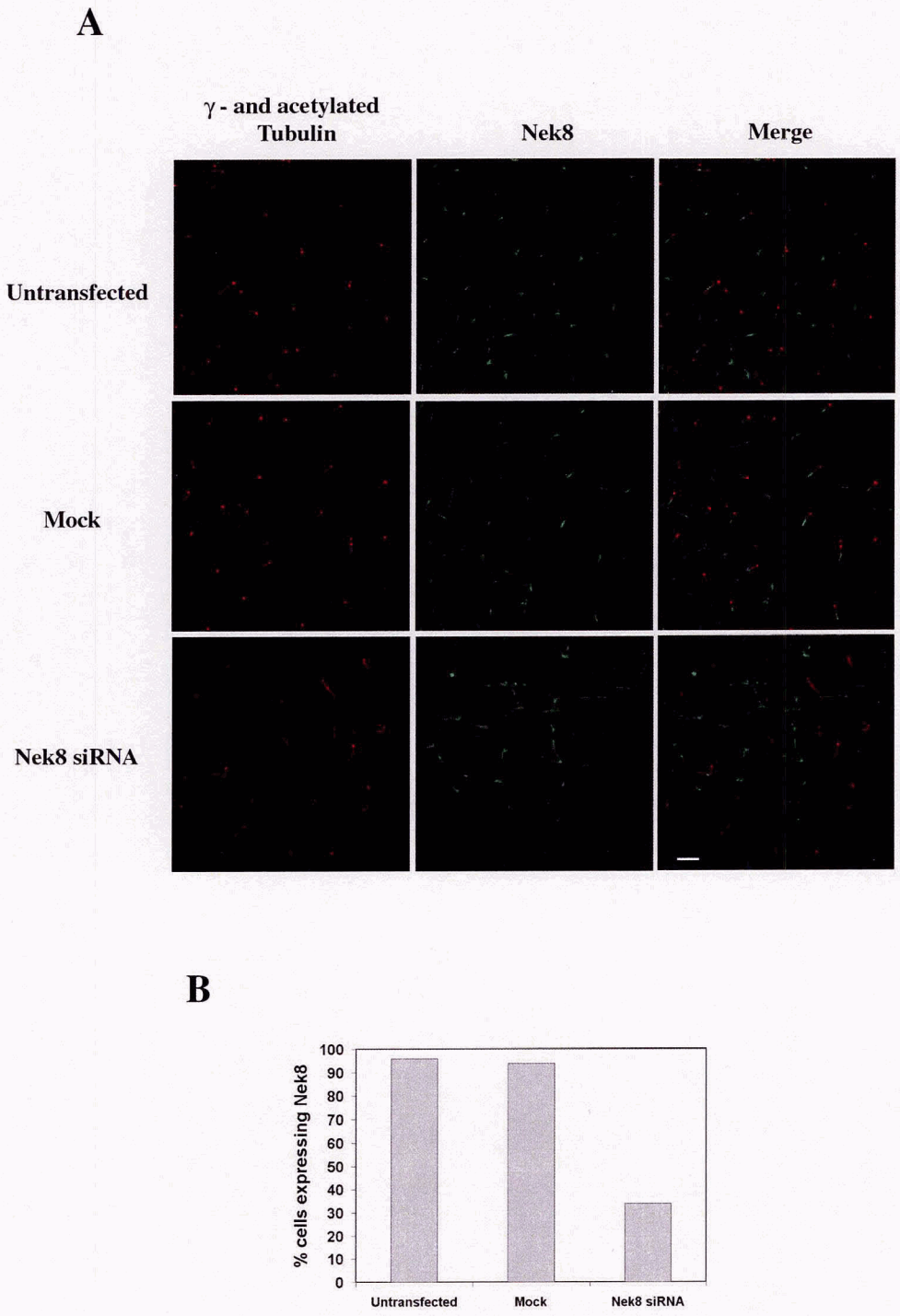

Figure 3-3 siRNA knockdown of mNek8 does not affect ciliogenesis.
(A) IMCD-3 cells were transfected with siRNA targeting mNek8 and incubated for 96 h. Cells were stained with antibodies against γ- and acetylated tubulin (red) and mNek8 (green). Bar = 5 μm. (B) Quantification of mNek8 loss from cilia. Two hundred cells from each experimental sample were analyzed for the presence of mNek8 signal in the cilium.

3.7 Reference List

Atala A, Freeman MR, Mandell J, Beier DR: Juvenile cystic kidneys (jck) (1993). A new mouse mutation which causes polycystic kidneys. *Kidney Int* 43: 1081–1085.

Bradley BA, Quarmby LM (2005). A NIMA-related kinase, Cnk2p, regulates both flagellar length and cell size in *Chlamydomonas*. *J Cell Sci* 118: 3317–3326.

Faragher AJ, Fry AM (2003). Nek2A kinase stimulates centrosome disjunction and is required for formation of bipolar mitotic spindles. *Mol Biol Cell* 14: 2876–2889.

Guay-Woodford LM (2003). Murine models of polycystic kidney disease: Molecular and therapeutic insights. *Am J Physiol Renal Physiol* 285: F1034–F1049.

Hou X, Mrug M, Yoder BK, Lefkowitz EJ, Kremmidiotis G, D'Eustachio P, Beier DR, Guay-Woodford LM (2002). Cystin, a novel cilia-associated protein, is disrupted in the cpk mouse model of polycystic kidney disease. *J Clin Invest* 109: 533–540.

Kubo A, Sasaki H, Yuba-Kubo A, Tsukita S, Shiina N (1999). Centriolar satellites: Molecular characterization, ATP-dependent movement toward centrioles and possible involvement in ciliogenesis. *J Cell Biol* 147: 969–980.

Liu S, Lu W, Obara T, Kuida S, Lehoczky J, Dewar K, Drummond IA, Beier DR (2002). A defect in a novel Nek-family kinase causes cystic kidney disease in the mouse and in the zebrafish. *Development* 129: 5839–5846.

Mack GJ, Rees J, Sandblom O, Balczon R, Fritzler MJ, Rattner JB (1998). Autoantibodies to a group of centrosomal proteins in human autoimmune sera reactive with the centrosome. *Arthritis Rheum* 41: 551–558.

Mahjoub MR, Rasi MQ, Quarmby LM (2004). A NIMA-related kinase, Fa2p, localizes to a novel site in the proximal cilia of *Chlamydomonas* and mouse kidney cells. *Mol Biol Cell* 15: 5172–5286.

Mochizuki T, Saijoh Y, Tsuchiya K, Shirayoshi Y, Takai S, Taya C, Yonekawa H, Yamada K, Nihei H, Nakatsuji N, Overbbek PA, Hamada H, Yokoyama T (1998). Cloning of inv, a gene that controls left/right asymmetry and kidney development. *Nature* 395: 177–181.

Mochizuki T, Wu G, Hayashi T, Xenophontos SL, Veldhuisen B, Saris JJ, Reynolds DM, Cai Y, Gabow PA, Pierides A, Kimberling WJ, Breuning MH, Deltas CC, Peters DJ Somlo S (1996). PKD2, a gene for polycystic kidney disease that encodes an integral membrane protein. *Science* 272: 1339–1342.

O'Connell MJ, Krien MJE, Hunter T (2003). Never say never. The NIMA-related protein kinases in mitotic control. *Trends Cell Biol* 13: 221–228.

Osmani AH, O'Donnell K, Pu RT, Osmani SA (1991). Activation of the nimA protein kinase plays a unique role during mitosis that cannot be bypassed by absence of the bimE checkpoint. *EMBO J* 10: 2669–2679.

Ou Y, Rattner JB (2000). A subset of centrosomal proteins are arranged in a tubular conformation that is reproduced during centrosome duplication. *Cell Motil Cytoskeleton* 47: 13–24.

Pazour GJ (2004). Intraflagellar transport and cilia-dependent renal disease: The ciliary hypothesis of polycystic kidney disease. *J Am Soc Nephrol* 15: 2528–2536.

Pazour GJ, San Agustin JT, Follit JA, Rosenbaum JL, Witman GB (2002). Polycystin-2 localizes to kidney cilia and the ciliary level is elevated in orpk mice with polycystic kidney disease. *Curr Biol* 12: R378–R380.

Pazour GJ, Dickert BL, Vucica Y, Seeley ES, Rosenbaum JL, Witman GB, Cole DG (2000). *Chlamydomonas* IFT88 and its mouse homologue, polycystic kidney disease gene Tg737, are required required for assembly of cilia and flagella. *J Cell Biol* 151: 709–718.

Pei Y (2003). Molecular genetics of autosomal dominant polycystic kidney disease. *Med Clin Exp* 26: 252–258.

Quarmby LM, Mahjoub MR (2005) Caught Nek-ing: Cilia and centrioles. *J Cell Sci* 118: 5161-5169.

Quarmby LM, Parker JDK (2005). Cilia and the cell cycle? *J Cell Biol* 169: 707–710.

The International Polycystic Kidney Disease Consortium (1995). Polycystic kidney disease: The complete structure of the PKD1 gene and its protein. *Cell* 81:289 – 298.

Wang S, Luo Y, Wilson PD, Witman GB, Zhou J (2004). The autosomal recessive polycystic kidney disease protein is localized to primary cilia, with concentration in the basal body area. *J Am Soc Nephrol* 15: 592–602.

Ward CJ, Hogan MC, Rossetti S, Walker D, Sneddon T, Wang X, Kubly V, Cunningham JM, Bacallao R, Ishibashi M, Milliner DS, Torres VE, Harris PC (2002). The gene mutated in autosomal recessive polycystic kidney disease encodes a large, receptor-like protein. *Nat Genet* 130: 259 – 269.

Ward CJ, Yuan D, Masyuk TV, Wang X, Punyashthiti R, Whelan S, Bacallao R, Torra R, LaRusso NF, Torres VE, Harris PC (2003). Cellular and subcellular localization of the ARPKD protein; fibrocystin is expressed on primary cilia. *Hum Mol Genet* 12: 2703–2710.

Yoder BK, Hou X, Guay-Woodford LM (2002). The polycystic kidney disease proteins, polycystin-1, polycystin-2, polaris, and cystin, are co-localized in renal cilia. *J Am Soc Nephrol* 13: 2508–2516.

CHAPTER 4:

Identification of Fa2p-interacting Proteins

4.1 Introduction

We have shown that Fa2p is localized to a specific region at the proximal end of cilia (the SOFA) during interphase, accumulates at the centriole/basal body prior to mitosis, and back at the SOFA at the onset of ciliogenesis in G_1 (Mahjoub *et al.*, 2004). This data raises some interesting questions: How is Fa2p targeted to the SOFA? What is the mechanism by which Fa2p is localized distinctly at the SOFA and restricted from assembling along the entire length of the axoneme? With what protein(s) is Fa2p interacting at the SOFA? Does Fa2p interact directly with the axonemal microtubules? Furthermore, we previously showed that Fa2p plays essential kinase-dependent roles in ciliary shedding, whereas it plays non-essential kinase-independent role(s) in mitosis (Mahjoub *et al.*, 2004). Although the ciliary and cell cycle activities of Fa2p may be unrelated, we hypothesize that Fa2p is part of a complex of proteins involved in the coordinate regulation of ciliary assembly/disassembly and cell cycle progression.

To shed some light on the role of Fa2p, I set out to identify proteins that interact with Fa2p and determine whether these proteins participate in deciliation, ciliogenesis, and cell cycle progression. Three approaches were used: (1) biochemical methods for purifying Fa2p and associated proteins; (2) molecular biological schemes to identify the SOFA-targeting sequence of Fa2p; (3) a genetic suppressor screen to identify

interactors/substrates of Fa2p. We predict that defining the activities of these proteins will reveal principles underlying sequential control of ciliogenesis and cell cycle progression.

4.2 Materials and Methods

4.2.1 Cell Strains and Culture

Wild-type *Chlamydomonas* strain cc137, mutant strains *pf2*, *pf6*, *pf9*, *pf14*, *pf16*, *pf20*, and *oda9* were obtained from the *Chlamydomonas* Genetics Center (Durham, NC). Rescue strain *fa2-1*;FA2HA, as well as B214;Cp60-HA were generated in our laboratory as described previously (Mahjoub *et al.*, 2004). Cells were maintained in liquid TAP medium or on plates containing 1.5% agar (Harris, 1989) at 22°C with constant illumination. All chemicals were purchased from Sigma-Aldrich (St. Louis, MO) unless otherwise indicated.

4.2.2 Axoneme Purification, Salt Extraction and Sucrose Gradients

Deflagellation was induced by dibucaine, and flagella were isolated as described previously (Witman, 1986). To purify axonemes, flagella were resuspended in buffer supplemented with 1% IGEPAL. For salt extractions, axonemes were pelleted by centrifugation, then resuspended at 10-16 mg/mL in HMEK buffer (10 mM HEPES, pH 7.4, 5 mM $MgSO_4$, 0.5 mM EDTA, 25 mM KCl, including protease inhibitor cocktail [Roche]) containing increasing concentrations of NaCl, KI or KCl (0.25 M, 0.3 M, 0.45 M, 0.5 M, and 0.6 M). Samples were centrifuged at 31,000Xg, and the salt extract was injected into a dialysis cassette (Pierce) and dialysed against 1L of HMEK buffer for 1, 2, 3 or 4 hours at 4°C. Samples were removed from the cassette, cleared by centrifugation at

31,000Xg, and 500 µL was loaded onto a 6mL 4-24% sucrose gradient. Sedimentation standards were loaded onto a parallel gradient and included BSA (4.4S, ~70 kDa), aldolase (7.3S, ~166 kDa), catalase (11.3S, ~250 kDa) and thyroglobulin (19.4S, ~670 kDa). Samples were spun overnight at 100,000Xg (30,000 rpm in a SW41 rotor; Beckman) at 4°C. 20 fractions were collected, and 40 µL aliquots were loaded onto an 8% SDS-PAGE gel for Western analysis. Blots were probed with anti-Fa2p as previously described (Mahjoub *et al.*, 2004), stripped and reprobed with anti-IC140 antibody diluted 10,000-fold (Yang and Sale, 1998).

4.2.3 Chemical Cross-linking

Purified axonemes were resuspended at 3mg/mL in HMEK (10 mM HEPES, pH 7.4, 5 mM $MgSO_4$, 0.5 mM EDTA, 25 mM KCl, including protease inhibitor cocktail) supplemented with increasing concentrations of cross-linkers. These include the zero-length cross-linker EDC [1-Ethyl-3-(3-Dimethylaminopropyl) carbodiimide Hydrochloride], which generates zero-length cross-links between free carboxyls and primary amines; and homobifunctional compounds which react with primary amines DFDNB (1,5-difluoro-2,4-dinitrobenzene), DMP (dimethyl pimelimidate) and DSS (disuccinimidyl suberate). Samples were incubated on ice for 30min, and reactions were quenched by addition of SDS-PAGE sample buffer containing 0.5M 2-mercaptoethanol. 120µg of protein from each cross-linking reaction was loaded onto a 6% SDS-PAGE gel and Western analysis using anti-Fa2p and anti-HA was performed as previously described (Mahjoub *et al.*, 2004). In some experiments, blots were stripped with a ReBlot Plus kit (Chemicon International; Temecula, CA) and reprobed with monoclonal antibodies against α-tubulin (clone B-5-1-2, Sigma; diluted 100,000-fold), anti-centrin

(clone 20H5), anti-HA (clone 3F10; Roche) or anti-acetylated tubulin (clone 611B-1, Sigma; diluted 100,000-fold).

To concentrate axonemes for immunoprecipitation experiments, axonemes at 3mg/mL were incubated with 20mM EDC as described above. 20 reactions (each with 150µg total protein) were combined, the reaction quenched by addition of 0.5M 2-mercaptoethanol and axonemes were concentrated by sedimentation at 31,000Xg for 30min at 4° C. Next, axonemes were resuspended in HMEK + 0.6M KI at a final concentration of 6mg/mL and incubated on ice for 30min. The sample was sedimented at 31,000Xg for 30min at 4° C, and the salt extract was dialysed as described above.

4.2.4 Immunoprecipitation experiments

Immunoprecipitation was performed as described by Fowkes and Mitchell (1998), with slight modification. Briefly, 500µL of extract was mixed with an equal volume of ice-cold IP buffer (HMEK plus 100mM NaCl, 0.1% Triton-X-100 and protease inhibitor cocktail), and presorbed with 25µl of 50/50 (vol/vol) protein-A or protein-G agarose beads (Sigma) for 30min on ice. 50 µL of either affinity purified rabbit anti-Fa2p (Rb 10495; Mahjoub et al., 2004), rat anti-HA (clone 3F10, Roche), mouse anti-HA (clone HA-7, Sigma) or mouse anti-α-tubulin (clone B-5-1-2, Sigma) was then added to presorbed extracts and incubated for 3-4 hours at 4°C. A 100µL volume of 50/50 (vol/vol) protein-A or protein-G agarose in IP buffer was added, the tubes were mixed gently for 3-4 hours at 4° C. The agarose beads were sedimented and washed three times with 1mL IP buffer. Immune complexes were eluted by addition of 100µL of 2X SDS-PAGE sample buffer and incubated in boiling water for 2 min. Equal amounts of protein from pre-IP (Input), immunoprecipitated (IP) and unbound fractions were loaded onto a 6% or 15%

SDS-PAGE gel and probed with either rabbit anti-Fa2p (diluted 500-fold), rat anti-HA antibody (diluted 1000-fold), mouse anti-centrin (clone 20H5; diluted 20,000-fold) or mouse anti-α-tubulin (clone B-5-1-2, diluted 10,000-fold).

4.2.5 Axoneme Rebinding Assay

Axoneme rebinding assays were performed as previously described (Yokoyama *et al.*, 2004), with modification. Wild-type and *fa2-1*;FA2HA axonemes were extracted at 10mg/mL in 500μL HMEK containing 0.6M NaCl; the extract containing FA2p-HA was retained and dialysed against HMEK (this is referred to as FA2HA NaCl Ext. in Figure 4-7B), while the extracted axonemes from the wild-type strain were washed once with 500μL HMEK buffer (referred to as Extracted Wt Axo.). The wild-type axonemes were sedimented, then resuspended in the 500μL of FA2HA NaCl Ext., and incubated at room temperature for 30min to facilitate rebinding. Axonemes were sedimented at 31,000Xg, and the supernatant was transferred to a new tube. Rebound axonemes were resuspended in 500μL of HMEK, and 6X SDS-PAGE sample buffer was added to each sample and incubated in boiling water for 2 min. Axoneme-equivalent volumes from each fraction were loaded onto an 8% SDS-PAGE gel, and Western analysis was performed with the anti-HA antibody as described above.

4.2.6 Molecular Biology

Sequence analysis of the Fa2p amino acid sequence was performed using the SMART algorithm (Simple Modular Architecture Research Tool; http://smart.embl-heidelberg.de/). The cDNA expression vector pGenD was a generous gift from J.D. Rochaix (University of Geneva, Switzerland; Fisher and Rochaix, 2001). The

paromomycin resistance vector pSI103 was kindly provided by P.Hegemann (University of Regensburg, Germany; Sizova *et al.*, 2001) and the Zeomycin resistance gene pSP124S was provided by S. Purton (University College London, England; Lumbreras *et al.*, 1998).

To generate the cDNA expression vector, pGenD was linearized by digestion with restriction enzymes *Nde*I and and *EcoR*I. Next, *FA2* cDNA was PCR amplified using primers that introduce 5' *Nde*I and 3' *EcoR*I restriction sites (forward, 5'-GCACATATGATGGCCCCGCCTGCGCCT- 3' and reverse, 5'-GCAGAATTCCTTGGCGCTGGTGTAGTA-3'). The PCR fragment was digested with *Nde*I and *EcoR*I then ligated into the pGenD vector above to give pFA2cDNA. Next, the 3XHA fragment was PCR amplified with primers that incorporate 5' and 3' *EcoR*I restriction sites and a stop codon (forward, 5'-CTGAGAATTCTACCCCTACGACGTGCCCGAC- 3' and reverse, 5'-TGATATCGAATTCCTAGCCCGGGGGCCGGCG- 3') using p3XHA (a plasmid encoding 3 repeats of the 9-amino acid hemagglutinin epitope; Finst *et al.*, 2000) as template. The product was digested with *EcoR*I and ligated into the unique *EcoR*I site at the 3′ end of pFA2cDNA vector to yield vector pFA2cDNA-HA. The selectable marker conferring resistance to paromomycin (*par*) was excised from pSI103 using flanking *Spe*I restriction sites, and ligated to pFA2cDNA-HA at a unique *Spe*I site upstream of the *PsaD* 5'UTR. Finally, the selectable marker *ble* was excised from pSP124S using flanking *Hind*III restriction sites and ligated to pFA2cDNA-HA at a unique *Hind*III site downstream of the *PsaD* 3′ UTR.

To generate the pFA2genomic-HA construct, the pFA2 (*Sac*I-*Sal*I) genomic vector was used as template for PCR using primers that eliminate the *FA2* gene while retaining the 5' and 3' UTR's. The primers also incorporate a 5' *Nde*I and 3' *Bgl*II restriction site (forward, 5'- GAAAGATCTTAGGGGGACGGACAT-3' and reverse, 5'-GGTCATATGCATTGTTGTCGCTGA-3'). The 3XHA epitope tag was subsequently amplified by PCR using primers that incorporate 5' NdeI and 3' BglII restriction sites (forward, 5'-GGTCATATGTACCCCTACGACGTGCCCGAC- 3' and reverse, 5'-GAAAGATCTCTAGCCCGGGGGCCGGCG- 3'). The PCR product was digested with *Nde*I-*Bgl*II and ligated into the vector above to yield pFA2promoter-HA. Next, the ~3.5 kb fragment of *FA2* genomic DNA (from the Start to Stop codon) was PCR amplified with primers that incorporate *Nde*I restriction sites at the 5' and 3' ends. The PCR product was digested by *Nde*I then ligated into pFA2promoter-HA linearized by digestion with *Nde*I, to yield vector pFA2genomic-HA. Finally, the selectable marker *ble* was excised from pSP124S using flanking *Hind*III restriction sites and ligated to pFA2genomic-HA at a unique *Hind*III site upstream of the *FA2* 5' UTR.

Nuclear transformation was performed as described previously (Finst *et al.*, 1998). Transformants were selected on 1.5% TAP medium plates supplemented with Zeomycin and assayed by Western and for deflagellation as described previously (Mahjoub *et al.*, 2004).

4.2.7 Genetic Suppressor Screen

Mutagenesis was performed as described by Harper and colleagues (1995), with the following modifications. *fa2-3;KD-FA2* cells were grown asynchronously in liquid TAP media to early log phase (~1X10^6 cells/mL). 1X10^8 cells were harvested by

centrifugation, and resuspended in 15mL of 10mM HEPES buffer (pH 7.4). The mono-alkylating agent ethylmethane sulfonate (EMS, Sigma), which induces GC- to- AT transition mutations, was added from a freshly prepared stock to a final concentration of 150mM. Cells were incubated with EMS for 1 hour at room temperature on an orbital shaker. Cells were then gently spun down in clean 50mL Falcon tubes, resuspended in 50mL of fresh TAP media to wash away residual EMS. This wash step was repeated twice more, and the cells were resuspended in 50mL of TAP media. Cell concentration was determined using a hemacytometer, and cells were plated onto 1.5% TAP-agar medium so that with ~30% survival (compared to non-mutagenized cells) around 100-200 colonies were expected per plate. Colonies were allowed to grow at room temperature with constant illumination for 7 days.

To test for rescue of the deflagellation defect, a motility assayed was employed as previously described, with modification (Finst *et al.*, 1998). Specifically, individual mutagenized colonies were picked into 96-well plates (Fisher Scientific) containing 200μL liquid TAP medium. Each plate also contained one well inoculated with wild-type cells as control. Cells were then allowed to grow for another 24-48 hours. Next, 50μL from each well was transferred to a new 96-well plate, and cells were examined microscopically to determine whether they were swimming; any colonies that were not motile were discarded (these comprised of paralyzed flagella mutants, short flagella mutants and bald cells). This step ensures that no false positives are isolated in the next step. We then pH-shocked the cells by adding 50μL of acid solution (40mM sodium acetate + 1mM calcium chloride). The pH was immediately raised by adding 50μL of 60mM sodium bicarbonate to each well. Cells were again inspected microscopically to

determine if they were motile: the control cells shed their flagella due to the pH shock, and are therefore immotile. The *fa2-3;KD-FA2* cells do not shed their flagella, and start to swim vigorously after roughly 5 minutes. Any potential suppressors would therefore be immotile, as they would also shed their flagella due to the pH shock. Any potential suppressors were then retested and examined microscopically under high magnification, looking for cells that had shed their flagella and freely floating flagella.

4.3 Results

4.3.1 Fa2p is Mislocalized in Axonemes of Various Flagellar Mutants

Flagella are non-essential organelles in *Chlamydomonas*, hence a large collection of paralyzed flagellar (*pf*) mutants lacking various components of the flagellar apparatus have been generated (reviewed in Silflow and Lefebvre, 2001). These include mutants lacking some, or all, components of inner dynein arms, outer dynein arms, radial spokes, and central pair microtubules (Silflow and Lefebvre, 2001). I took advantage of some of these mutants to determine whether Fa2p is associated with one (or more) known components of axonemes. I reasoned that if Fa2p is lacking in axonemes isolated from a specific mutant, then Fa2p is most likely interacting with that complex of proteins.

Flagella were isolated from wild-type cells and a range of *pf* mutants and analysed by Western blot. Also, a fraction of the flagella from each mutant was demembranated (to remove the membrane and matrix proteins) and the axonemes analysed by Western. To our surprise, Fa2p was missing in mutant flagella lacking inner and outer dynein arms, radial spokes and central pair microtubules (Figure 4-1). Specifically, wild-type levels of Fa2p were observed in flagella and axonemes isolated from *pf6* (lacking long projection

on C1 tubule of the central pair; Rupp *et al.*, 2001) and *pf*16 (lacking the C1 tubule of the central pair; Smith and Lefebvre, 1996). However, Fa2p was missing from both flagella and axonemes of *pf*20 (Figure 4-1), which completely lacks the central pair microtubules (Smith and Lefebvre, 1997). Fa2p was also missing in *pf*14 (lacking radial spokes; Diener *et al.*, 1993), *pf*9 (inner dynein arm deficient; Myster *et al.*, 1997) and *oda*9 (lacking outer dynein arms; Wilkerson *et al.*, 1995) fractions. Interestingly, Fa2p was present in the flagella fraction, but missing in axonemes isolated from *pf*2 mutants (that lack a subunit of the dynein regulatory complex; Rupp and Porter, 2003). This suggested that, while Fa2p was present in the flagellar fraction from *pf*2 mutants, the protein is not anchored to the axoneme-proper as in wild-type. It is interesting to note that all of these mutants were able to deflagellate, suggesting that the aberrant localization of Fa2p in these cells did not abrogate its function during deflagellation (see Discussion).

The mislocalization of Fa2p in a variety of flagellar mutants was perplexing. To our knowledge, Fa2p is the first axonemal protein to show this general mislocalization pattern. Indeed, this method has been used successfully to identify the axonemal localization of various proteins, including protein phosphatases PP1 and PP2 (Yang *et al.*, 2000), a novel Tctex-related light chain (DiBella *et al.*, 2004), and various radial spoke and central pair associated proteins (Smith and Yang, 2004). It is possible that the protein (or complex of proteins) anchoring Fa2p to the axoneme is sensitive to perturbations of core axonemal proteins. This suggests that the Fa2p-associated complex is dependent on the proper assembly of the main axonemal proteins, however there is no data to support this theory. Thus, a more direct approach of identifying Fa2p-interacting proteins was required.

4.3.2 Salt Extraction and Sucrose Density Gradient Analysis

I previously showed that most of the Fa2 protein segregates with the flagellar fraction following deflagellation, and remains tightly associated with axonemes following removal of the flagellar membrane by detergent treatment (see Chapter 2, Figure 2-2). To determine whether Fa2p can be extracted from axonemes using salt-containing buffers, axonemes were harvested from wild-type or *fa2-1*;FA2HA strains and incubated with buffer containing increasing concentrations of NaCl (which has been shown to remove dynein arms but not radial spoke proteins) or KI (which extracts most proteins including radial spokes). I see that Fa2p is completely extracted from axonemes in the presence of 0.6M NaCl (Figure 4-2A).

The architecture of flagellar axonemes is such that most axonemal proteins assemble into larger complexes (Smith and Yang, 2004; Cole, 2003; King, 2003; Kamiya, 2002). Therefore, I wanted to determine whether the Fa2p-containing salt extract also contained protein(s) that may be interacting with Fa2p. I predicted that, following dialysis (to remove the salt), Fa2p would re-associate with these protein(s), which could subsequently be purified and identified. The dialyzed extract was fractionated on a 4-24% sucrose gradient, and fractions were analysed by Western blotting. Fa2p appeared to migrate around 4S, which is the sedimentation rate expected of the monomeric form of the protein (Figure 4-2B). If Fa2p was associated with other protein(s), I would have expected a shift in the sucrose gradient relative to the size of this protein complex. However, this was not observed, whereas the control protein, IC140 (Intermediate Chain of inner arm dynein; Yang and Sale, 1998) migrated as a complex of ~18S as expected (Figure 4-2B). This data suggested that Fa2p may not be associated

with a larger protein complex. However, there are alternative possibilities: (1) Although Fa2p was extracted with salt, the potential Fa2p-binding protein(s) might not, and hence the downstream analysis was incomplete; (2) Following extraction, Fa2p might lose the ability to rebind these protein(s), possibly due to protein misfolding; (3) The sucrose gradient fractionation step caused dissociation of Fa2p from its binding protein(s). Ultimately, an alternative approach to identifying Fa2p-associated proteins was needed.

4.3.3 Fa2p Interacts with Two Axonemal Proteins *In situ*.

Cross-linking of axonemal proteins has been a successful method of identifying binding partners in *Chlamydomonas* axonemes (Benashski and King, 2000; Patel-King *et al.*, 2002; Takada *et al.*, 2002). The reason for this success is likely due to the highly organised structure of the axoneme with very uniform protein-protein interactions. Using purified axonemes harvested from wild-type or *fa2-1*;FA2HA strains, I empirically tested various protein cross-linkers including homobifunctional compounds (DFDNB, DMP and DSS) and the carbodiimide reagent EDC, which generates zero-length cross-links between free carboxyls and primary amines.

Axonemes were incubated with increasing concentrations of the various cross-linkers, and samples were analysed by Western blot. Interestingly, I observed two predominant cross-linked bands in experiments using EDC (Figure 4-3). The higher-migrating band was a cross-linked product of approximately 130 kDa (arrows in Figure 4-3), while a less robust cross-linked product of ~90 kDa was also observed (arrow-heads in Figure 4-3). The same two cross-linked products were observed in experiments using axonemes from wild-type cells (probed with anti-Fa2p antibody; Figure 4-3A) or *fa2-1*;FA2HA cells (probed with anti-HA antibodies; Figure 4-3B).

To identify the Fa2p-associated proteins, I first sought to increase the yield of these cross-linked products in order to facilitate purification. Subsequently, I could obtain peptide fingerprints using MALDI-ToF Mass Spectroscopy of proteolytic fragments to identify the corresponding genes from the *Chlamydomonas* genome and ciliary proteome. Axonemes were harvested from *fa2-1*;FA2HA cells and incubated with EDC as described above, then subjected to an extra concentrated step by sedimentation (see Materials and Methods). I then tested whether the ~130 kDa and ~90 kDa cross-linked products could be extracted from axonemes using high-salt buffers. Figure 4-4A shows that most of the cross-linked products was extracted by 0.6M KI. The salt extract was then dialyzed, and immunoprecipitation was performed using two different anti-HA antibodies (Figure 4-4B). The two antibodies precipitated ~75% of monomeric Fa2p (arrows; compare Input and Unbound lanes), as well as almost all of the cross-linked products (asterisk). However, the yield from these experiments insufficient to allow for Mass Spectroscopy analysis. This is in spite of the fact that we started with ~20-fold more cross-linked axonemes than in published protocols, and a larger amount of starting material was not feasible.

One reason for poor protein recovery may be due to the low abundance of the Fa2 protein. Indeed, most experiments that have yielded successful results have been done using proteins found along the entire length of the axoneme (Benashski and King, 2000; Patel-King *et al.*, 2002; Takada *et al.*, 2002). Nevertheless, this approach did provide us with clues regarding two possible proteins (or protein complexes) that interact with Fa2p at the SOFA. Because I used a zero-length cross-linker, I know that Fa2p interacts directly with a ~20 kDa protein, as well as a protein (or complex of proteins) that is ~60

kDa in size. Although the identity of these proteins remains to be determined, three possible candidates (based on molecular weight) are katanin, centrin and tubulin.

Katanin exists as a heterodimer in vertebrate cells (McNally and Vale, 1993). The p80 subunit is a WD40 protein essential for localizing the catalytic (p60) subunit to centrosomes and spindle poles. The p60 subunit of katanin is an ATPase in the AAA family, and possesses microtubule severing activity (reviewed in Quarmby, 2000). The *Chlamydomonas* katanin (Cp60) has been cloned and is implicated in the deflagellation pathway (Lohret *et al.*, 1998; Lohret *et al.*, 1999). Specifically, Cp60 was shown to have axonemal microtubule severing activity, and is localized on the outer-doublet microtubules at the transition zone, proximal to the SOFA (Lohret *et al.*, 1999). Due to its proposed role in deflagellation, katanin is an obvious candidate for the ~60 kDa Fa2p-binding protein identified above. Although immuno-EM localization data indicates that katanin is localized more proximally, at the transition zone, and remains associated with the cell body post deflagellation (Lohret *et al.*, 1999), Western analysis of purified axonemes showed that a small amount of Cp60 segregated with the severed flagella (Figure 4-5A). Therefore, I repeated the cross-linking experiments using axonemes purified from a strain expressing an HA-tagged Cp60, to see if this protein becomes cross-linked to Fa2p. This strain was used because we currently do not have an antibody against endogenous Cp60. Under the conditions that yield the EDC cross-linked Fa2p products, no cross-linked bands are observed when probed for Cp60-HA (Figure 4-5B). Thus, this ruled Cp60 out as the ~60 kDa protein identified in the cross-linking experiments. However, we cannot dismiss the possibility that endogenous Cp60 interacts with Fa2p in the axoneme, based solely on these experiments.

One candidate Fa2p-binding protein that fulfils the 20 kDa size requirement is centrin. *Chlamydomonas* centrin is a 20 kDa calcium binding protein localized to various regions of the basal body apparatus, including the striated fibers that connect the two basal bodies together, as well as fibers that connect the basal body to the nucleus. Furthermore, centrin is found in the stellate fibers inside the transition zone (Salisbury *et al.*, 1988; Sanders and Salisbury, 1989; Taillon *et al.*, 1992). Centrin has been implicated in deflagellation (Sanders and Salisbury 1989; Sanders and Salisbury, 1994), by a mechanism of calcium-induced contraction of centrin fibers in the transition zone, although this remains controversial (discussed in Quarmby, 2004). Western analysis of cellular fractions indicated that a small amount of centrin segregated with purified axonemes (Figure 4-6A). Similar to the Cp60-HA experiment above, I probed for centrin on Western blots of EDC cross-linked axonemes to determine whether the small cross-linked product observed was indeed centrin. However, the result was unclear; the axonemal cross-linking yielded numerous centrin bands by immunoblot analysis, making it difficult to identify a band that corresponds to the Fa2p cross-linked product. Therefore, I performed co-immunoprecipitation experiments to test whether centrin could co-precipitate with Fa2p. Wild-type or *fa2-1*;FA2HA axonemes were extracted with 0.6M NaCl, dialyzed, and immunoprecipitation was performed using anti-Fa2p or anti-HA antibodies (see Materials and Methods). Almost all of Fa2p was immunoprecipitated using three different antibodies; however, centrin did not co-immunoprecipitate in any of the experiments (Figure 4-6B). This suggested that centrin was not the ~20 kDa Fa2p-binding protein, although it is possible that, following extraction, Fa2p loses the ability to rebind centrin. The identity of the ~20 kDa protein remains unknown.

4.3.4 Extracted Fa2p can Rebind Axonemes

I next tested the possibility that Fa2p is binding tubulin, an obvious candidate binding-protein as Fa2p might be sitting directly on the microtubules forming the axonemes. As mentioned in the cross-linking experiments above, Fa2p appeared to interact with a protein of approximately ~60 kDa. This is close to the 55 kDa molecular weight of tubulin, and led me to examine whether axonemal Fa2p can bind tubulin. To test this, I performed three separate experiments: (1) Western blots of cross-linked axonemes probed with anti-Fa2p (e.g. Figure 4-3) were stripped and reprobed with antibodies against tubulin (alternatively, antibodies against acetylated-tubulin where used, since microtubules of the axoneme are modified by acetylation). However, these blots were inconclusive, as I could not determine whether the same bands were being identified by the tubulin antibodies as the Fa2p antibodies (data not shown). (2) A split-lane Western blotting method was also used. Briefly, axonemes were cross-linked as described above then loaded into a wide lane on an SDS-PAGE gel. Following transfer to nitrocellulose, this lane was cut down the middle, and one half was probed with anti-Fa2p antibody, while the other half was probed with tubulin antibodies. The two halves of the membrane were then put back together during antibody detection. Once again, I could not definitively determine whether the same protein bands were being identified by the two antibodies. In both of the above experiment, the blots identified a large number of tubulin cross-linked products, as would be expected. However, the blots had high levels of background (even though the exposure time was ~1 second, as well as large dilution of the anti-tubulin antibodies), likely due to the high amount of tubulin present in each lane (data not shown). Lower amounts of protein loading did not permit visualization of the faint Fa2p cross-linked bands. Based on these problems, this approach was abandoned.

The third approach was to perform co-immunoprecipitation experiments using antibodies that precipitate Fa2p, as mentioned above. These blots were then probed with antibodies that recognize tubulin. Figure 4-6B shows that, unlike centrin, alpha-tubulin co-immunoprecipitated with Fa2p. Although a small amount of tubulin precipitated in control experiments lacking anti-Fa2p antibodies (Figure 4-6B, Mock panel), higher amounts of tubulin precipitated in the presence of anti-Fa2p antibodies. This was evident is cases where larger amounts of Fa2p are visible (e.g. Mouse anti-HA panel). Furthermore, the reciprocal immunoprecipitation experiment performed using anti-α-tubulin antibodies demonstrated that Fa2p precipitates with tubulin (Figure 4-6C). Although we cannot conclude that Fa2p directly interacts with tubulin, this result suggested that such an interaction may exist.

The final method I used to determine whether Fa2p binds tubulin was to perform an axonemal rebinding assay. Some axonemal proteins, for example a central-pair kinesin motor protein (Yokoyama *et al.*, 2004), can be extracted with an ionic buffer then can rebind to extracted axonemes once the salt has been removed by dialysis. A schematic showing the axoneme rebinding assay is shown in Figure 4-7A. Briefly, axonemes were harvested from *fa2-1*;FA2HA cells, and extracted with 0.6M NaCl. Following dialysis, equivalent amounts of this extract were incubated with NaCl-extracted axonemes isolated from a wild-type strain (not expressing Fa2p-HA). This was done in order to eliminate the presence of any FA2p-HA present on the extracted axonemes, so that any Fa2p-HA bound to axonemes comes from the extract only (Figure 4-7A). Over 90% of extracted Fa2p-HA can rebind extracted axonemes (Figure 4-7B).

The high affinity of Fa2p-HA for extracted axonemes was interesting, however, this is not an indication that Fa2p can bind microtubules directly. Because a NaCl extract was used as the starting material, many other axonemal proteins were present, thus Fa2p might bind axonemes through an intermediate protein. Furthermore, from the Western blot data it was unclear whether Fa2p is rebinding axonemes strictly at the SOFA (where it is normally) or along the entire length of the microtubules (i.e. has a general affinity for microtubules). To address this issue, indirect immunofluorescence microscopy was performed on axonemes (following the rebinding step with the NaCl extract) to determine where the Fa2p-HA localized. However, repeated attempts where unsuccessful; no Fa2p-HA signal was observed on the rebound axonemes by immunofluorescence (data not shown). One possible reason for the lack of staining is that following salt extraction, axoneme rebinding and fixation steps, the HA-epitope becomes masked.

A more direct method of testing the microtubule-binding properties of Fa2p would be to express and purify the protein, then perform binding assays with *in vitro* synthesized microtubules. However, repeated attempts at expressing Fa2p in *E.coli* failed. Fa2p was either not expressed at all, or was rapidly degraded when expressed even at low levels (data not shown). This may be due to the codon bias presented by the high (68%) GC content of the *FA2* cDNA, as well as other issues such as stability, toxicity, and proper protein folding. To circumvent these problems, eukaryotic expression systems may need to be utilized, such as mammalian or insect cell lines. However, that is beyond the scope of this thesis.

4.3.5 Fa2p SOFA-targeting Domain

A proteomic study of purified *Chlamydomonas* flagella has identified roughly 360 proteins, many of which have orthologs in humans (Pazour *et al.*, 2005). However, no consensus flagellar targeting sequence has yet been identified in either organism. Furthermore, little is known about the SOFA region of flagella and the mechanism(s) of protein localization to this distinct area. Clearly, a mechanism must exist to confer the asymmetric distribution of proteins localized specifically at this region of the axoneme. This may come in the form of a specific targeting domain found in the peptide sequences of SOFA proteins. Alternatively, scaffolding proteins may exist that are at the proximal end of the axoneme. As such, SOFA-targeted proteins would bind these scaffolds and be retained strictly at the SOFA. I sought to identify a fragment of the Fa2 amino acid sequence that is necessary and/or sufficient to target Fa2p to the SOFA (I refer to this as the SOFA-targeting sequence), with the hopes of shedding some light on other proteins that may also be localized (or participate in Fa2p localization) to this region.

Examination of the Fa2p amino acid sequence, using a variety of protein analysis software, did not yield any known motifs aside from the kinase domain. However, there are a number of regions with low sequence complexity (LSC) within the Fa2p sequence (Figure 4-8A; identified by the SMART software; http://smart.embl-heidelberg.de/). These LSC regions appear rich in certain amino acids such as proline, alanine, glycine and glutamine, while one region is almost exclusively comprised of serine/threonine/tyrosine (Figure 4-8A). Although the significance of these regions remains unclear, they provided starting point as targets for truncation analysis.

To facilitate expression of truncated versions of Fa2p, a cDNA-based expression vector (Fisher and Rochaix, 2001) was engineered to contain an HA-tag (Figure 4-8B). As proof of principle, I sought to express the full length *FA2* cDNA containing a C-terminal HA-tag. The vector was transformed into *fa2* mutant cells, and transformants were assayed by Western for expression of the Fa2p-HA. Of the ~200 colonies screened, none expressed the protein or rescued the deflagellation defect in the *fa2* mutants. In contrast, ~30% of transformants containing the *FA2HA* genomic construct (Mahjoub *et al.*, 2004) express the protein. The lack of expression using cDNA now appears to be a common phenomenon in the *Chlamydomonas* research community. Indeed, it is one of the few weaknesses of the *Chlamydomonas* model, and a robust method of expressing cDNA is yet to be developed. Therefore, I turned back to the genomic construct for the truncation mutation analysis.

Again, as a first step I wanted to show that the full length *FA2* genomic construct (containing a C-terminal HA-tag) can express and localize to the SOFA. The *FA2* genomic construct was engineered to contain an HA-epitope tag immediately prior to the stop codon (Figure 4-8C). This vector was similar to the genomic expression vector used in Chapter 2 (Figure 2-1 and Mahjoub *et al.*, 2004) but the HA-tag was inserted right at the end of the gene, instead of in the sixth exon (compare Figure 2-1 with Figure 4-8C). The vector was transformed into *fa2* mutant cells, and transformants were assayed by Western as previously described. Once again, no protein expression was detected in 56 transformants assayed (data not shown).

The failure of expression from the full length *FA2* gene construct is perplexing, but may be due to the placement of the HA-tag. To test this, the construct was engineered

to contain the HA-tag N-terminally (Figure 4-8C). That construct also failed to yield protein expression in 50 transformants colonies. Thus, the HA-tag appears to interfere with gene expression when at either terminus of the gene. Therefore, there is no guarantee that truncated fragments of the genomic *FA2* DNA would express in this vector, so the approach was abandoned. The redesign of a genomic *FA2* construct was done to ease the construction and analysis of subsequent truncation steps. However, due to the lack of expression from this construct, the *FA2HA* genomic vector described in Chapter 2 will be used as the template for mutagenesis. This approach is not trivial, as there are no convenient restriction enzyme sites that allow deletion of small regions of the gene. Secondly, the *FA2HA* construct is roughly 10 kilobases in size, making site-directed mutagenesis challenging. Furthermore, it requires sequencing of large (~9000 bases) fragments of DNA after each deletion step.

4.3.6 Genetic Screen for *fa2* Suppressors

Another way of discovering potential Fa2p-interacting proteins is by identifying genetic interactors. I performed a chemical mutagenesis screen, using EMS, to identify point mutations that would suppress the *fa2* deflagellation defect. I hypothesized that point mutations in potential suppressors may enhance/increase their deciliation activity without affecting other essential cellular activities, such as a possible role in the cell cycle. Precedence for this comes from experiments showing that the kinase activity of Fa2p is essential for its role in the deciliation pathway, but not for cell cycle progression, separating the two functions (Chapter 2; Mahjoub *et al.*, 2004). Specifically, a kinase-dead (KD)- *FA2* construct containing an amino acid substitution of the invariant lysine (K46R) in the ATP-binding loop, fails to rescue the deciliation phenotype when

transformed into *fa2* mutants. However, the cell cycle profile of these cells is comparable to wild-type, and the protein is localized to the SOFA similar to wild-type Fa2p (Chapter 2; Mahjoub *et al.*, 2004). This strain (*fa2-3;KD-FA2*) was the target strain for a suppressor screen using EMS mutagenesis.

The first phase entailed using EMS to mutagenize *fa2-3;KD-FA2* cells, which were subsequently subjected to a deciliation treatment (see Materials and Methods). A motility assay was used to identify cells rescued for the deciliation phenotype. The second phase of analysis would involve examination of *fa2* suppressed strains for effects of the suppressor on the delays in G_2/M and ciliogenesis. Next, backcrosses would be performed to determine the phenotype of the new mutation in the absence of the *fa2* mutation. The presence of an independent phenotype would facilitate genetic mapping, but if necessary the suppressor mutations could be mapped in the context of the *fa2* allele (i.e. the *fa2/suppressor* strain would be crossed into a mapping strain, S1D2, which also contains a *fa2* mutation). Finally, we would generate diploid strains to determine whether the suppressors are dominant or recessive.

Using this rapid motility based assay, I (with assistance from undergraduate students Andrea Lee and Sarah Chow) screened 65,170 mutagenized *fa2-3;KD-FA2* colonies. Of these, 1090 (1 in 60 colonies or 1.7%) were identified as motility mutants (representing unwanted paralyzed flagella mutants, short flagella mutants and bald cells), and were excluded from further analysis. Unfortunately, none of the remaining mutagenized cells rescued the deflagellation defect. One possible explanation for the lack of *fa2* suppressors identified by this screen is that more mutagenized colonies need to be examined, to ensure thorough coverage of the *Chlamydomonas* genome. Because I was

using a strain containing a *FA2* point mutation as my target strain (*fa2-3;KD-FA2)*, I predicted that a revertant colony might be isolated, where the K46R mutation has been changed back to lysine. The failure to isolate a revertant indicates that the screen was not saturated. Although it is impossible to determine the exact extent of mutagenesis in our screen, a comparison can be made to a study by Loppes (1970), who used EMS mutagenesis to isolate *Chlamydomonas* arginine auxotrophs. With an lethality rate of 50% (identical to our experiments), Loppes isolated arginine auxotrophs at a rate of 1:282 (or 0.35%). Since there are 8 genes involved in the arginine biosynthetic pathway, this correlates to a mutation rate of 0.043% per gene.

Another comparison is the original mutagenesis screen to identify deflagellation mutants, where 26,000 colonies were assayed and yielded 13 deflagellation null mutants (1 in 2000 colonies screened; Finst *et al.*, 1998). Furthermore, a recent screen to identify suppressors of the *mat3* mutation in *Chlamydomonas* yielded 19 suppressors from 20,000 colonies screened (1 in 1052; Fang and Umen, 12th International Conference on the Cell and Molecular Biology of *Chlamydomonas*, abstract # 28). *MAT3* encodes the *Chlamydomonas* homologue of the retinoblastoma (Rb) tumor suppressor, and *mat3* mutant cells are small in size (Umen and Goodenough, 2001). The screen identified the transcription factors E2F and Dp1, both established members of the Rb pathway (Fang and Umen, 12th International Conference on the Cell and Molecular Biology of *Chlamydomonas*, abstract # 28). It is important to note that although both of the above screens obtained less coverage than our EMS screen, both used insertional mutagenesis (with exogenous DNA) to randomly insert into the nuclear genome. Insertional mutagenesis typically generates single gene mutations, and usually leads to null mutants,

and thus is significantly different than our screen. Ultimately, our EMS screen was unsuccessful in identifying the rare types of protein modifications we were looking for (see Discussion below).

4.4 Discussion

The biochemical approach to identifying interactors of Fa2p has led to some interesting, yet perplexing, results. The mislocalization of Fa2p in a range of paralyzed flagellar mutants is confusing, as no obvious mechanism(s) for this exist. Further complicating the issue is that the analysis was performed on axonemes isolated from these mutants; hence deflagellation is unaffected in these cells even though Fa2p is unstable/mislocalized in the purified flagella and axonemes. One explanation for this is that Fa2p is sufficiently anchored at the SOFA to induce deflagellation in these *pf* mutants, but is unstable due to the *pf* mutations. Another possibility is that while at the SOFA, Fa2p may be on the proximal side of the severing site in the mutants, and is therefore retained by the cell body during the cell fractionation. It would be interesting to perform immunofluorescence localization of endogenous Fa2p in these mutants, and see whether Fa2p indeed remains attached to the cell body-side of the SOFA post deflagellation. Unfortunately, indirect immunofluorescence using the anti-Fa2p antibody does not produce a specific signal (discussed in Chapter 2). Nevertheless, it would appear that the aberrant localization of Fa2p in these cells does not abrogate its function during deflagellation. Indeed, the role of Fa2p in deflagellation may simply be in assembly of the axonemal severing complex. Our lab previously developed an *in vitro* assay for axonemal microtubule severing wherein axonemal-basal body complexes were isolated from whole cells then tested for the ability to deflagellate (Lohret *et al.*, 1998). Calcium,

but not ATP, is necessary to activate axonemal severing in this system. This data suggests that the Fa2p kinase was not likely to play a direct role in signaling calcium-induced deflagellation, but may be important for directing assembly of a microtubule severing complex during axonemal assembly. Thus, the severing complex would be already assembled in the *pf* mutants.

Fa2p can be extracted from axonemes using high-salt buffers, but removal of the salt by dialysis does not appear to facilitate rebinding to a large protein(s) complex as indicated by sucrose gradient sedimentation. Indeed, various conditions were tested including varying salt concentrations for extractions, types of salt used, and dialysis conditions (see Materials and Methods). The first instance of a Fa2p-interacting protein came from cross-linking experiments performed on purified axonemes. Two proteins (or protein complexes) were identified that bind directly to Fa2p, with molecular weights of ~20 kDa and ~60 kDa respectively. However, purification of these complexes proved to be difficult, most likely due to the low abundance of Fa2p in axonemes as well as the low abundance of the cross-linked products (see Figure 4-3). The identity of these proteins remains unknown, however, I hypothesized that katanin, centrin or tubulin may be the Fa2p-binding partners. The immunoprecipitation experiments suggested that tubulin interacted with Fa2p, and I subsequently showed that salt-extracted Fa2p has high affinity for extracted axonemes. However, I cannot conclude that the protein binds tubulin or microtubules directly.

An alternate approach to identify Fa2p-interactors was to perform a chemical mutagenesis screen. However, this assay was not fruitful. The failure to identify *fa2* suppressors is disappointing, but may provide insight into the role of Fa2p at the SOFA.

Our original hypothesis was that modifications to certain proteins would overcome the *fa2* deflagellation defect, without affecting cell cycle progression. One obvious class of proteins that, when mutated, might suppress the *fa2* phenotype are those implicated in the deflagellation pathway (*ADF1, FA1* and katanin; Finst *et al.*, 1998; Lohret *et al.*, 1999). *ADF1* was discovered in a screen for deflagellation mutants and putatively encodes an ion channel; *adf1* cells are defective in the Ca^{2+} - influx step during deflagellation, but are able to deflagellate if the cells are permeabilized to allow Ca^{2+} into the cell (Quarmby and Hartzell, 1994; Finst *et al.*, 1998). In contrast, the *fa* mutants fail to deflagellate even if calcium is introduced into the cell. This places the *ADF1* gene product upstream of the Fa proteins in the deflagellation pathway (Finst *et al.*, 1998; Quarmby, 2004). As such, it is difficult to imagine a mutation in *ADF1* that would allow it to bypass the *fa2* mutation, thus ruling it out as a candidate. The other essential deflagellation gene, *FA1*, encodes a 171 kDa coiled-coil protein shown to be localized to the flagellar transition zone (Finst *et al.*, 2000). Because of the identical deflagellation phenotype, it is unknown whether Fa1p is upstream or downstream of Fa2p in the signaling pathway. Nonetheless, it is possible that Fa2p interacts with, and regulates (e.g. via phosphorylation), Fa1p. In that scenario, it is possible that mutations in Fa1p that mimic phosphorylation (for example, substitution of a serine or threonine by aspartic or glutamic acid) could suppress the *fa2* phenotype. Furthermore, it is conceivable that activating mutations in Fa1p could suppress the *fa2* defect. The final protein implicated in this pathway is katanin (Cp60). As previously mentioned, katanin has been shown to localize on the outer-doublet microtubules at the transition zone, and is implicated in the axonemal microtubule severing step during deflagellation, putatively placing it downstream of Fa2p in this

pathway (Lohret *et al.*, 1998; 1999). Interestingly, although the original insertional mutagenesis screen for the deflagellation mutants yielded multiple alleles of *adf1*, *fa1* and *fa2*, no katanin mutants were isolated (Finst *et al.*, 1998). One possible explanation is that null mutants of katanin would be lethal, as katanin has been implicated in mitosis (Quarmby, 2000). In this screen, we entertained the possibility that Cp60 point mutants could induce axonemal microtubule severing in the absence of Fa2p catalytic activity. Again, one possibility would be a mutation that causes increased activity of Cp60, perhaps via a phospo-mimic mutation. In *Xenopus*, katanin activity can be regulated by inhibition (via interaction with microtubule-associated proteins; MAPs) or stimulation (by a polo-like kinase, Plx1; McNally *et al.*, 2002). It is possible that similar mechanisms of regulation exist in *Chlamydomonas* for Cp60; mutations in these proteins may alter Cp60 activity such that it bypasses the *fa2* phenotype.

Another candidate modification would be to other NIMA-related kinases. The *Chlamydomonas* genome expresses 10 other Neks, some of which are localized to the flagella (reviewed in Quarmby and Mahjoub, 2005). Specifically, *CNK6* was identified in a proteomic study of *Chlamydomonas* flagella (Pazour *et al.*, 2005), but the specific flagellar localization of the protein is yet to be determined. Cnk2p has been localized to puncta along the length of the axoneme, and affects flagellar length and cell size (Bradley and Quarmby, 2005). Although not strictly at the SOFA, some Cnk2p staining is observed in the SOFA region. Furthermore, the flagellar proteome had identified ~90 signal transduction proteins, including 21 protein kinases that have not previously been localized to the flagella (Pazour *et al.*, 2005). We predicted that one (or more) of these kinases may acquire a mutation such that they are constitutively active, and thus be able

to phosphorylate targets of Fa2p. However, no such mutants were identified. This may indicate that Fa2p's role is highly specific and cannot be bypassed by other kinases. Finally, it is important to note that mutations to substrates of Fa2p may be lethal, since they could also be involved in aspects of cell cycle regulation, similar to Fa2p. As such, these mutants could not have been isolated as part of this mutagenesis screen.

4.5 Figures

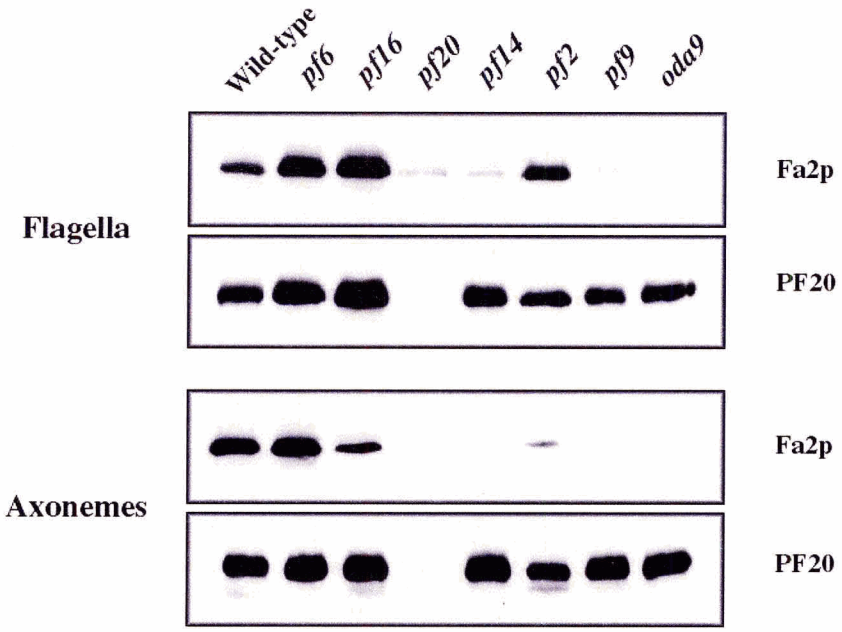

Figure 4-1 Fa2p is mislocalized in various flagellar mutants
Immunoblot of flagellar and axonemal fractions isolated from a series of mutants. 30μg of either flagella or axonemal protein was loaded onto an 8% SDS-PAGE gel. Blots were probed with anti-Fa2p, stripped and reprobed with anti-PF20. Strains used: Wild-type, *pf*6 (lacking long projection on C1 tubule of the central pair), *pf*16 (lacking the C1 tubule of the central pair), *pf*20 (lacks central pair microtubules), *pf*2 (lacks a component of inner dynein arms), *pf*14 (lacking radial spokes), *pf*9 (inner dynein arm deficient) and *oda*9 (lacking outer dynein arms).

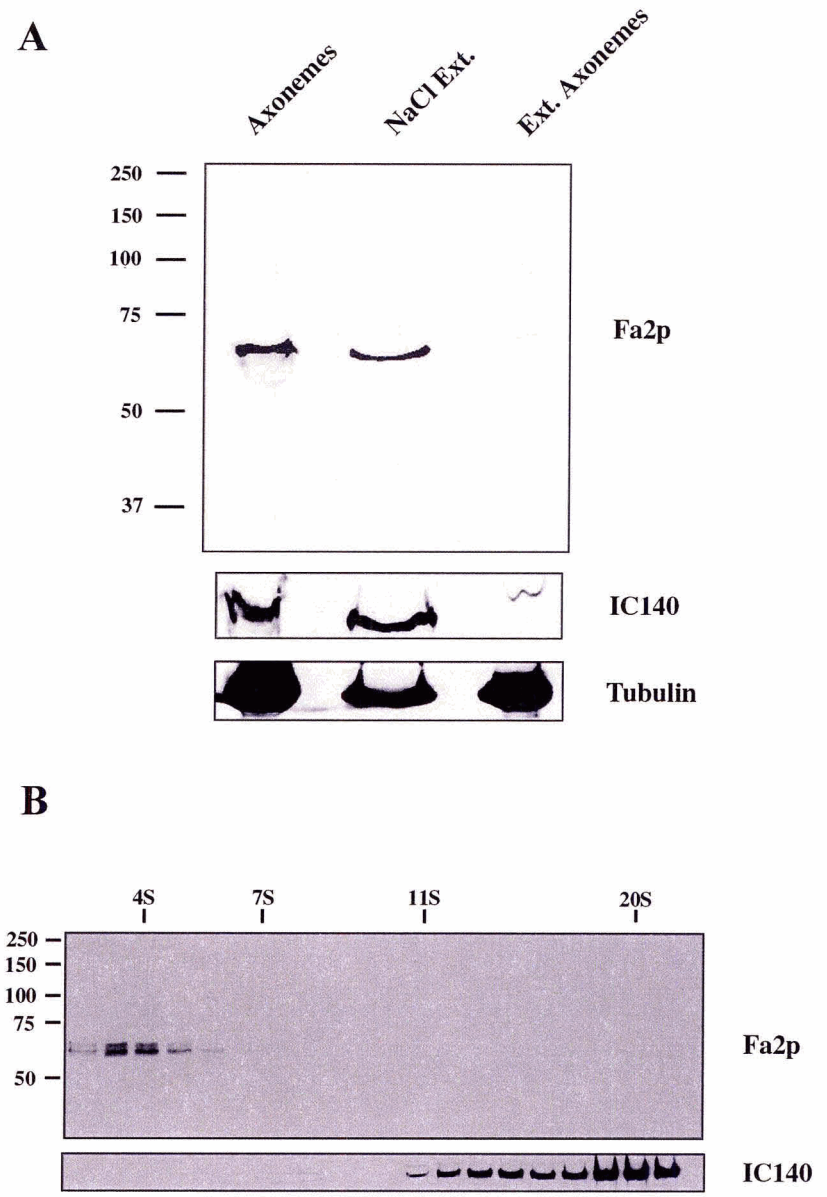

Figure 4-2 Salt-extracted Fa2p sediments as a monomer in sucrose gradients.
(A) Immunoblot of wild-type axonemes extracted with 0.6M NaCl. Flagellar-equivalent amounts of protein were loaded in each lane, and blots were probed with anti-Fa2p. The membrane was subsequently stripped and reprobed with antibodies against IC140 then α-Tubulin. (B) Western blots of sucrose gradient fractions. The 0.6M NaCl extract was dialysed then loaded onto a 4-24% sucrose gradient and sedimented overnight. 20 fractions were collected, and an equal volume from each was loaded onto an 8% SDS-PAGE gel. Blots were probed with anti-Fa2p, stripped then reprobed with anti-IC140. Sedimentation standards used: BSA (4.4S, ~70 kDa), aldolase (7.3S, ~166 kDa), catalase (11.3S, ~250 kDa) and thyroglobulin (19.4S, ~670 kDa).

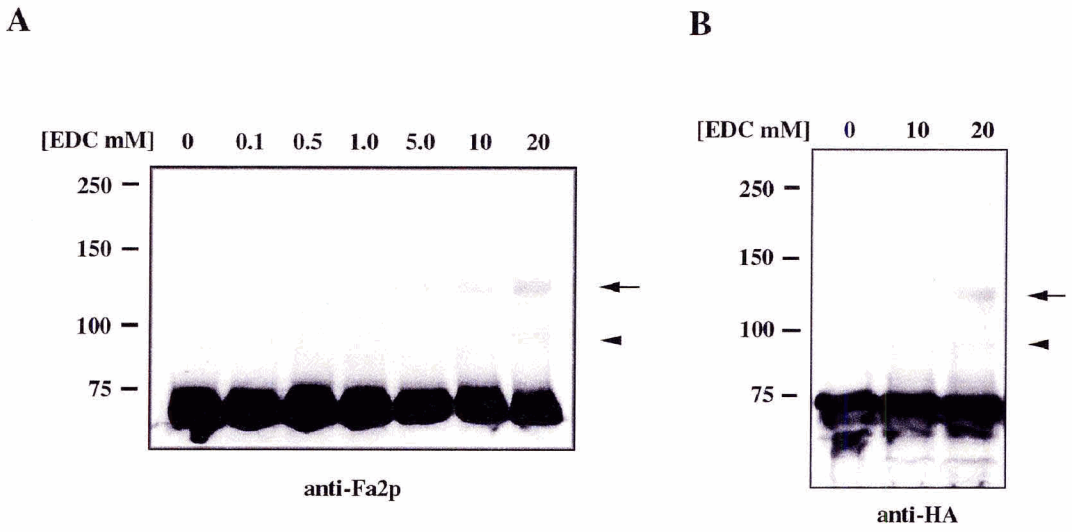

Figure 4-3 Axonemal cross-linking identifies two Fa2p-interacting protein complexes. Immunoblots of axonemes isolated from wild-type (A) and *fa2-1*;FA2HA (B) cells and incubated with the indicated concentrations of the zero-length cross-linker EDC. We note the occurrence of two cross-linked species, a ~130 kDa band (arrows) and a ~90 kDa band (arrowhead), in both experiments. Blots were probed with anti-Fa2p (A) or anti-HA (B) antibodies.

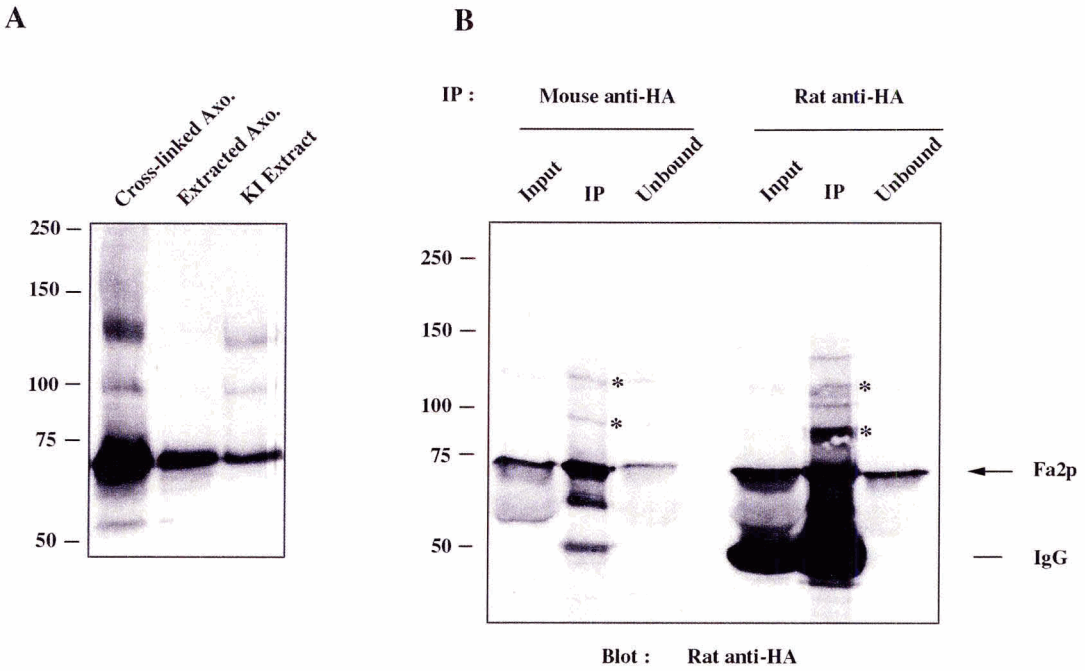

Figure 4-4 Salt extraction and immunoprecipitation of Fa2p cross-linked products. (A) *fa2-1*:FA2HA axonemes were incubated with 20mM EDC, sedimented then resuspended in buffer containing 0.6M KI. Flagellar-equivalent amounts of each fraction were separated by an SDS-PAGE gel and probed with anti-Fa2p antibody. Both the ~130 kDa and ~90 kDa cross-linked products are extractable with 0.6M KI. (B) *fa2-1*:FA2HA axonemes were isolated and incubated with 20mM EDC. Samples were then pooled and concentrated as described in Materials and Methods. The concentrated, cross-linked axonemes were extracted in HMEK buffer containing 0.6M KI, then dialysed against HMEK buffer. Immunoprecipitation was performed using two monoclonal anti-HA antibodies as indicated. Samples were incubated with protein-G agarose beads, and immune complexes were precipitated by sedimentation. Equal amounts of protein from dialysed KI-extract (Input), precipitated proteins (IP) or unbound supernatant (Unbound) were separated by SDS-PAGE gel, then probed with the Rat anti-HA antibody. The ~130 kDa and ~90 kDa cross-linked species are indicated by an asterisk.

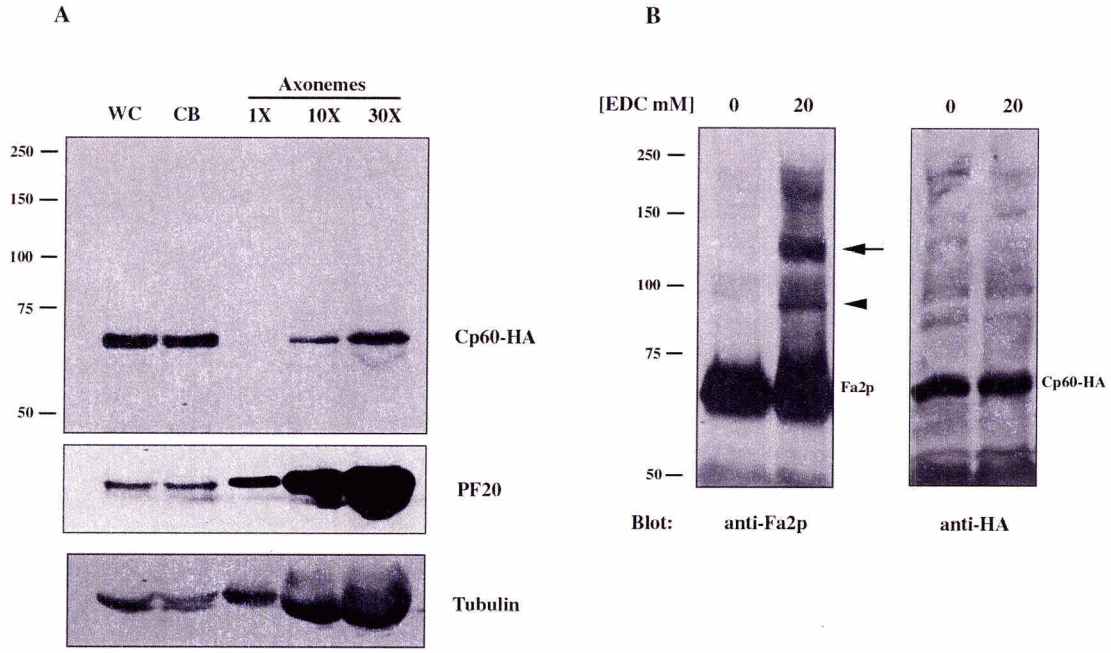

Figure 4-5 Cellular fractionation and axonemal cross-linking of cells expressing Cp60-HA.

(A) Immunoblot of cellular fractions from wild type cells expressing an HA-tagged Cp60 construct indicates that a small amount of Cp60-HA is found in the severed flagella. Cells were deflagellated with dibucaine, and equivalent numbers of whole cells (WC), cell bodies (CB), and axonemes were loaded in each lane. In addition, 10-fold and 30-fold concentrations of axonemes were included. Blots were probed with anti-HA (top), stripped and reprobed with anti-PF20 then anti-α-Tubulin antibodies as indicated. (B) Immunoblots of axonemes isolated from wild-type;Cp60-HA cells and incubated with the indicated concentrations of the zero-length cross-linker EDC. Blots were probed with anti-Fa2p (left panel) or anti-HA (right panel) antibodies. We note the occurrence of the two Fa2p cross-linked species, a ~130 kDa band (arrows) and a ~90 kDa band (arrowhead), similar to previous experiments. However, these cross-linked products are not observed when probing for Cp60-HA.

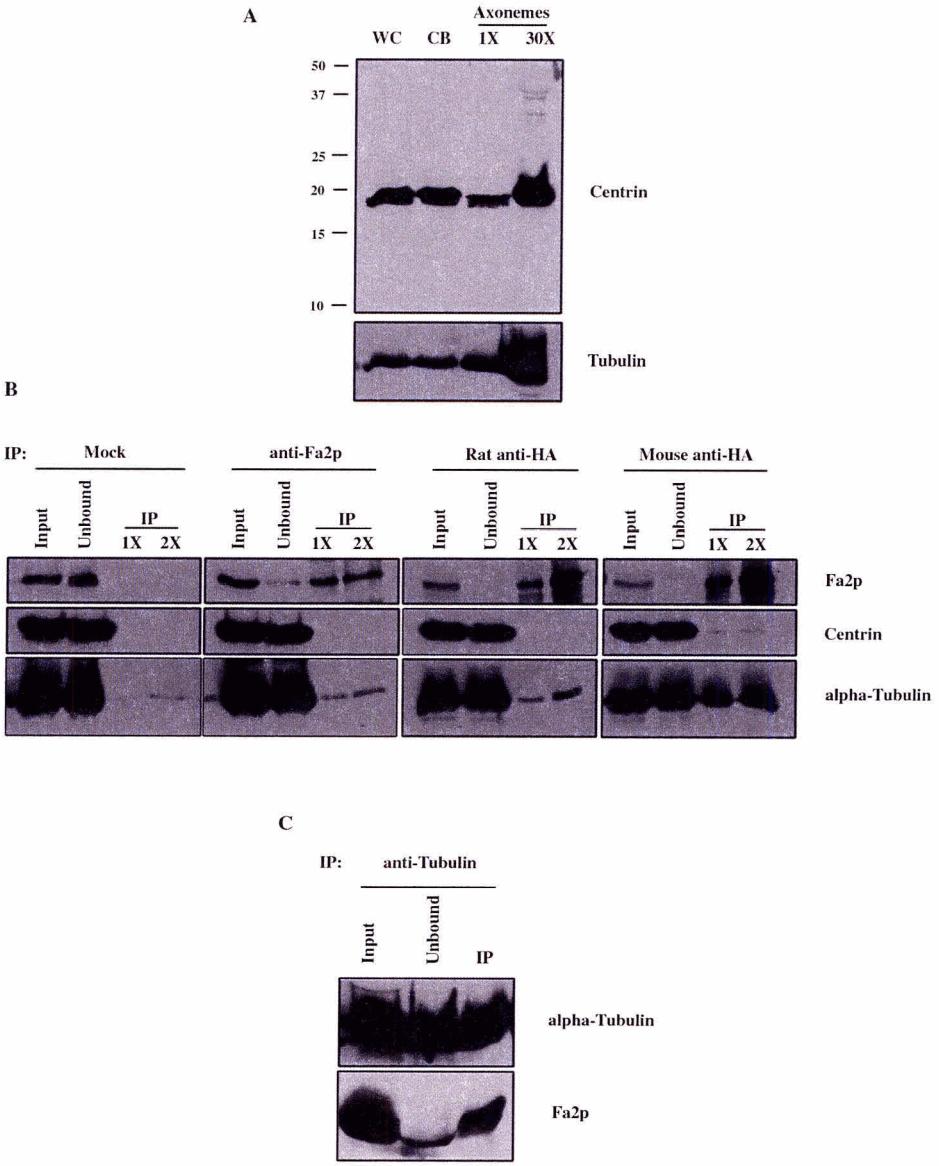

Figure 4-6 Cellular fractionation and immunoprecipitation from axonemal salt extracts. (A) Immunoblot of cellular fractions from wild type cells indicates that a small amount of centrin is found in axonemes. Cells were deflagellated with dibucaine, and equivalent numbers of whole cells (WC), cell bodies (CB), and axonemes were loaded in each lane. In addition, a 30-fold concentration of axonemes was included. Blots were probed with anti-centrin (top), stripped and reprobed with anti-α-Tubulin antibodies. (B) Immunoblots from immunoprecipitation experiments indicates that tubulin, and not centrin, can co-immunoprecipitate with Fa2p. Axonemes were extracted with 0.6M NaCl, dialyzed then incubated with either anti-Fa2p, monoclonal rat anti-HA or mouse anti-HA, as indicated. Equivalent concentrations of extract (Input), the flow-through (Unbound), and immunoprecipitates (IP) were loaded from each sample and analyzed by Western. In addition, a 2-fold concentration of the IP fraction was included, to help identify any possible weak signals. Blots were probed with anti-Fa2p (top row), anti-centrin (middle row) or anti-α-Tubulin (bottom row). (C) The reciprocal immunoprecipitation experiment, using anti-α-Tubulin, co-precipitates Fa2p from axonemal extracts.

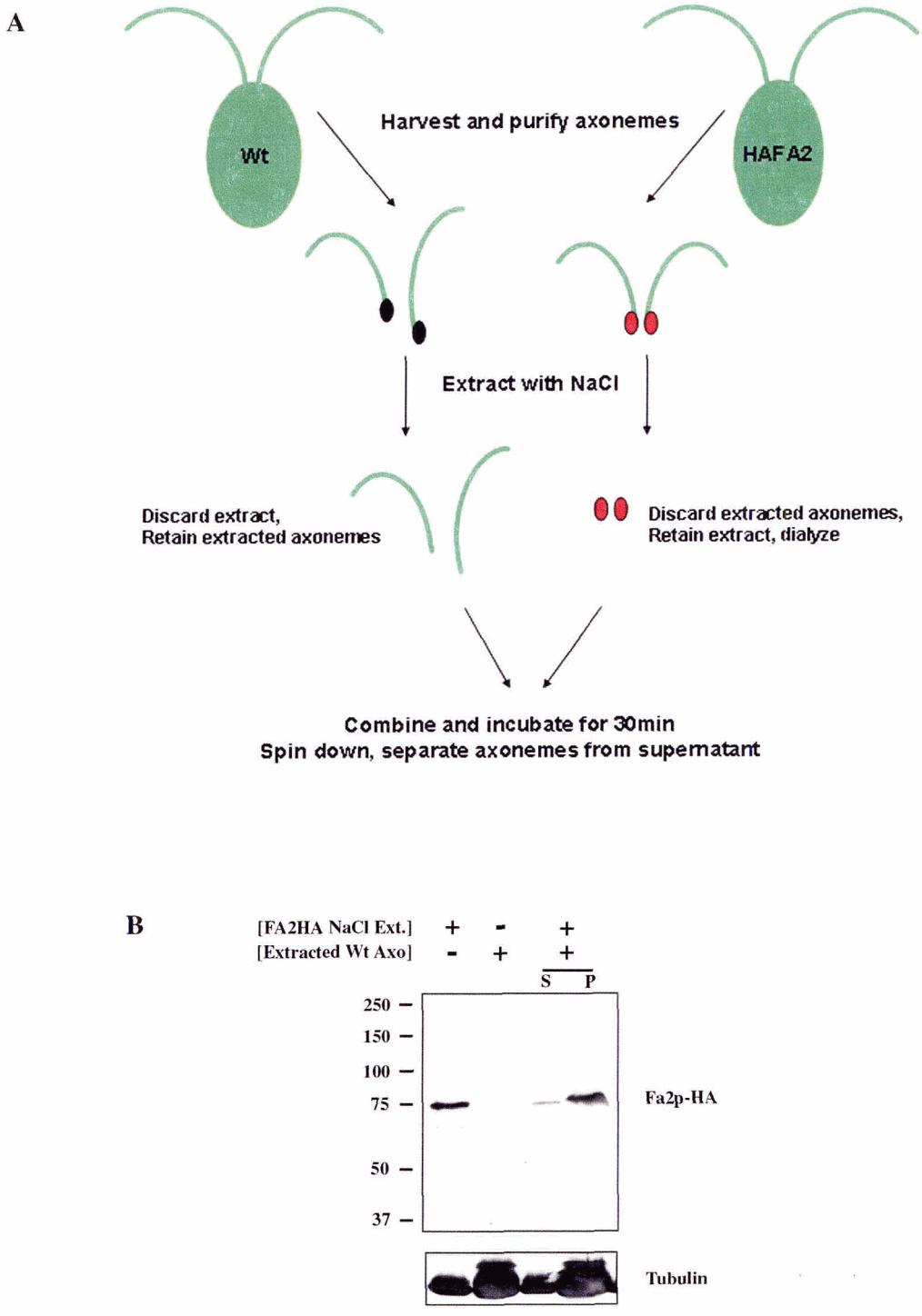

Figure 4-7 Salt-extracted Fa2p can rebind extracted axonemes.
(A) Cartoon schematic demonstrating the axoneme rebinding assay. (B) Western blot of supernatant (S) and pellet (P) fractions after incubation of dialyzed NaCl extract isolated from *fa2-1*:FA2HA cells with extracted wild-type axonemes. Flagellar-equivalents of each fraction were separated by SDS-PAGE, probed with anti-Fa2p, stripped then reprobed with anti-α-Tubulin antibodies.

A

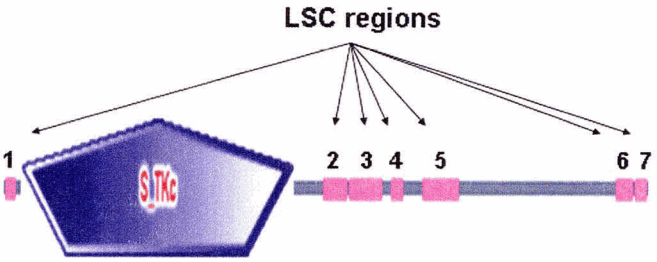

	pI
LSC1 (2-11): APPAPAPPPA	5.5
LSC2 (307-330): GGVATAPPPQQQVGTPPRGVPGPP	9.8
LSC3 (332-363): HPFASPHGGGGGAPPPYPAQPSPHSPYPYQQG	7.0
LSC4 (372-384): RPGSGRSPGPGPG	12.0
LSC5 (402-437): YPSPQHQQPPQQQQGGYGGGYSPPQPYGHQQQQPSP	6.9
LSC6 (588-604): ARGAGGGGGYARAADDA	6.0
LSC7 (605-616): TSYVSSTSYYTS	5.2

B

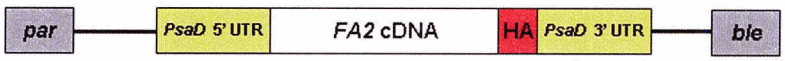

C

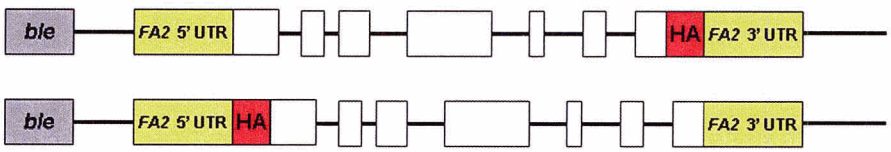

Figure 4-8 *FA2* constructs used for truncation analysis.
(A) Schematic of Fa2 amino acid sequence showing the N-terminal kinase domain and seven regions of low sequence complexity (LSC), as identified by the SMART software (image was obtained and modified from http://smart.embl-heidelberg.de/). Amino acid sequences from each LSC are shown, along with the isoelectric charge of each segment. (B) Schematic showing *FA2HA* cDNA expression construct containing a C-terminal HA-tag. The vector was also engineered to contain two antibiotic resistance markers: a paromomycin resistance gene (*par*) and a Zeomycin resistance gene (ble). (C) Schematic of the *FA2HA* genomic construct engineered to contain an N-terminal or C-terminal HA-tag, and a Zeomycin resistance gene.

4.6 Reference List

Benashski S.E., King S.M. (2000). Investigation of protein-protein interactions within flagellar dynein using homobifunctional and zero-length crosslinking reagents. *Methods.* 22: 365-371.

Bradley B.A., Quarmby L.M. (2005). A NIMA-related kinase, Cnk2p, regulates both flagellar length and cell size in *Chlamydomonas. J. Cell Sci.* 118: 3317-3326.

Cole D.G. (2003). The intraflagellar transport machinery of *Chlamydomonas reinhardtii. Traffic.* 4: 435-442.

DiBella L.M., Smith E.F., Patel-King R.S., Wakabayashi K., King S.M. A novel Tctex2-related light chain is required for stability of inner dynein arm I1 and motor function in the *Chlamydomonas* flagellum. *J. Biol. Chem.* 279: 21666-21676.

Diener D.R., Ang L.H., Rosembaum J.L. (1993). Assembly of flagellar radial spoke proteins in *Chlamydomonas*: identification of the axoneme binding domain of radial spoke protein 3. *J. Cell Biol.* 123: 183-190.

Finst, R.J., P.J. Kim and L.M. Quarmby. 1998. Genetics of the deflagellation pathway of *Chlamydomonas reinhardtii.* Genetics. *149*: 927-936.

Finst, R.J., P.J. Kim, E. Griffis and L.M. Quarmby. 2000. Fa1p is a 171 kDa protein essential for axonemal microtubule severing in *Chlamydomonas.* J. Cell Science *113*: 1963-1971.

Fisher N., Rochaix J.D. (2001). The flanking regions of PsaD drive efficient gene expression in the nucleus of the green alga *Chlamydomonas reinhardtii. Mol. Genet. Genomics* 265: 888-894.

Fowkes M.E., Mitchell D.R. (1998). The role of preassembled cytoplasmic complexes in assembly of flagellar dynein subunits. *Mol. Biol. Cell* 9: 2237-2247.

Harper J.D.I, Wu L., Sakuanrungsirikul S., John P.C.L. (1995). Isolation and partial characterization of conditional cell division cycle mutants in *Chlamydomonas. Protoplasma* 186: 149-162.

Harris E.H. 1989. The *Chlamydomonas* Sourcebook. Academic Press. Inc., Berkeley. CA.

Kamiya R. (2002). Functional diversity of axonemal dyneins as studied in *Chlamydomonas* mutants. *Trends Genet.* 19: 162-167.

King S.M. (2003). Organisation and regulation of the dynein microtubule motor. *Cell Biol, Int.* 27: 213-215.

Lohret, T.A., F.J. M^{c}Nally and L.M. Quarmby. 1998. A role for katanin-mediated axonemal microtubule severing in *Chlamydomonas* deflagellation. *Mol. Biol. Cell* 9: 1195-1207.

Lohret, T.A., Zhao, L., and Quarmby, L.M. (1999). Cloning of Chlamydomonas p60 katanin and localization to the site of outer doublet severing during deflagellation. *Cell Motil Cytoskeleton* 43, 221-231.

Loppes R. (1970). Selection of arginine-requiring mutants in *Chlamydomonas reinhardtii* after treatment with three mutagens. *Experimentia* 26: 660-661.

Lumbreras, V., D.R. Stevens, and S. Purton. 1998. Efficient foreign gene expression in *Chlamydomonas reinhardtii* mediated by an endogenous intron. *Plant J. 14*: 441-448.

Mahjoub M.R., Rasi M.Q., Quarmby L.M. (2004). A NIMA-related kinase, Fa2p, localizes to a novel site in the proximal cilia of *Chlamydomonas* and mouse kidney cells. *Mol Biol Cell* 15: 5172–5286.

McNally F.J., Vale R.D. (1993). Identification of katanin, and ATPase that severs and disassembles stable microtubules. *Cell* 75: 419-429.

McNally K.P., Buster D., McNally F.J. (2002). Katanin-mediated microtubule severing can be regulated by multiple mechanisms. *Cell Motil. Cytoskel.* 53: 337-349.

Myster S.H., Knott J.A., O'Toole E., Porter M.E. (1997). The *Chlamydomonas* Dhc1 gene encodes a dynein heavy chain subunit required for assembly of the I1 inner arm complex. *Mol. Biol. Cell* 8: 607-620.

Patel-King R.S., Benashski S.E., King S.M. (2002). A bipartite Ca2+ regulated nucleoside-diphosphate kinase system with in the *Chlamydomonas* flagellum. The regulatory subunit p72. *J. Biol. Chem. 277*: 34271-34279.

Pazour G.J., Agrin N., Leszyk J., Witman G.B. (2005). Proteomic analysis of a eukaryotic cilium. *J. Cell Biol.* 170: 103-113.

Quarmby LM, Mahjoub MR (2005) Caught Nek-ing: Cilia and centrioles. *J Cell Sci* 118: 5161-5169.

Quarmby, L.M. (2004). Cellular deflagellation. *Int Rev Cytol* 233, 47-91.

Quarmby L.M. (2000). Cellular Samurai: katanin and the severing of microtubules. *J. Cell Sci.* 113: 2821-2827.

Quarmby L.M., Hartzell H.C. (1994). Two distinct, calcium-mediated, signal transduction pathways can trigger deflagellation in *Chlamydomonas reinhardtii. J. Cell Biol.* 124: 807-815.

Rupp G., Porter M.E. (2003). A subunit of the dynein regulatory complex in *Chlamydomonas* is a homologue of a growth arrest-specific gene product. *J. Cell Biol.* 162: 47-57.

Rupp G., O'toole E., Porter M.E. (2001). The *Chlamydomonas* PF6 locus encodes a large alanine/proline-rich polypeptide that is required for assembly of a central pair projection and regulates flagellar motility. *Mol. Bio. Cell* 12: 739-751.

Salisbury, J.L., A.T. Baron, Sanders M.A.. (1988). The centrin-based cytoskeleton of *Chlamydomonas reinhardtii*: Distribution in interphase and mitotic cells. J. Cell Biol. *107*: 635-641.

Sanders, M.A., Salisbury J.L. (1989). Centrin-mediated microtubule severing during flagellar excision in *Chlamydomonas reinhardtii*. J Cell Biol. *108*:1751-1760.

Sanders, M.A., Salisbury J.L. (1989). Centrin plays an essential role in microtubule severing during flagellar excision in *Chlamydomonas reinhardtii. J. Cell Biol.* 124: 795-805.

Silflow C.D., Lefebvre P.A. (2001). Assembly and motility of eukaryotic cilia and flagella. Lessons from *Chlamydomonas reinhardtii. Plant Physiol.* 127: 1500-1507.

Sizova I., Fuhrmann M., Hegemann P. (2001). A Streptomyces rimosus aphVIII gene coding for a new type phosphotransferase provides stable antibiotic resistance to *Chlamydomonas reinhardtii. Gene.* 277: 221-229.

Smith E.F., Lefebvre P.A. (1996). PF16 encodes a protein with armadillo repeats and localizes to a single microtubule of the central pair apparatus in *Chlamydomonas* flagella. *J. Cell Biol.* 132: 359-370.

Smith E.F., Lefebvre P.A. (1997). PF20 gene product contains WD repeats and localizes to the intermicrotubule bridges in *Chlamydomonas* flagella. *Mol. Biol. Cell* 8: 455-467.

Smith E.F., Yang P. (2004). The radial spokes and central apparatus: mechano-chemical transducers that regulate flagellar motility. *Cell Motil. Cytoskeleton.* 57: 8-17.

Taillon B., Adler S., Suhan J., Jarvik J. (1992). Mutational analysis of centrin: An EF-hand protein associated with three distinct contractile fibers in the basal body apparatus of *Chlamydomonas. J. Cell Biol.* 119: 1613-1624.

Takada S., Wilkerson C.G., Wakabayashi K., Kamiya R., Witman G.B. (2002). The outer arm-docking complex: composition and characterization of a subunit (oda1) necessary for outer arm assembly. *Mol. Biol Cell* 13: 1015-1029.

Umen J.G., Goodenough U.W. (2001). Control of cell division by a retinoblastoma protein homolog in *Chlamydomonas. Genes Dev.* 15: 1652-1661.

Wlkerson C.G., King S.M, Koutoulis A., Pazour G.J., Witman G.B. (1995). The 78,000 M(r) intermediate chain of *Chlamydomonas* outer arm dynein is a WD-repeat protein required for arm assembly. *J. Cell Biol.* 129: 169-178.

Witman G.B. 1986. Isolation of *Chlamydomonas* flagella and flagellar axonemes. Methods Enzymol. *134*: 280-290.

Yokoyama R., O'toole E., Ghosh S., Mitchell D.R. (2004). Regulation of flagellar dynein activity by a central pair kinesis. *Proc. Nat. Acad. Sci.* USA. 101: 17398-17403.

Yang P., Sale W.S. (1998). The *Mr* 140,000 Intermediate Chain of *Chlamydomonas* flagellar inner arm dynein is a WD-repeat protein implicated in dynein arm anchoring. *Mol. Biol. Cell* 9: 3335-3349.

Yang P., Fox L., Colbran R.J., Sale W.S. (2000). Protein Phosphatases PP1 and PP2A are located in distinct positions in the *Chlamydomonas* flagellar axoneme. *J. Cell Sci.* 113: 91-102.

CHAPTER 5:

Conclusions and Future Directions

The dual role for Fa2p in deciliation and cell cycle progression is interesting, yet many questions remain about how it performs this dual function. In this study we have shown an asymmetric localization of Fa2p at a unique site, near the proximal region of the cilium, where it is aptly placed to perform a role in deciliation. Furthermore, we infer a translocation of the protein into the cell during flagellar disassembly (preceding mitosis), where it remains associated with the spindle poles. We theorize that this MTOC localization may be key to its role in cell division. However, a few questions remain: why would a protein essential for deciliation regulate cell cycle progression? What does deciliation provide for the cell? And what is the mechanism of Fa2p targeting to the SOFA?

5.1 Ciliary Disassembly and Mitosis

In most ciliated cells, from *Chlamydomonas* to mammals, flagella are resorbed prior to cell division (Bloodgood, 1974; Reider *et al.*, 1999; Pazour and Witman, 2003). Resorption involves disassembly of the axoneme from the distal tip of the flagella, and continues through to the removal of the transition zone (Cavalier-Smith, 1974). This process frees the basal bodies, allowing them to act as centrosomes/MTOC during mitosis (Silflow and Lefebvre, 2001). However, it was shown long ago that immediately preceding cell division, the basal bodies detach from the resorbing flagella, and that this detachment occurs at the transition zone (Johnson and Porter, 1967). Although many

studies since have focused on the resorption aspect, no experiments have been conducted to determine whether this detachment is required to release the basal bodies. One hypothesis is that although disassembly at the tip is the major contributor, the final steps require a severing event at the transition zone to free up the basal bodies. This idea is supported by recent data suggesting a link between flagellar disassembly and deflagellation; a model has been proposed where brief fractures in the microtubules at the SOFA facilitate disassembly at this region (Parker and Quarmby, 2003). Thus, in *fa2* mutants this essential severing step is missing, and cells are delayed until disassembly completes the resorption process. However, this model would predict that other deflagellation mutants, namely *adf1* and *fa1* cells, would also have a cell cycle delay due to slower disassembly. Examination of the cell cycle profile of these mutants shows that they are wild-type for cell cycle progression (Mahjoub, Bradley, Parker and Quarmby, unpublished data). This indicates that the cell cycle delay in *fa2* cells is not simply a consequence of the defect in axonemal microtubule severing.

A more likely scenario is that Fa2p acts as a checkpoint signal, relaying information to the cell that the cilium has been disassembled, thus permitting cell cycle progression. Fa2p translocation into the cell occurs during the final stages of flagellar resorption (Chapter 2). It seems possible that the increased cellular/MTOC accumulation of Fa2p transmits information about the stage of ciliary disassembly to the cell. In this model, Fa2p binds to interacting proteins at the spindle poles and provides a mitotic "go-ahead" signal to the cell. We do not believe that this signal is mediated via phosphorylation, as a kinase-inactive form of Fa2p can mediate cell cycle progression as in wild-type. Instead, Fa2p may act as a scaffold on which mitotic regulators bind to the

MTOC. There is precedence for this type of checkpoint signaling between ciliary disassembly and cell cycle progression: Pan and colleagues (2004) have shown that a *Chlamydomonas* paralog of Aurora kinase (CALK) acts as an effector of disassembly, in a checkpoint system that responds to developmental cues. Specifically, the authors showed that CALK is phosphorylated in conditions where cells disassemble their cilia including deflagellation, pre-zygotic flagellar resorption and resorption induced by disrupting IFT (Pan *et al.*, 2004). In contrast, CALK is dephosphorylated when flagella reassemble. The authors propose that ciliated cells have a sensory pathway that detects the state of flagella assembly/disassembly, and that CALK acts as a cellular effector for this pathway (Pan *et al.*, 2004). As such, Fa2p may be interacting with similar effectors, relaying information to the cell about the state of flagellar disassembly prior to mitosis.

5.2 Mechanisms of SOFA Targeting

Fa2p is assembled onto the axoneme at the SOFA in the very early stages of ciliary assembly, following deciliation or cell division. This localization is restricted to a narrow region, and is observed in both *Chlamydomonas* and when exogenously expressed in kidney epithelial cells (Chapter 2). To our knowledge, Fa2p was the first axonemal protein identified to show specific affinity for this region. Little is known about the SOFA, although recent data suggest that this ciliary domain may be important in various aspects of ciliary function. Previously, EM studies have shown that the proximal region of the *Chlamydomonas* axoneme lacks certain structures, such as radial spokes. Furthermore, this region is distinguished by the presence of a distinct subset of inner dynein arms that are found exclusively in this domain (Piperno and Ramanis, 1991). More recently, it was shown that a membrane protein (AGG2) essential for mediating

light orientation during *Chlamydomonas* phototaxis is localized to the SOFA (Iomini *et al.*, 2006). Although co-localization studies with Fa2p were not performed, the authors note that the AGG2 signal remains with the proximal region of severed flagella, similar to Fa2p (Iomini *et al.*, 2006). Finally, a component of nexins (inter-doublet links that connect the outer doublet microtubules) called p187 was recently observed to be localized to a proximal ~1 μm portion of the axoneme (Yanagisawa and Kamiya, 12th International Conference on the Cell and Molecular Biology of *Chlamydomonas*, abstract # 144). This finding is interesting since nexins are found along the entire length of the axoneme, yet asymmetry exists in the nexin components. So how is the longitudinal compartmentalization of the axoneme established? Specifically, what is the mechanism that confines Fa2p to this distinct region? One mechanism that may control this asymmetry is the sequential modification of tubulin making up the axoneme.

Microtubules of the ciliary axoneme are subjected to several types of evolutionarily conserved post-translational modifications, including acetylation, detyrosination, polyglutamylation, and polyglycylation (L'Hernault and Rosenbaum, 1985; Johnson, 1998; Redeker *et al.*, 1994; Pechart *et al.*, 1999). Although these modifications occur on cytoplasmic and other microtubular structures, I will focus on the axonemes for the purpose of this discussion. Most of the axonemal α-tubulin is acetylated on a single lysine residue located in the N-terminus of the protein, and this acetylation appears to be an indicator of stabilized microtubules (LeDizet and Piperno, 1987; Maruta *et al.*, 1986). Detyrosination (removal of a carboxy-terminal tyrosine of α-tubulin) is observed along the length of the axoneme, however, it is enriched in the B-tubules of the doublets and reduced or absent from A-tubules and the central pair (Johnson, 1998).

Similarly, polyglutamylation of tubulin was observed predominantly on the B-tubules of *Chlamydomonas* axonemes (Lechtreck and Geimer, 2000). Interestingly, polyglutamylated tubulin is present predominantly in the proximal region of the cilium, but lacking in the transition zone (Lechtreck and Geimer, 2000). The staining region is larger than, but encompasses, the SOFA. This pattern of polyglutamylation has also been reported in rodent lung epithelial cells, *Paramecium* and primary cilia (Bobinnec *et al.*, 1998; Pechart *et al.*, 1999). Furthermore, differences in the developmental timing of detyrosination and polyglutamylation modifications exist: ciliary assembly begins with tyrosinated tubulin, until the cilium is roughly half length. Detyrosinated tubulin is then detected midway through ciliary assembly. In contrast, polyglutamylation precedes detyrosination and becomes visible immediately after the onset of flagellar regeneration (Lechtreck and Geimer, 2000; Johnson, 1998).

The differential modifications of tubulin, and their timing, may provide insight into the asymmetric localization of Fa2p on the axoneme. The cross-linking studies in Chapter 4 identified two Fa2p-binding proteins in axonemal preparations, one of which is roughly the size of tubulin. Furthermore, I showed that Fa2p can co-immunoprecipitate with tubulin, and that salt-extracted Fa2p rebound extracted axonemes with high affinity, supporting the hypothesis that Fa2p may be directly sitting on the microtubules of the axoneme. I envision a mechanism by which, during flagellar regeneration, Fa2p is targeted to the proximal axoneme and binds to one isoform of tubulin. As the axonemal tubulin is further modified, Fa2p localization becomes restricted.

Finally, the posttranslational modifications mentioned above are involved in mediating the interaction of axonemes with microtubule-associated proteins, motors and

intermediate filaments (Rosenbaum, 2000 and references within). These include the binding of dynein arms, as well as kinesin motors, to the axoneme. It would be interesting to see whether disruption of these, or other, tubulin modifications affect Fa2p localization (see below). These ideas also apply to the asymmetrically localized mNek8 protein, which is found predominantly in the proximal region of primary cilia, similar to Fa2p.

5.3 Future Directions

There is still much to be learned about how Fa2p exerts its effect on deciliation and cell cycle progression. Furthermore, little is known about the proteins that interact with, regulate or are regulated by Nek1 and Nek8. Studies of the two mammalian Neks are currently being conducted by graduate students in the Quarmby lab, Mark White and Melissa Trapp. In this section, I will focus on future experiments with Fa2p.

A key to understanding Fa2p function is to identify interacting proteins, substrates and proteins that regulate Fa2p activity during deflagellation and cell cycle progression. Our biochemical and genetic studies did not identify such a protein, but did point towards a possible interaction with tubulin. To determine whether this interaction is genuine, a saturation experiment is being conducted. This experiment is similar to the axonemal-rebinding assay described in Figure 4-7, except that extracted axonemes will be incubated with increasing amounts of Fa2p-containing salt extract. Our hypothesis is that at an extract-to-axoneme ration of 1:1, the majority of Fa2p would be in the axonemal fraction (similar to figure 4-7B). However, as exceeding amounts of extract are added, we predict to see a saturation point for Fa2p rebinding. These experiments will help us determine whether the Fa2p-tubulin interaction is significant, or whether it is an artefact.

The next step would be to investigate this interaction: (a) purified, recombinant Fa2p can be used in *in vitro* microtubule-binding studies to test the affinity of binding to polymerized microtubules. We can then narrow down the portion of the Fa2 peptide that is interacting with tubulin, by using deletion mutants. (b) Perturbation of tubulin modifications in *Chlamydomonas*. This will be performed in collaboration with the Gaertig lab (University of Georgia), and involves performing RNAi of the *Chlamydomonas* homologs of the tubulin modifying enzymes. Preliminary BLAST searches using the *Tetrahymena* TTLL1 (tubulin tyrosine ligase-like 1) sequence have identified 11 target *Chlamydomonas* genes. RNAi constructs for these genes will be transformed into wild-type cells and transformants assayed for flagellar (or other) phenotypes. Any RNAi-positive colonies will be assayed for Fa2p localization and assembly at the SOFA. (c) Perturbation of tubulin modifications in ciliated epithelial cells (e.g. by antibody injection or siRNA), followed by localization of transfected Fa2p.

I am also interested in obtaining a higher resolution localization pattern of Fa2p on the axoneme. Specifically, I would like to know if the protein is associated with the outer-doublets, central pair or other axonemal structures. A finer resolution localization of Fa2p may provide insight into structures/protein complexes that anchor Fa2p to the SOFA. To answer these questions, immuno-EM studies will be performed using anti-Fa2p or anti-HA antibodies (on wild-type or Fa2p-HA cells, respectively). *fa2* mutant cells can be used as negative controls in both cases. Due to our lack of experience with electron microscopy, we will secure collaborations with other *Chlamydomonas* researchers. Identification of the axonemal localization of Fa2p may also provide insight into its role in the axoneme.

Once a robust construct for expressing Fa2p is developed, we can identify the axonemal targeting domain of Fa2p. This fragment can then be used in yeast two-hybrid studies to fish in a *Chlamydomonas* cDNA library and identify putative interactors. The deletion constructs will also be helpful in dissecting the domain(s) involved in translocation of Fa2p into the cell during flagellar resorption.

Another avenue of investigation is to identify substrates of Fa2p, since it is a protein kinase. Ideally, we would compare the phospho-proteins present in flagella isolated from wild-type and *fa2* mutants. However, *fa2* cells do not shed their flagella, making this experiment impossible. An alternate approach is to isolate flagellar-basal body complexes (FBBCs) from both strains, and compare the phosphor-proteins by 2D gel analysis. We predict that in *fa2* FBBCs, one (or more) proteins will be lacking in phosphorylation. Ideally, these proteins can then be excised and identified by Mass Spectroscopy. This experiment requires that protein yield be high enough to allow peptide sequencing. Unlike the cross-linking experiments, we are not dependent on the weak interaction of Fa2p with another protein, or numerous purification steps. Thus, this experiment is significantly different, and may allow the direct identification of a Fa2p substrate. At the very least, it will provide us with information regarding the molecular weight and isoelectric charge of these substrates; these can then be used to mine the flagellar proteome for candidate proteins.

Another fundamental question is whether Fa2p is activated during deciliation or cell cycle progression. Some members of the Nek family are activated by phosphorylation, sometimes via autophosphorylation (reviewed in Quarmby and Mahjoub, 2005). Examination of lysates containing endogenous Fa2p have not yielded

any information on whether the protein is phosphorylated pre – or post-deciliation. In rare cases, Fa2p was observed to migrate as a doublet in SDS-PAGE gels (e.g. Figure 4-2B). However, phosphatase treatment of such extracts did not affect the migration pattern. It is possible that other posttranslational modifications may be occurring, or that the doublet is due to slight amounts of protein degradation. However, more thorough experiments need to be done to test the phosphorylation possibility; one experiment would be to use purified recombinant Fa2 protein *in vitro* to perform phosphorylation assays using generic kinases (alternatively, we can just use Fa2p to test for autophosphorylation). The phosphorylation sites can be identified by peptide sequencing and Mass Spectroscopy; we can then make the corresponding mutation(s) in the serine/threonine/tyrosine residues of the gene, and transform that into *Chlamydomonas*. We will then test transformants for rescue of deciliation and cell cycle progression, identifying residues essential in activation of Fa2p.

This work will increase our understanding of the fundamental problem of the regulation of axonemal microtubule severing. Understanding this essential cellular process has broad implications for human health (reviewed in Quarmby, 2004). For example, sterility can be the result when testicular sperm deflagellate in response to ingested toxins; infection results when respiratory epithelia deciliate in response to excessive tobacco smoke (Quarmby, 2004). Furthermore, elucidating the roles of proteins, such as Fa2p, involved in the coordinate regulation between cilia and the cell cycle may provide insight into mechanisms of various human diseases, such as polycystic kidney disease, infertility and blindness.

5.4 Reference List

Bloodgood RA. 1974. Resorption of organelles containing microtubules. *Cytobios* 9:143-161.

Bobinnec Y., Khodjakov A., Mir L.M., Rieder C.L., Edde B., Bornens M. (1998). Centriole disassembly in vivo and its effect on centrosome structure and function in vertebrate cells. *J. Cell Biol.* 143: 1575-1589.

Cavalier-Smith, T. 1974. Basal body and flagellar development during the vegetative cell cycle and the sexual cycle of *Chlamydomonas reinhardtii. J. Cell Sci.* 16: 529-556.

Iomini C., Linya L., Wenjum M., Dutcher S.K., Piperno G. (2006). Two flagellar genes, AGG2 and AGG3, mediate orientation to light in Chlamydomonas. *Curr. Biol.* 16: 1147-1153.

Johnson K.A. (1998). The axonemal microtubules of the *Chlamydomonas* flagellum differ in tubulin isoforms content. *J. Cell Sci.* 111: 313-320.

Johnson, U.G. and K.R. Porter. 1968. Fine structure of cell division in *Chlamydomonas reinhardi.* Basal bodies and microtubules. *J. Cell Biol.* 38: 403-425.

L'Hernault S.W., Rosenbaum J.L. (1985). Reversal of the posttranslational modification on *Chlamydomonas* flagellar alpha-tubulin occurs during flagellar resorption. *J. Cell Biol.* 100: 457-462.

Lechtreck K.F., Geimer S. (2000). Distribution of polyglutamylated tubulin in the flagellar apparatus of green flagellates. *Cell Motil. Cytosk.* 47: 219-235.

LeDizet M, Piperno G. (1987). Identification of an acetylation site of *Chlamydomonas* alpha-tubulin. *Proc. Natl. Acad. Sci. USA.* 84: 5720-5724.

Maruta H., Greer K., Rosenbaum J.L. (1986). The acetylation of alpha-tubulin and its relationship to the assembly and disassembly of microtubules. *J. Cell. Biol.* 103: 571-579.

Pan, J., Q. Wang, and W.J. Snell. 2004. An aurora kinase is essential for flagellar disassembly in *Chlamydomonas*. *Dev. Cell* 6: 445-451.

Parker, J.D.K. and L.M. Quarmby. 2003. *Chlamydomonas fla* mutants reveal a link between deflagellation and intraflagellar transport. *BMC Cell Biology.* 4: 11.

Pazour, G.J., Witman, G.B. (2003). The vertebrate primary cilium is a sensory organelle. *Curr Opin Cell Biol* 15, 105-110.

Pechart I., Kann M.L., Levilliers N., Bre M.H., Fouquet J.P. (1999). Composition and organization of tubulin isoforms reveals a variety of axonemal models. *Biol. Cell* 91: 685-697.

Piperno G., Ramanis Z. (1991). The proximal portion of *Chlamydomonas* flagella contains a distinct set of inner arm dyneins. *J. Cell Biol.* 112: 701-709.

Quarmby LM, Mahjoub MR (2005) Caught Nek-ing: Cilia and centrioles. *J Cell Sci* 118: 5161-5169.

Quarmby, L.M. (2004). Cellular deflagellation. *Int Rev Cytol* 233, 47-91.

Redeker V., Levilliers N., Scmitter J.M., Le Caer J.P., Rossier J., Adoutte A., Bre M.H. (1994). Polyglycylation of tubulin: a posttranslational modification in axonemal microtubules. *Science* 266: 1688-1691.

Rieder CL, Jensen CG and Jensen LCW. 1979. The resorption of primary cilia during mitosis in a vertebrate (PtK)1 cell line. *J Ultrastr Res* 68:173-185.

Rosenbaum J.L. (2000). Cytoskeleton: Functions for tubulin modifications at last. *Curr. Biol.* 10: R801-R803.

Silflow, C.D. and P.A. Lefebvre. 2001. Assembly and motility of eukaryotic cilia and flagella. Lessons from *Chlamydomonas reinhardtii. Plant Physiol.* 127: 1500-1507.